

NASA-CR-168310

NASA-CR-168310
19840008313

NASA CR-168310
MCR-83-624



National Aeronautics and
Space Administration

**CRYOGENIC FLUID
MANAGEMENT EXPERIMENT
TRUNNION VERIFICATION TESTING**

by W.J. Bailey, and D.A. Fester

MARTIN MARIETTA DENVER AEROSPACE

prepared for

NASA Lewis Research Center

Contract NAS3-23245

LIBRARY COPY

1984

LANGLEY RESEARCH CENTER
LIBRARY, NASA
HAMPTON, VIRGINIA

13 1 1 RN/NASA-CR-168310

DISPLAY 13/2/1

84N16381*# ISSUE 7 PAGE 985 CATEGORY 31 RPT#: NASA-CR-168310 NAS
1.26:168310 MCR-83-624 CNT#: NAS3-23245 83/12/00 107 PAGES

UNCLASSIFIED DOCUMENT

UTTL: Cryogenic Fluid Management Experiment (CFME) trunnion verification testing
TLSP: Final Report, Nov. 1981 - Sep. 1983

AUTH: A/BAILEY, W. J.; B/FESTER, D. A.

CORP: Martin Marietta Aerospace, Denver, Colo. AVAIL.NTIS SAP: HC A06/MF
A01

MAJS: /*CRYOGENIC FLUID STORAGE/*FATIGUE (MATERIALS)/*LIQUID HYDROGEN/*SHAFTS
(MACHINE ELEMENTS)/*STORAGE TANKS

MINS: / EPOXY COMPOUNDS/ GLASS FIBERS/ LAMINATES

ABA: S.L.

ABS: The Cryogenic Fluid Management Experiment (CFME) was designed to
characterize subcritical liquid hydrogen storage and expulsion in the
low-g space environment. The CFME has now become the storage and supply
tank for the Cryogenic Fluid Management Facility, which includes transfer
line and receiver tanks, as well. The liquid hydrogen storage and supply
vessel is supported within a vacuum jacket to two fiberglass/epoxy
composite trunnions which were analyzed and designed. Analysis using the
limited available data indicated the trunnion was the most fatigue
critical component in the storage vessel. Before committing the complete
storage tank assembly to environmental testing, an experimental assessment

ENTER:

1. Report No. NASA CR-168310		2. Government Accession No.		3. Recipient's Catalog No.	
4. Title and Subtitle Cryogenic Fluid Management Experiment (CFME) Trunnion Verification Testing				5. Report Date December 1983	
				6. Performing Organization Code	
7. Author(s) W. J. Bailey and D. A. Fester				8. Performing Organization Report No. MCR-83-624	
9. Performing Organization Name and Address Martin Marietta Denver Aerospace P.O. Box 179 Denver, Colorado 80201				10. Work Unit No.	
				11. Contract or Grant No. NAS3-23245	
12. Sponsoring Agency Name and Address NASA Lewis Research Center 21000 Brookpark Road Cleveland, Ohio 44135				13. Type of Report and Period Covered Final Report Nov. 1981 to Sept. 1983	
				14. Sponsoring Agency Code	
15. Supplementary Notes Project Manager, Harold J. Kasper, NASA Lewis Research Center, Cleveland, Ohio 44135					
<p>16. Abstract Cryogenic liquid storage and supply systems will play an important role in meeting missions/requirements of future NASA and DOD payloads. A first step in the development of these spacecraft systems is to obtain engineering performance data. The Cryogenic Fluid Management Experiment (CFME) was designed to characterize subcritical liquid hydrogen storage and expulsion in the low-g space environment. The CFME has now become the storage and supply tank for the Cryogenic Fluid Management Facility (CFMF), which includes transfer line and receiver tanks, as well.</p> <p>The liquid hydrogen storage and supply vessel is supported within a vacuum jacket by two fiberglass/epoxy composite trunnions which were analyzed and designed under Contract NAS3-21591. Analysis using the limited available data indicated the trunnion was the most fatigue critical component in the storage vessel. Before committing the complete storage tank assembly to environmental testing, an experimental assessment was performed to verify the capability of the trunnion design to withstand expected vibration and loading conditions.</p> <p>Three tasks were conducted to evaluate trunnion integrity. The first determined the fatigue properties of the trunnion composite laminate material. Tests at both ambient and liquid hydrogen temperatures showed composite material fatigue properties far in excess of those expected. Next, an assessment of the adequacy of the trunnion designs was performed (based on the tested material properties). Trunnion structural fatigue integrity tests were then performed for expected loading conditions over a seven mission life. Finally, four trunnions were fabricated for use on the CFMF test article and flight experiment.</p>					
17. Key Words Cryogenic Storage Composite Support Trunnion Composite Fatigue Properties E-glass/S-glass Epoxy Laminate Composite Fatigue Testing Cryogenic Fluid Management Facility			18. Distribution Statement Unclassified - Unlimited		
19. Security Classif. (of this report) Unclassified		20. Security Classif. (of this page) Unclassified		21. No. of Pages 88	
				22. Price NO	

CRYOGENIC FLUID MANAGEMENT
EXPERIMENT TRUNNION
VERIFICATION TESTING

Final Report

December 1983

by

William J. Bailey

and

Dale A. Fester

Prepared for

NATIONAL AERONAUTICS AND SPACE ADMINISTRATION

Lewis Research Center

Contract NAS3-23245

Martin Marietta Denver Aerospace
Denver, Colorado 80201

FOREWORD

This report was prepared by the Martin Marietta Corporation, Denver Aerospace, under Contract NAS3-23245. The contract was administered by the Lewis Research Center of the National Aeronautics and Space Administration, Cleveland, Ohio. The technical period of performance was from November 1981 to September 1983.

The following NASA-LeRC individuals contributed to Project Management of the program:

Mr. Eugene P. Symons
Mr. Harold J. Kasper

The authors wish to acknowledge the contributions of the following individuals to this program:

Dale A. Fester - Program Manager
William J. Bailey - Technical Director
Susan W. Pawlowski - Dynamics and Stress Analysis
Terence Coxall - Stress Analysis
Paul R. Kerstetter - Stress Analysis
Duncan A. Boyce - Composites Analysis
Robert S. Bollinger - Stress Analysis
Donald A. Stang - Materials Composites Engineering
Ted F. Kiefer - Materials Test Engineering
John S. Marino - Design
Joseph M. Toth, Jr. - Composites Technology
John W. Tuthill - Structural Test

The data in this report are presented with the International System of Units as the primary units and English Units as secondary units. All calculations and graphs were made in English units and converted to the International units.

TABLE OF CONTENTS

	<u>Page</u>
LIST OF FIGURES	iii
LIST OF TABLES	v
SUMMARY	vi
 I. INTRODUCTION	 I-1
A. Task I - Determination of Fatigue Properties of Trunnion .	I-5
B. Task II - CFME Materials Trunnion Design Assessment . . .	I-6
C. Task III - Determination of CFME Trunnion Structural Integrity	 I-6
 II. DETERMINATION OF FATIGUE PROPERTIES OF TRUNNION	
MATERIAL (Task I)	II-1
A. Test Specimen Design	II-1
B. Definition of Test Philosophy	II-8
C. Static Tension Test Results	II-11
D. Fatigue Test Description	II-13
E. Ambient Temperature Fatigue Test Results	II-18
F. Liquid Hydrogen Temperature Fatigue Test Results	II-23
 III. CFME TRUNNION DESIGN ASSESSMENT (Task II)	 III-1
A. Stress and Dynamic Analysis	III-3
B. Trunnion Design Modification	III-9
 IV. DETERMINATION OF CFME TRUNNION STRUCTURAL INTEGRITY	 IV-1
A. Testing Philosophy	IV-1
B. Trunnion Fabrication	IV-2
C. Structural Fatigue Test Fixture	IV-13
D. Structural Fatigue Test Description	IV-13
E. Trunnion Structural Integrity Test Results	IV-20
 V. CONCLUSIONS AND RECOMMENDATIONS	 V-1
 APPENDIX A ABBREVIATIONS AND ACRONYMS	 A-1
REFERENCES	R-1
DISTRIBUTION LIST	D-1

LIST OF FIGURES

<u>FIGURE</u>	<u>TITLE</u>	<u>Page</u>
I-1	Cryogenic Fluid Management Experiment	I-2
I-2	Cryogenic Fluid Management Facility	I-3
I-3	Trunnion Mounting Configuration	I-4
II-1	Original Test Specimen Configuration	II-2
II-2	Interim Test Specimen Configuration	II-3
II-3	Interim Test Specimen/Test Machine Interface	II-4
II-4	Selected Laminate Test Specimen Configuration	II-6
II-5	Selected Laminate Test Specimen/Test Machine Interface	II-7
II-6	X Direction Stress/Strain Diagram for CFME Laminate	II-9
II-7	Laminate Load/Strain Curve	II-12
II-8	Test Specimen/Test Machine Installation	II-14
II-9	Specimen Fatigue Test Setup	II-15
II-10	Assembled Test Fixture Configuration	II-16
II-11	Specimen Fatigue Test Setup with Cryostat Installed	II-17
II-12	CFME Trunnion Laminate S/N Curve for Ambient Temperature	II-21
II-13	Ambient Temperature Laminate Specimen Test Deflection Data	II-22
II-14	CFME Trunnion Laminate Stiffness Degradation	II-24
II-15	Failed Ambient Test Specimen R-8	II-26
II-16	CFME Trunnion Laminate LH ₂ Temperature S/N Curve	II-27
II-17	CFME Trunnion Laminate Deflection at LH ₂ Temperature	II-28
II-18	Failed LH ₂ Test Specimen H-5	II-29
III-1	CFME Trunnion Laminate S/N Curve Comparison with 321-SS and 6061-T6 Al	III-2
III-2	CFME Trunnion Stress Analysis Diagrams	III-5
III-3	Trunnion Fatigue Loading Conditions	III-6
III-4	CFME Fixed Trunnion Assembly	III-11
III-5	CFME Floating Trunnion Assembly	III-12
III-6	Back-up Ring Assembly	III-13
III-7	Back-up Ring Installation	III-14

LIST OF FIGURES

<u>FIGURE</u>	<u>TITLE</u>	<u>Page</u>
IV-1	CFME Fixed Trunnion Assembly (Rev. B)	IV-3
IV-2	CFME Floating Trunnion Assembly (Rev. B)	IV-4
IV-3	Fixed Trunnion Manufacturing Tooling	IV-5
IV-4	End Insert and Spacer Constraint Tooling	IV-6
IV-5	Flange Constraint Tooling	IV-7
IV-6	Floating Trunnion Manufacturing Tooling	IV-10
IV-7	Fixed Trunnion Configuration	IV-11
IV-8	Floating Trunnion Configuration	IV-12
IV-9	CFME Trunnion Fatigue Test Set-up	IV-14
IV-10	CFME Trunnion Structural Integrity Test Set-up Details	IV-15
IV-11	CFME Trunnion Test Instrumentation Locations	IV-16
IV-12	Failed Fixed Trunnion in Test Setup	IV-21
IV-13	Floating Trunnion Static Test Deflection Data	IV-23
IV-14	Floating Trunnion Static Test Strain Data	IV-24
IV-15	Fixed Trunnion Static Test Deflection Data	IV-25
IV-16	Fixed Trunnion Static Test Strain Data	IV-26

LIST OF TABLES

<u>TABLE</u>	<u>TITLE</u>	<u>Page</u>
II-1	Laminate Static Data	II-11
II-2	Fatigue Test Specimen Loading Conditions	II-18
II-3	Ambient Temperature Fatigue Test Results	II-19
II-4	Liquid Hydrogen Temperature Fatigue Test Results	II-25
III-1	Design Load Factors	III-3
III-2	20,000 Cycle Fatigue Loading (0σ to 2σ)	III-8
III-3	2,540 Cycle Fatigue Loading Margin Testing (2σ to 3σ) . . .	III-8
IV-1	Trunnion Test Summary	IV-20

SUMMARY

Cryogenic liquid storage and supply systems will play an important role in meeting mission requirements of future NASA and DOD payloads. A first step in the development of spacecraft subcritical cryogenic storage systems is to obtain engineering data on the performance of these systems. The Cryogenic Fluid Management Experiment (CFME) was designed to characterize subcritical liquid hydrogen storage and expulsion in the low-g space environment. The Cryogenic Fluid Management Facility (CFMF) has expanded the CFME concept into an integrated supply and receiver tank design which will prove more versatile in characterizing low-g cryogenic performance. Martin Marietta is designing the CFMF under Contract NAS3-23355 using previously designed CFME supply tankage, including the composite support trunnions. The trunnions comprise the first hardware fabrication for the project.

The CFME liquid hydrogen storage vessel is supported within a vacuum jacket by two fiberglass/epoxy composite trunnions which were analyzed and designed under Contract NAS3-21591. Analysis had shown a trunnion damage factor of 0.813 which when compared to a maximum of 1.0 leads to identification of the trunnion as the most fatigue critical component in the storage vessel. Since limited analytical or experimental investigations existed on the fatigue life of composites at cryogenic temperature, an experimental assessment was desired of the capability of the trunnion design to withstand vibration and loading conditions. Before committing the complete storage tank assembly to environmental testing, an experimental assessment was performed to verify the capability of the trunnion design to withstand expected vibration and loading conditions.

Three tasks were conducted to evaluate trunnion integrity. The first determined the fatigue properties of the trunnion composite laminate material. Tests at both ambient and liquid hydrogen temperatures showed composite material fatigue properties far in excess of those expected. As a result, a new damage factor of less than 0.1 was determined. Next, an assessment of the adequacy of the trunnion designs was performed (based on the tested material properties) and minor changes were made primarily to facilitate fabrication. Flight configuration trunnions were then fabricated and structural fatigue integrity tests were performed for both expected

conditions and for margin so that cumulative damage could be assessed. Results showed that the trunnion designs were more than adequate to meet expected loading conditions over a seven-mission life. Finally, after the trunnion design was experimentally verified, four trunnions were fabricated for use on the CFMF test article and flight experiment.

I. INTRODUCTION

Mission plans for future NASA and DOD payloads include a wide variety of applications which require orbital cryogenic liquid storage and supply systems. These applications range from the use of small quantities of liquid helium for experimental cooling to the use of thousands of liters of cryogenics in the next generation of orbit-to-orbit transfer vehicles. Composite support structures will play an important role in these systems. This project was conducted to evaluate and experimentally verify the composite support system design for the Cryogenic Fluid Management Experiment (CFME) shown in Figure I-1. This experiment is designed to provide a thorough characterization of low-g cryogenic liquid expulsion and provide a data base from which efficient thermal designs for subcritical cryogen storage systems can be generated.

The CFME design essentially becomes the LH_2 supply tank for the expanded CFME concept, shown in Figure I-2. A transfer line, LH_2 receiver tank, associated plumbing and pressurization systems are included to provide chilldown, liquid transfer and resupply performance data. For the purposes of this report, however, the supply tank trunnions will be referred to as the "CFME Trunnions".

The capability of the CFME to meet the seven-mission requirement was determined to be extremely sensitive to the fatigue life of the composite trunnions at cryogenic temperatures. Because of the limited extent of analytical or experimental treatment of the fatigue life of composites at cryogenic temperatures, an early verification of design and performance capability was provided by this program.

The CFME composite support trunnion was analyzed and designed in detail under contract NAS3-21591 (Ref 1). The vacuum jacket girth ring interfaces with the liquid hydrogen storage vessel through two support trunnions. The trunnion mount configuration is shown in Figure I-3. This design resulted from an assessment which considered both the thermal requirements and the structural design as driven by fatigue for seven-mission life. One trunnion is adjusted to the proper position prior to final closeout welding of the support tube assembly by a threaded and vented fitting. It is called the

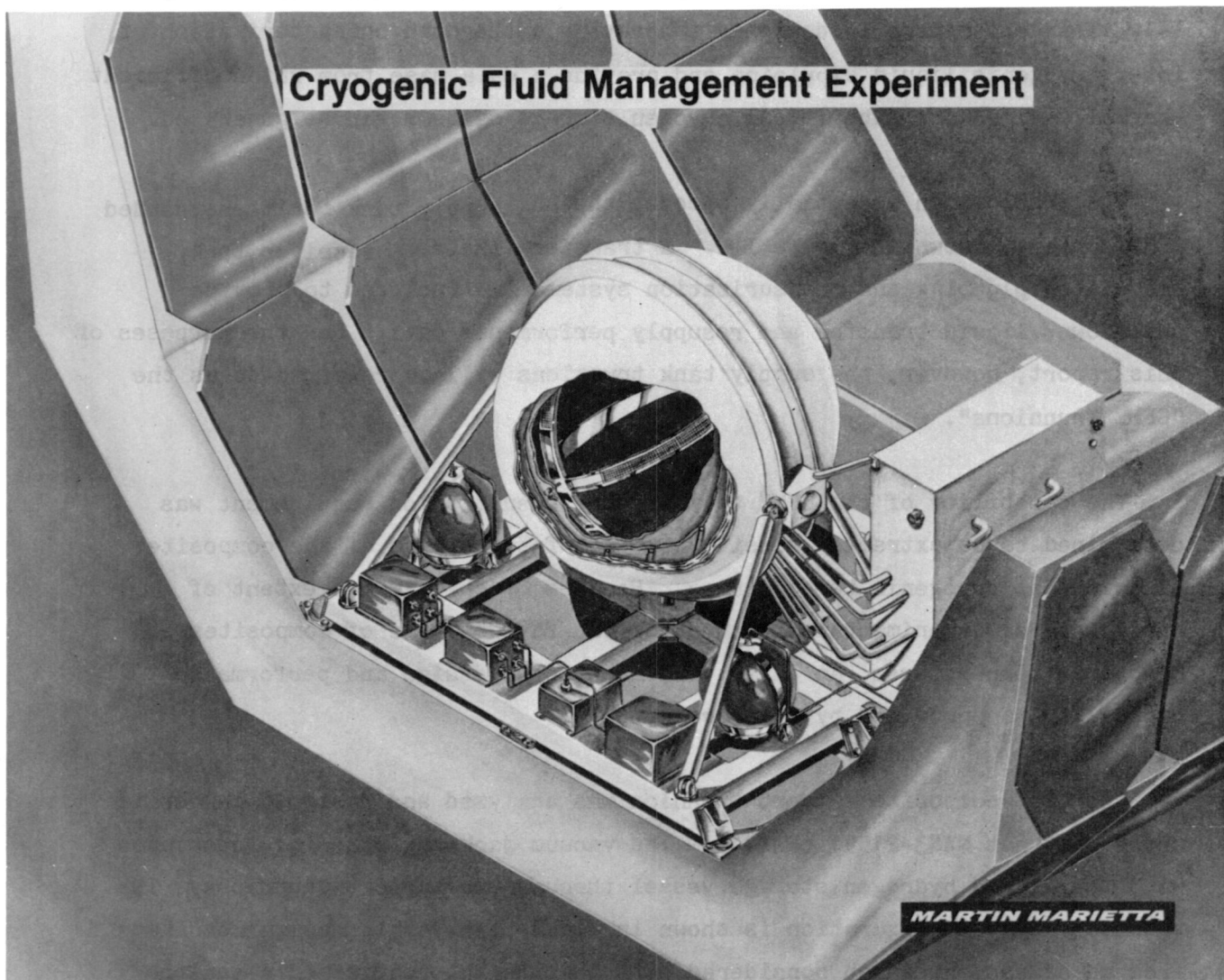


Figure I-1 Cryogenic Fluid Management Experiment

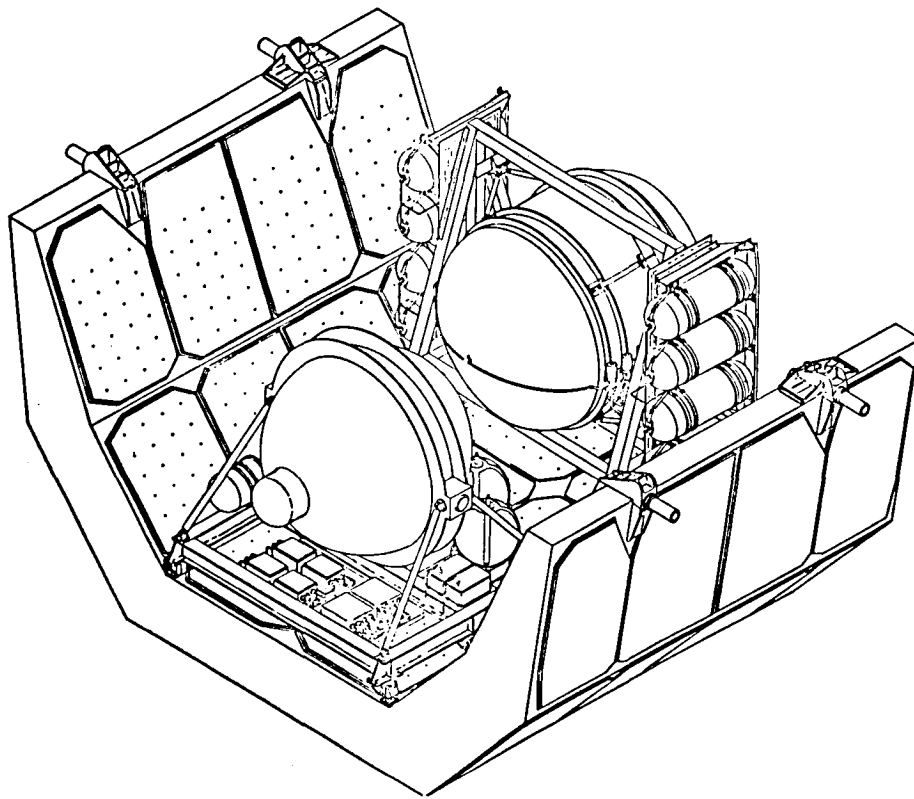


Figure I-2 Cryogenic Fluid Management Facility

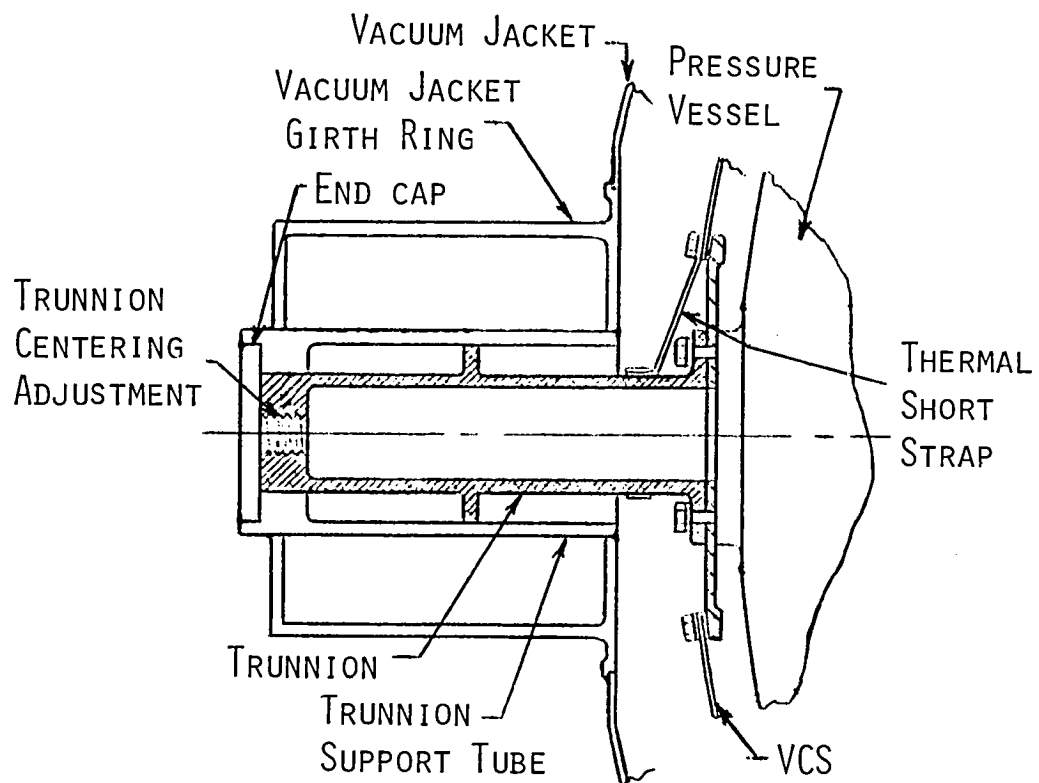


Figure I-3 Trunnion Mounting Configuration

fixed trunnion. The other trunnion allows for contraction and expansion of the pressure vessel and is termed the floating trunnion. The pressure vessel is therefore slightly offset (unsymmetrical support) in the unloaded condition, but becomes symmetrical in the loaded (cold and contracted) condition.

The CFME Trunnion Verification Testing Program was divided into three tasks which were designed to evaluate and experimentally verify the CFME trunnion design.

A. Task I- Determination of Fatigue Properties of Trunnion Materials

A test matrix and test plan (Ref 2) to establish the basic mechanical property data for the trunnion fiberglass/epoxy material were prepared and submitted to the NASA Project Manager for review and approval. The CFME Trunnion Test Plan, CFME-80-32 (Ref 3) submitted as a part of Contract NAS3-21591 was used as the basis for the laminate material property tests.

Laminate material test specimens were designed and fabricated, the test system was constructed and fatigue tests were performed at ambient and liquid hydrogen temperatures. Collected data were used to generate S/N curves (stress amplitude vs cycles) for the laminate material.

All data reduced from the Task I effort indicated that the CFME trunnion laminate material is significantly stiffer (and capable of supporting more load) than suggested from the properties used during the original analysis. Stiffness increased as the laminate temperature decreased. Ambient temperature fatigue tests showed significantly increased cycle life beyond that indicated by the original analytical S/N curve.

B. Task II - CFME Trunnion Design Assessment

The basic property data obtained from the tests conducted in Task I were used to assess the adequacy of the CFME trunnion design for the seven-mission life. Results were compared with dynamic and stress analyses previously performed on the trunnion configurations (Ref 4). The design of the trunnions was then modified to incorporate improvements suggested by the following:

- 1) Task I data reduction;
- 2) Manufacturing processes and development evaluations;
- 3) Stress and dynamic analysis;
- 4) Customer concerns;
- 5) Technical reviews.

CFME trunnion drawings numbered 849CFME1035 and 849CFME1036 were updated to reflect appropriate configuration changes.

C. Task III - Determination of CFME Trunnion Structural Integrity

A test matrix and test plan (Ref 5) to establish the structural integrity of the CFME trunnions were prepared and submitted to the NASA Project Manager for review and approval. The CFME Trunnion Test Plan (Ref 3) was used as the basis for the structural integrity tests; however, only the fatigue portions of the testing described therein were included.

Three test trunnions (one fixed and two floating) were fabricated and successfully tested under fatigue loads over a spectral distribution up to and including limit loads for 20,000 cycles. Two of the trunnions (one fixed and one floating) were subjected to margin testing for an additional 2,540 cycles at a load level up to and including ultimate load (1.5 times limit load). All test trunnions were then loaded to failure, which occurred at 1.9 to 2.3 times limit load. These failures occurred above the design ultimate load even after completion of fatigue tests.

Based on these successful test results, four deliverable trunnions (two fixed and two floating) were then fabricated for use on the CFME test article and flight experiment.

II. DETERMINATION OF FATIGUE PROPERTIES OF TRUNNION MATERIAL (Task I)

The Task I effort consisted of the following activities:

- 1) Procurement of contract materials;
- 2) Establishment of test specimen configuration;
- 3) Definition of test philosophy;
- 4) Test plan preparation;
- 5) Materials and process specification preparation;
- 6) Test fixture design;
- 7) Test facility setup;
- 8) Test specimen fabrication;
- 9) Test procedure preparation;
- 10) Ambient temperature fatigue testing;
- 11) Liquid hydrogen temperature fatigue testing;
- 12) Fatigue testing data reduction.

The following sections detail the Task I effort.

A. Test Specimen Design

Three test specimen configurations were considered using an iterative development to achieve a design which would meet the following criteria:

- 1) Compatible with test machine interface;
- 2) Compatible with test machine capacity (66,750 N (15,000 lbs) maximum);
- 3) Minimize specimen/test machine load alignment complexity;
- 4) Withstand buckling in compression;
- 5) Positive attachment to minimize slipping;
- 6) Same specimen design for ambient and LH₂;
- 7) Design compatible with LH₂.

Since composite tension-compression fatigue testing represents a field where little documentation is available, this iteration of specimen configuration was necessary to develop a preferred design.

An evaluation of the proposed test specimen configuration was conducted after it was determined that both the specimen gage section and the test fixture clamping jaws were inadequate for tension-compression fatigue loading. The original design (taken from Ref. 3), shown in Figure II-1, had an insufficient cross-sectional area in the gage section. In addition, it was felt that the difference in thermal contractions of the composite and the stainless steel clamping jaws would not provide an adequate grip for a long-term cyclic fatigue test at LH₂ temperatures.

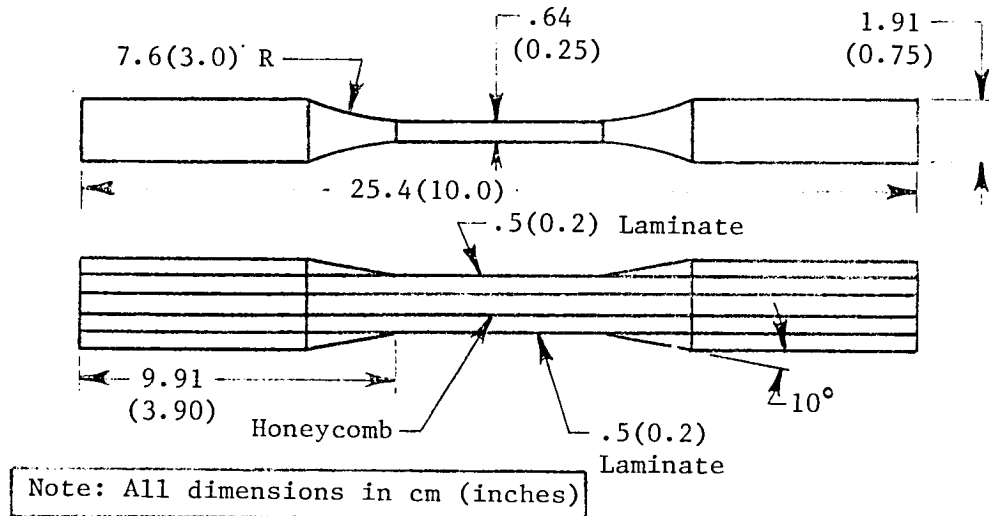


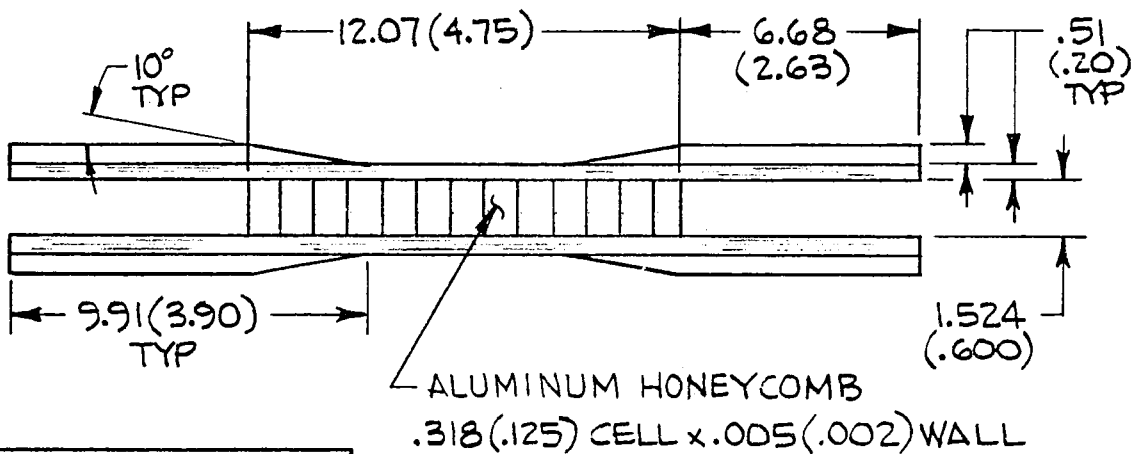
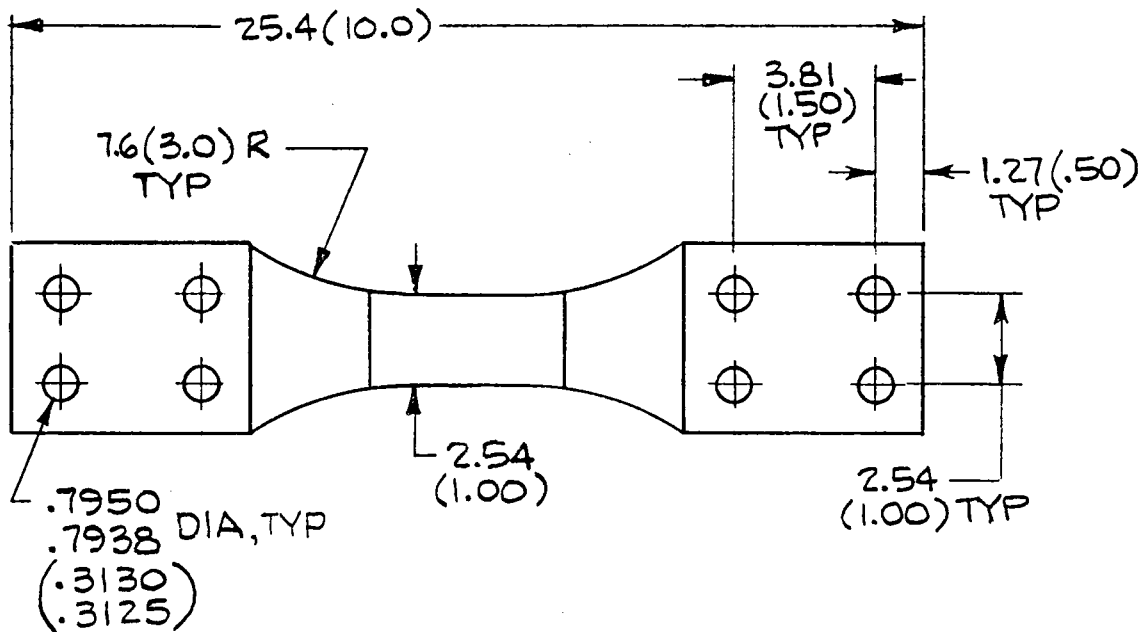
Figure II-1 Original Test Specimen Configuration

A new specimen configuration was proposed (Figure II-2), which had an increased width in the gage section and a clevis arrangement at each end for interface with the tongues of the testing machine (Figure II-3). Specimen securing was provided by a four bolt attachment at each end. This configuration was assessed from the stand point of complexity of manufacture and chance for success in obtaining the required information from the test series. Objections to this design were:

- 1) End configuration and proper alignment required match drilling of the specimen clevis and the test machine tongue;
- 2) The honeycomb center, added to minimize buckling of the laminate material during the compression half of the loading cycle, presented problems related to maintaining the bond to each half of the specimen;

SPECIMEN LAYUP												
0°	45°	0 ₂ °	45°	0 ₂ °	45°	0 ₂ °	45°	0 ₂ °	45°	0 ₂ °	45°	0°
.03	.023	.061	.023	.061	.023	.061	.023	.061	.023	.061	.023	.03
(.012)	(.009)	(.024)	(.009)	(.024)	(.009)	(.024)	(.009)	(.024)	(.009)	(.024)	(.009)	(.012)

CLOTH (TYP)
 ROVING (TYP)



NOTE: ALL DIMENSIONS
 IN CM (INCHES)

Figure II-2 Interim Test Specimen Configuration

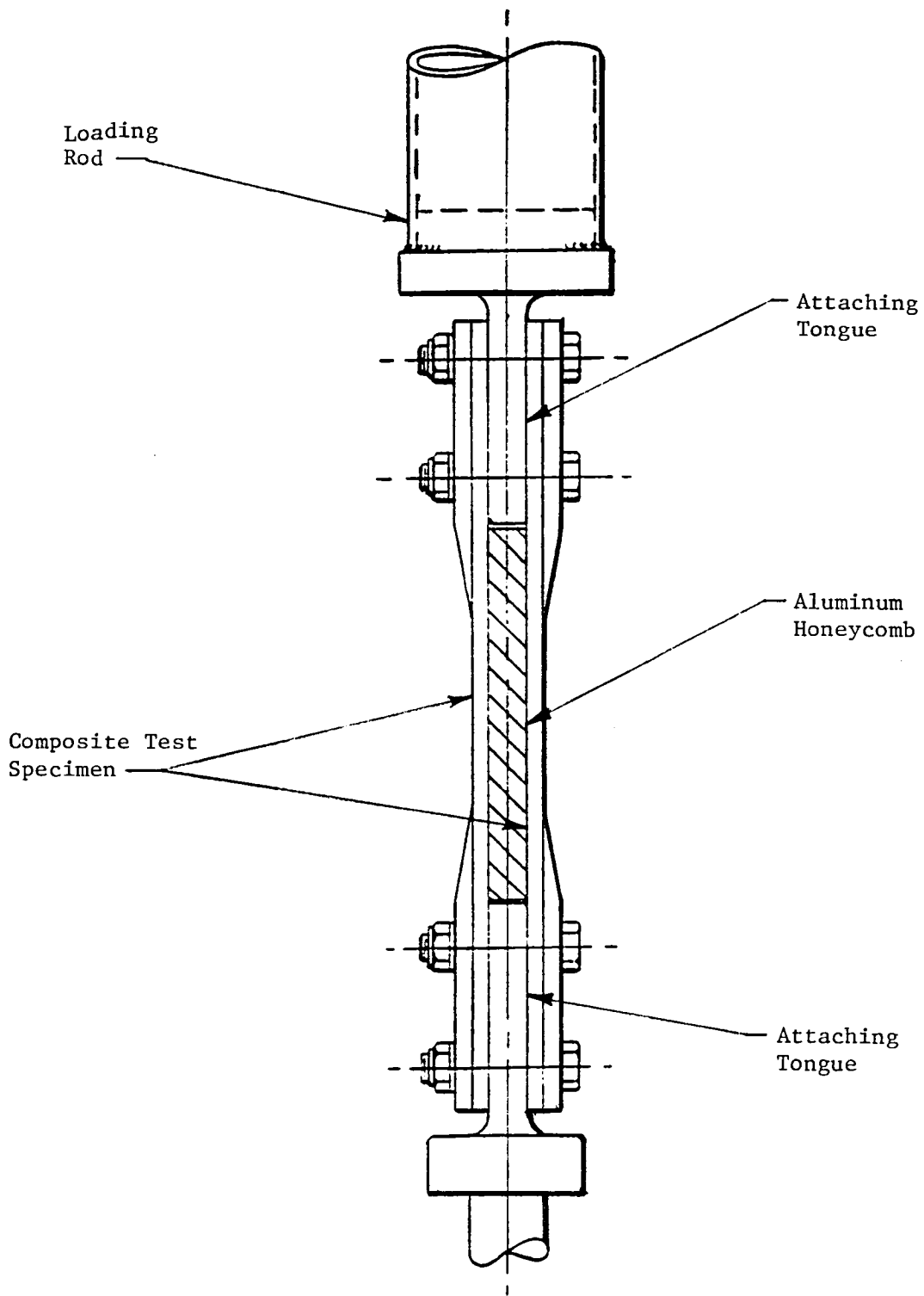


Figure II-3 Interim Test Specimen/Test Machine Interface

- 3) Trapped air within the honeycomb would be unacceptable during LH_2 testing resulting in the need for using a perforated honeycomb or having to punch holes through all of the honeycomb cells;
- 4) Having a double coupon, doubled the size of the load applied by the testing machine and increased the size of the supporting structure of the cryostat, resulting in a higher heat leak;
- 5) The width of the coupon, 3.56 cm (1.4 in.), and the fact that the specimens were off the centerline of the loading would create the potential for the stress in each side to be unequal, which was unacceptable.

Re-evaluation subsequently led to a simplified single laminate design to reduce fabrication and test problems. The resulting specimen configuration, shown in Figure II-4, consisted of a single laminate 0.51 cm (0.2 in.) thick supported by doublers at each end. The overall length of the specimen was reduced from 25.4 cm (10 in.) to 17.78 cm (7 in.) and the length of the gage section was reduced from 5.59 cm (2.2 in.) to 2.54 cm (1.0 in.) This change minimized buckling concerns during specimen compression and aligned the centerline of the coupon with the load line of the test machine. The four bolt attachment was maintained with the coupon tongue interfacing with a test fixture clevis at each end, as shown in Figure II-5. Since the overall gage section of the specimen was cut in half, the loading required from the test machine was reduced by the same magnitude.

The original material lay-up, shown in Figure II-2, was also re-evaluated and a new lay-up was designed for both the test specimens and trunnion configurations. The new lay-up is shown in Figure II-4 and has the following advantages over the old lay-up:

- 1) E-glass cloth on the outside avoided the possibility of 0° unidirectional ply peeling of the S-glass roving. This consideration was the driving factor to change the lay-up configuration;

SPECIMEN LAYUP									
-45	0°	+45°	0°	+45°	-45°	0°	+45°	0°	-45°
.023	.091	.023	.091	.023	.023	.091	.023	.091	.023
(.009)	(.036)	(.009)	(.036)	(.009)	(.009)	(.036)	(.009)	(.036)	(.009)

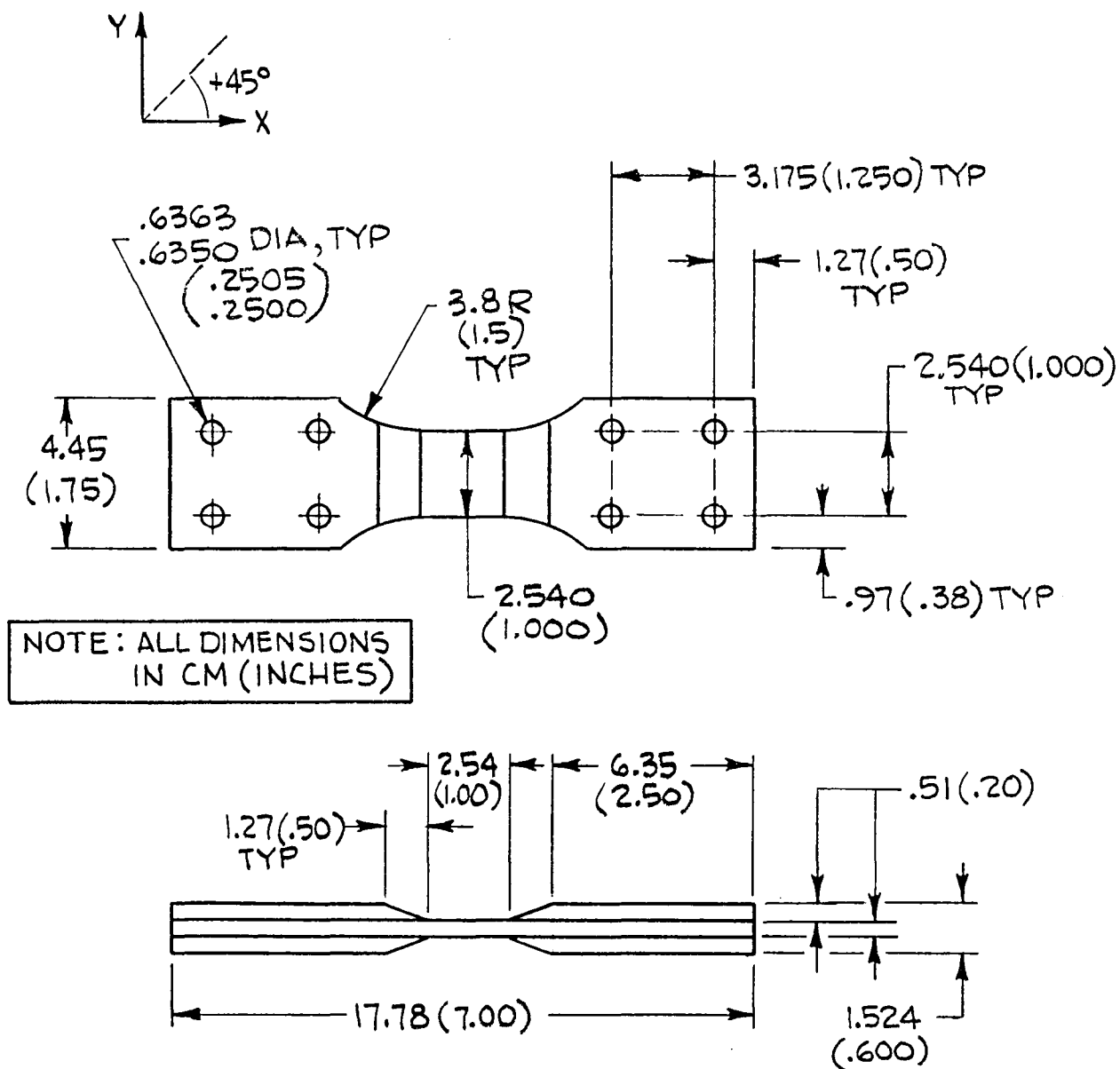


Figure II-4 Selected Laminate Test Specimen Configuration

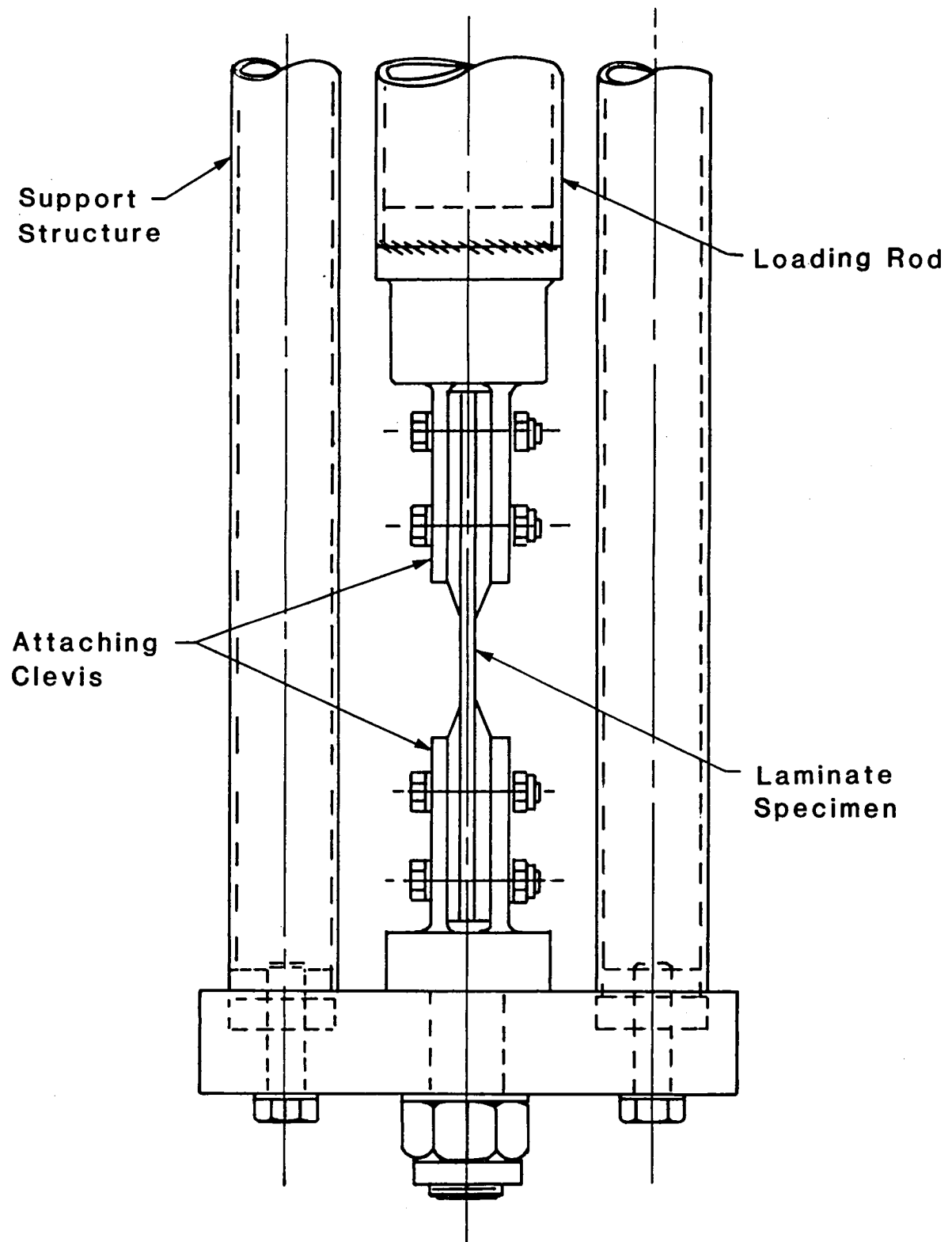


Figure II-5 Selected Laminate Test Specimen/Test Machine Interface

- 2) Extension-shear coupling and bending-twisting coupling was reduced by using orientations of -45° and $+45^{\circ}$ fabric plies (E-glass cloth) when compared to that offered by the original lay-up which used only $+45^{\circ}$ orientations.

Analysis of this new lay-up was performed using the SQ5 computer program; results indicated that the strength and in-plane elastic constants of the new lay-up were the same as the old. In both cases, the laminate thickness was 0.50 cm (0.198 in.).

The laminate test material consisted of multiple layers of S-glass roving and style 1581 E-glass cloth in a 934 epoxy resin system assembled in the configuration shown in Figure II-4. Laminate thickness after cure averaged 0.47 cm (0.185 in.), which was slightly under the expected 0.50 cm (0.20 in.). The fatigue test specimens were fabricated from one layer of laminate material, 0.47 cm (0.185 in.) thick, bonded to reinforcing tabs at each end (see Figure II-4). Reinforcing tabs were fabricated from E-glass cloth only to reduce manufacturing complexity. Tabs were bonded to the laminate along one face and beveled at approximately 20 degrees to provide for a gradual transfer of load from the tabs to the specimen gage section. End thickness was then machined to 1.62 cm (0.60 in.) to provide a tight fit in the test fixture clevis. Holes were matched drilled to provide for proper bolting to the clevis.

B. Definition of Test Philosophy

A close look was taken at the test philosophy of the specimen fatigue tests, the object of the testing and the data expected from Task I testing. How the results of these tests would be used were also considered.

The inherent fact that the laminate was composed of two materials (S-glass roving in the 0° plies, and E-glass cloth in the 45° plies) with greatly varying stiffnesses posed the problem of how a failure of the laminate could be detected. A review of the trunnion stress analysis (Ref 5) showed that the calculations were all based on an assumed laminate ultimate strength of 334,650 kN/m² (48,500 psi) when in fact this number more closely represented the ultimate strength of just the 45° E-glass cloth (as shown by

the knee in the curve in Figure II-6). The ultimate strength of the overall laminate was analytically determined by the SQ5 program to be on the order of $1,104,000 \text{ kN/m}^2$ (160,000 psi) after failure of all 45° plies (1/3 of the laminate), as shown in Figure II-6. The object of the testing therefore was to determine, if possible, the loading and cycling values which would indicate a failure of the 45° E-glass cloth. This failure, however, was not visually observable and could only be obtained through proper test instrumentation (strain gage and deflection readings). The effect of this failure mode on the overall laminate stiffness was also required for material property evaluation.

Four laminate specimen static tension tests at ambient temperature were defined to determine if failure of the 45° E-glass cloth could be detected. These static test specimens were identical to those proposed for the fatigue tests (see Figure II-4). The four specimens were instrumented with strain gages to obtain the stress/strain curve for the specimens (a decrease in slope represents a decrease in specimen stiffness or a decrease in longitudinal elastic modulus). Figure II-6 shows the stress/strain diagram generated by the SQ5 Computer program for the CFMF trunnion laminate. Data collected from these tests was used to try to verify this curve and the ability of the test instrumentation to determine the location of the "knee" on the stress/strain curve. This point denotes a decrease in the elastic modulus of the laminate due to a failure of the 45° E-glass plies. The ultimate strength of the laminate was also determined from these tests.

Failure of the fatigue specimen (for the purpose of this program) was defined as the cycle at which a 10% increase from the initial deflection of the specimen occurred if in fact such a change took place before catastrophic failure of the entire laminate. The loading conditions for both the ambient and LH_2 fatigue tests were determined from the data collected from the three tension tests and were identified as a percentage (100%, 80%, 60% and 40%) of the loading required to fail the 45° E-glass cloth in the laminate. A cycle limit of 1,000 cycles, 5,000 cycles, 20,000 cycles, and 40,000 cycles respectively, was established as the point at which the test would be terminated should no failure occur. A representative S/N curve for the laminate was generated for this load distribution.

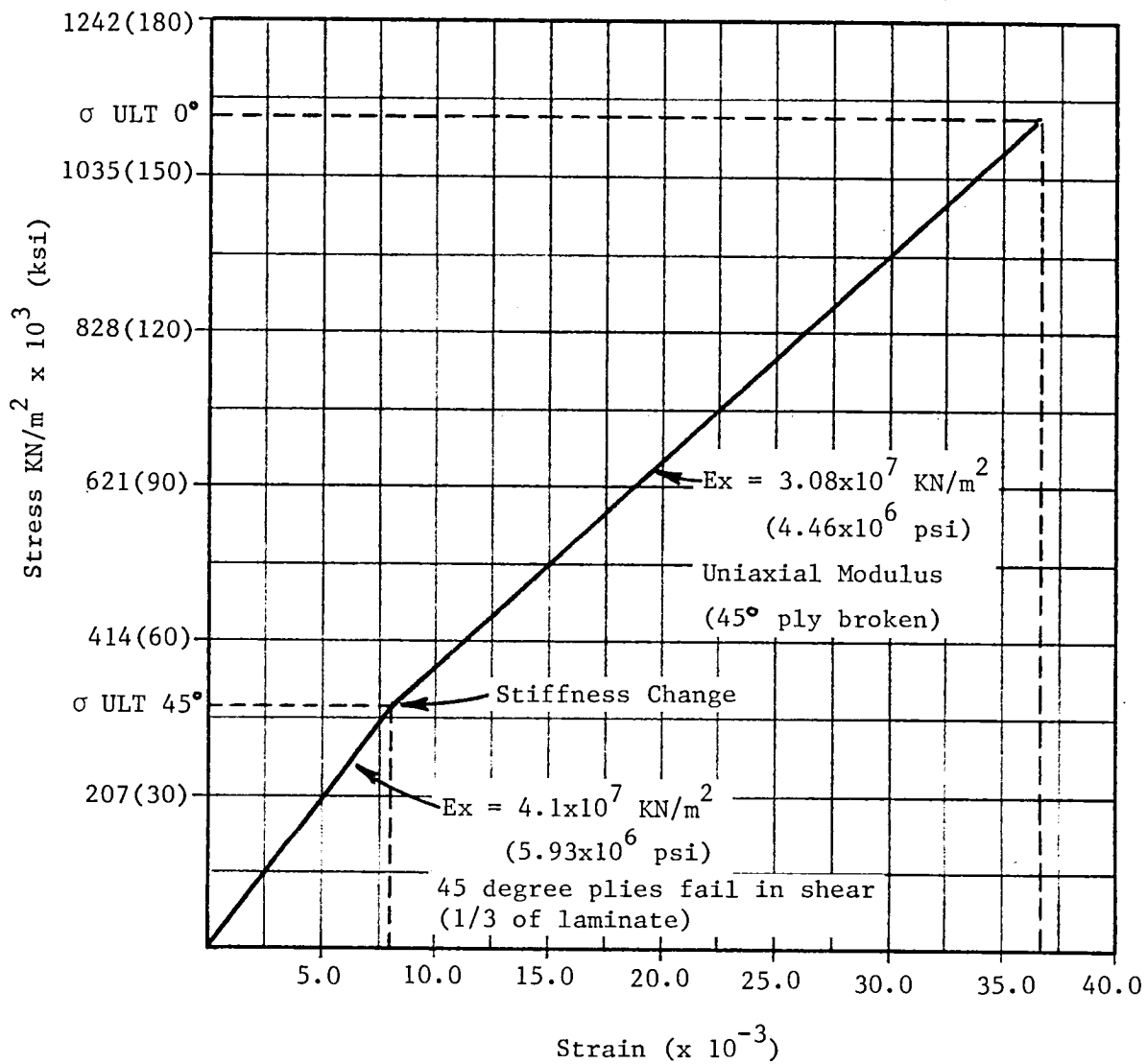


Figure II-6 X-Direction Stress/Strain Diagram for CFME Laminate

C. Static Tension Test Results

Four static tension tests were conducted to determine 45° E-glass cloth failure. One test was conducted to determine ultimate failure of the laminate. Results of these tests are presented in Table II-1.

Table II-1 Laminate Static Data

<u>Specimen Number</u>	<u>Load at First Indication of Failure</u>		<u>Actual Stress</u>	
	N	(lb)	kN/m ²	(psi)
1	64,525	(14,500)	567,420	(82,235)
2	53,400	(12,000)	483,510	(70,074)
3	54,512	(12,250)	480,240	(69,600)
4*	149,520	(33,600)	1,324,800	(192,000)

* Ultimate failure test

The specimens had strain gages installed for specimen alignment and data collection. Figure II-7 shows the load/strain curve for specimen number 4. This test consisted of two specimen loadings; the first loading resulted in a discontinuity at 53,400 N (12,000 lb) after which the load was decreased to zero; the second loading also resulted in a discontinuity between 53,400 N (12,000 lb) and 55,625 N (12,500 lb), another at 73,425 N (16,500 lb) and specimen failure at 149,520 N (33,600 lb). The strain gage failed at 93,450 N (21,000 lb).

Specimens number 2 and 3 were dye penetrant inspected and x-rayed. Results of this inspection revealed no evidence of E-glass cloth failure but did show a crack which was propagated from the gage section into the doubler where the radius of the doubler meets the gage section. It was believed that this damage was the result of a stress concentration in this area due to the specimen design and not due to actual failure in the 45° E-glass material.

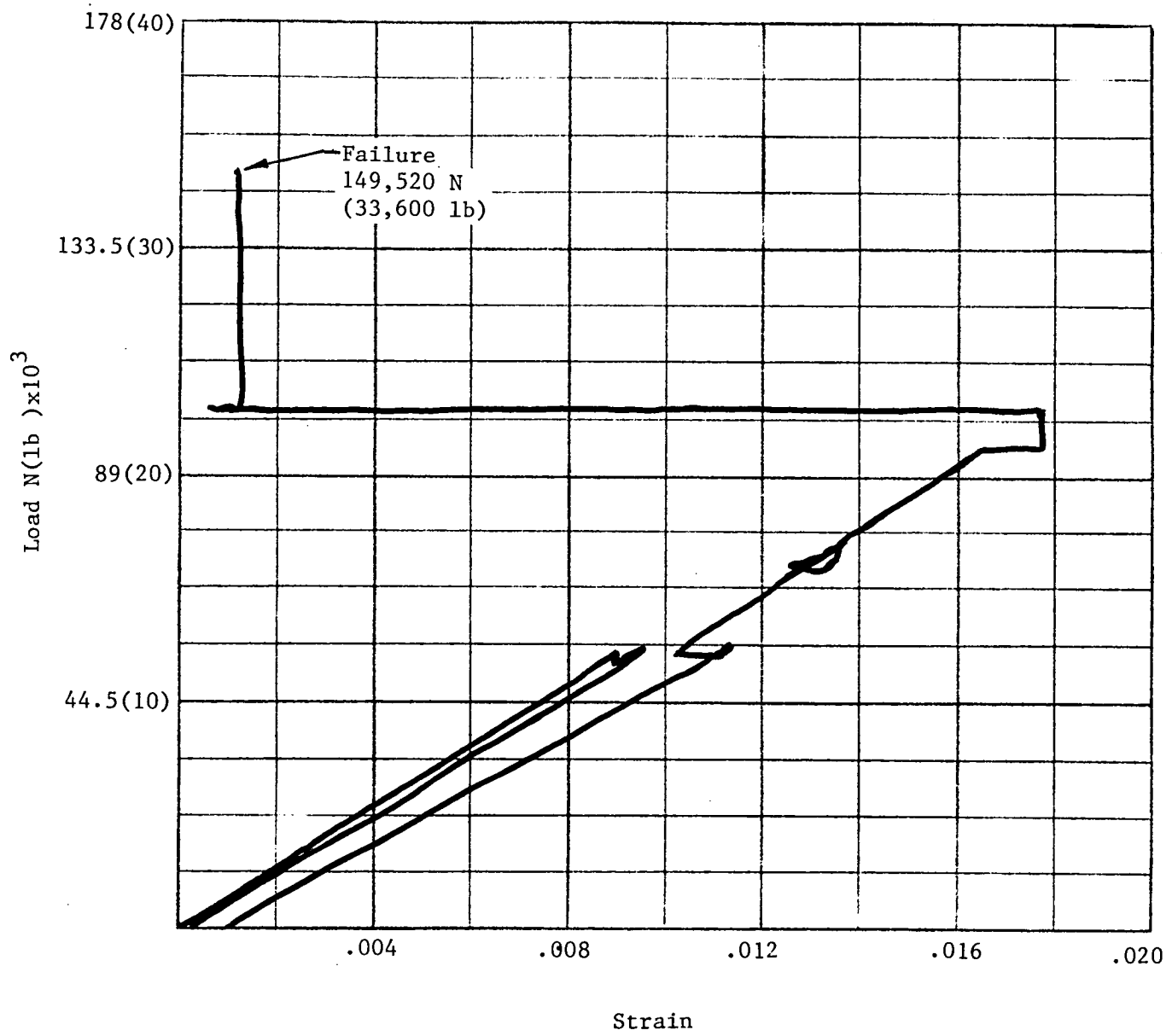


Figure II-7 Laminate Load/Strain Curve

The expected change in slope of the stress/strain curve due to the decreasing longitudinal elastic modulus of the specimen did not occur. The lowest of the three loads, 53,400 N (12,000 lb), where discontinuity of the stress/strain curve appeared, was selected as an arbitrary "failure" point. This point became the base line for the 100%, 80%, 60% and 40% loading conditions for the ambient temperature fatigue tests. This compares to the 40,940 N (9,200 lb) used in the original CFME trunnion analysis and is 30% greater. The actual tested stress value at this so-called "failure" point was $483,000 \text{ kN/m}^2$ (70,000 psi) compared to the $317,400 \text{ kN/m}^2$ (46,000 psi) used in the analysis. These preliminary results indicated a much stronger laminate than originally predicted.

D. Fatigue Test Description

Figure II-8 shows the composite tension-compression test specimen bolted in four places at each end through the test fixture attaching clevis. The lower clevis was rigidly attached to the bottom of the fixture while the top clevis was an extension of the load-bearing rod. A guide attached to the three structural supports provided for true positioning and alignment of the specimen with the load. The assembled test fixture is shown in Figure II-9; it consisted of a MTS servohydraulic testing machine with the load cylinder mounted at the top of the unit. The load cell was flange bolted to the fixture load-bearing rod which passed through the lid of the cryostat. A flexible rubber bellows sealed the loading rod to the lid and prevented hydrogen from escaping during cryogenic use.

The first test series was conducted in air at ambient temperature using the cryostat fixture without the cryogenic reservoir. Figure II-9 shows the test setup configured for these tests. The second test series was conducted with the specimen immersed in LH_2 . Figures II-10 and II-11 show the assembled test fixture with the cryostat reservoir installed.

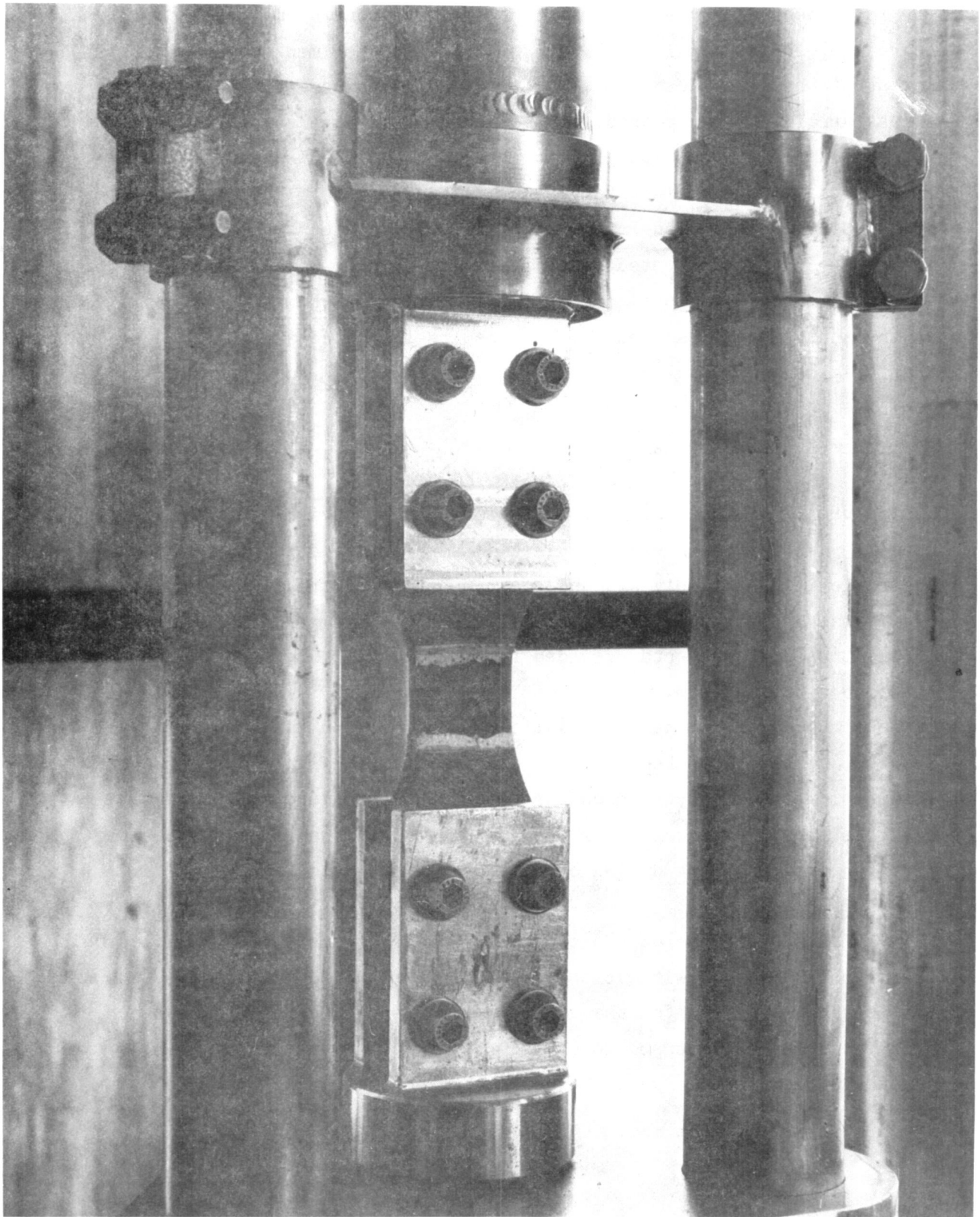


Figure II-8 Test Specimen/Test Machine Installation

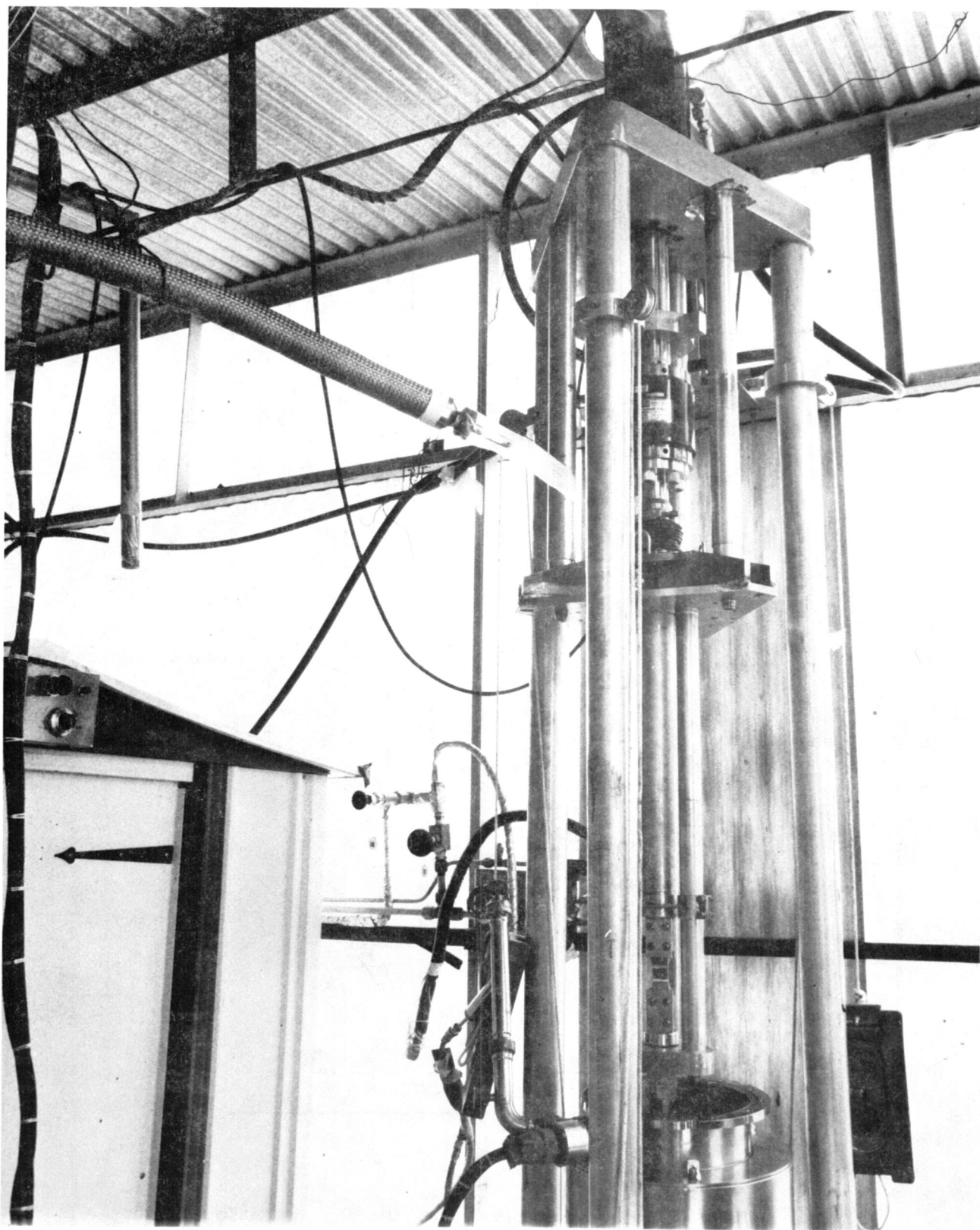


Figure II-9 Specimen Fatigue Test System

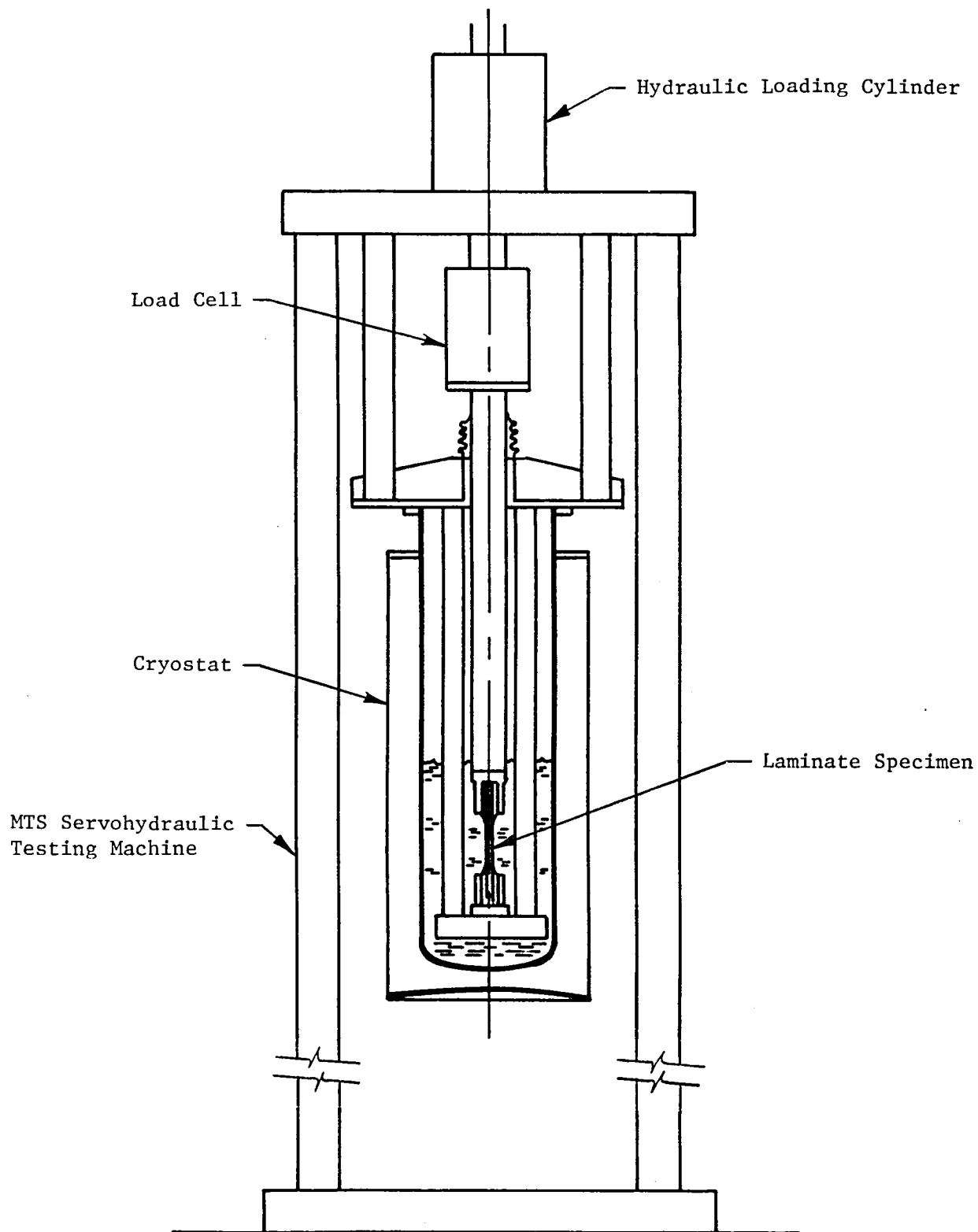


Figure II-10 Assembled Test Fixture Configuration

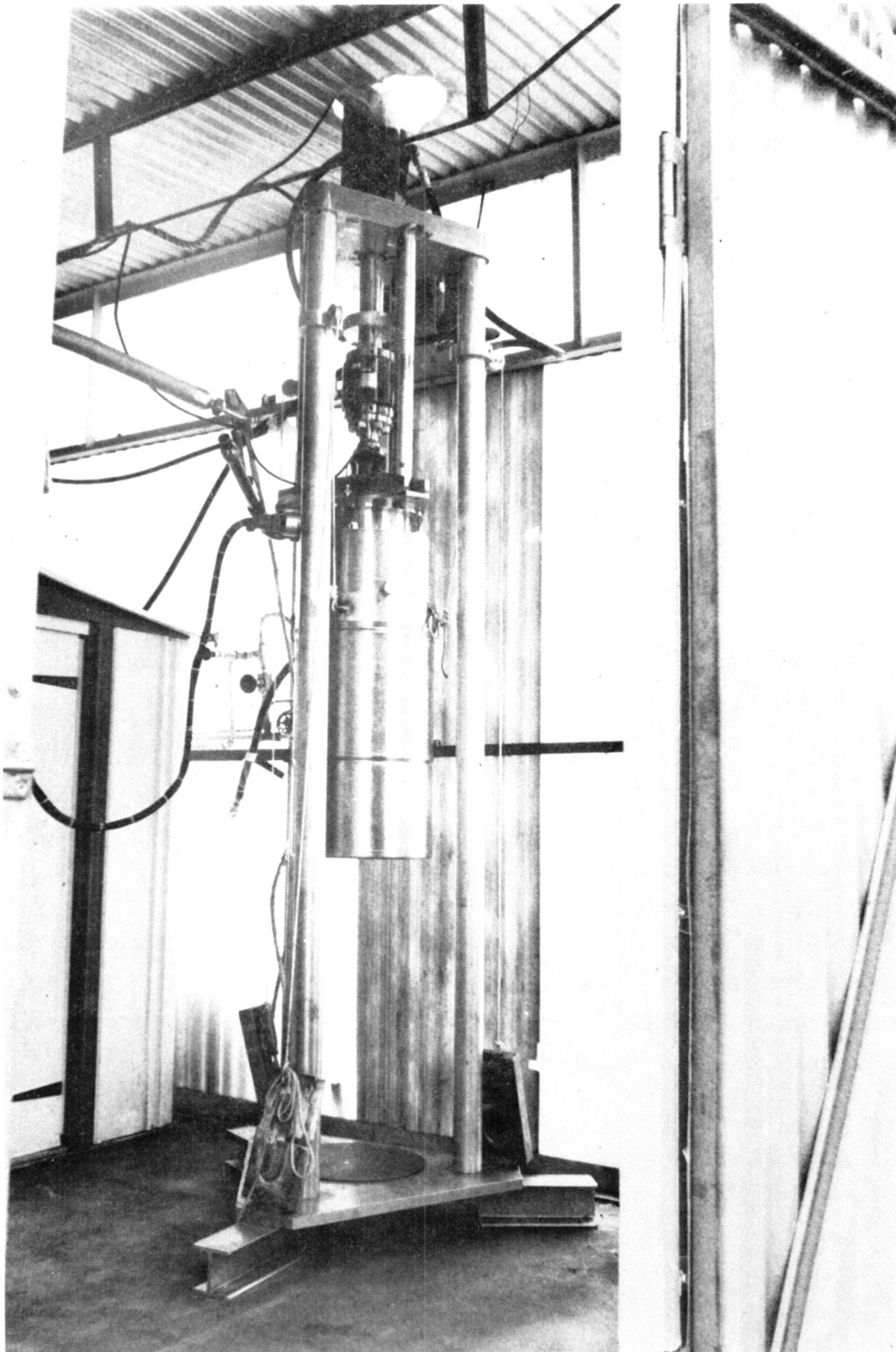


Figure II-11 Specimen Fatigue Test Setup with Cryostat Installed

Specimen loading values are shown in Table II-2 and are the same for both ambient and cryogenic conditions. The values are listed as a percentage of the base line value of 53,400 N (12,000 lb) which was determined from static tension test results. Average specimen stress for the given loading conditions are also given.

Table II-2 Fatigue Test Specimen Loading Conditions (R = -1)

Loading Amplitude		Stress Amplitude		Percentage of
<u>N</u>	<u>(lb)</u>	<u>kN/m²</u>	<u>(psi)</u>	<u>maximum loading</u>
53,400	(12,000)	448,500	(65,000)	100
42,720	(9,600)	358,800	(52,000)	80
32,040	(7,200)	269,100	(39,000)	60
21,360	(4,800)	179,400	(26,000)	40

Deformation of the test specimen is proportional to the longitudinal stiffness of the specimen. By monitoring the deflection of the specimen and observing any change, the rate of stiffness degradation (or damage caused by fatigue) could be observed.

E. Ambient Temperature Fatigue Test Results

Results of the ambient temperature fatigue tests are presented in Table II-3. Specimens were tested at 100%, 80%, 60% and 40% of the 53,400 N (12,000 lb) baseline which generated specimen failures over a range of stress suitable for the generation of the desired S/N curve.

Table II-3 Ambient Temperature Fatigue Test Results (R = -1)

<u>Specimen Number</u>	<u>Loading Amplitude N (lb)</u>	<u>Stress Amplitude kN/m² (psi)</u>	<u>Cycles to Failure</u>	<u>Maximum Cycle Test Limit*</u>
R-3	53,400 (12,000)	448,500 (65,000)	128	1,000
R-5	42,720 (9,600)	359,490 (52,100)	1,878	5,000
R-2	42,720 (9,600)	358,800 (52,000)	1,938	5,000
R-7	32,040 (7,200)	278,070 (40,300)	8,800	20,000
R-8	32,040 (7,200)	264,960 (38,400)	12,200	20,000
R-4	21,360 (4,800)	182,850 (26,500)	66,000+	40,000
R-9	21,360 (4,800)	180,090 (26,100)	40,000+	40,000

* Test to be terminated if no failure occurs.

The two specimens tested at the 40% level, 21,360 N (4,800 lb), survived 40,000 cycles as specified in the test plan while all of the other specimens failed before the specified maximum cycle test limit was reached. In an attempt to achieve failure at the 40% level, one of the two specimens was cycled to failure, which occurred at 66,000 cycles. This failure occurred at the bolt holes and was attributed to the specimen design. Therefore, this was not considered a valid data point; failure of the gage section would have occurred at a higher cycle level. The second 40% specimen (R-9) which survived 40,000 cycles was re-installed into the test setup and cycled under 80% load 42,720 N (9,600 lb) in an attempt to calculate a damage factor which was assumed to be cumulative in a linear fashion. At the 80% level, this specimen failed at 1076 cycles. Failure was again attributed to the specimen design since failure did not occur in the gage section. However, using this data and the linear damage rule resulted in the following:

$$\frac{1076 \text{ cycles}}{1900 \text{ cycles}} + \frac{40,000}{X} = 1.0$$

X = 92,166 cycles to failure for the 40% level where 1900 is the approximate number of cycles to failure for the two 80% specimens, R-2 and R-5

Figure II-12 shows the ambient temperature S/N curve obtained from the data of Table II-3. Also shown for comparison is the analytical curve used in the original CFME Trunnion design analysis (Ref 1).

It should be noted that the original concept for failure of the laminate was to detect 45° ply failure of the E-glass cloth by monitoring specimen deflection. When the deflection increased by 10%, failure (for the purposes of this test) would have occurred in accordance with the definition stated. Figure II-13 shows the recorded deflection for five of the seven ambient temperature specimens. Deflections for the two 40% level tests did not indicate any change in deflection for the first 40,000 cycles. The frequency of loading was increased from 2 Hz to 4 Hz. The capability of the recorders was exceeded and no deflection data were obtained. Also shown on Figure II-13 is the deflection of specimen R-9 over the last 1076 cycles at 42,720 N (9,600 lb) which followed the first 40,000 cycles at 21,360 N (4,800 lb).

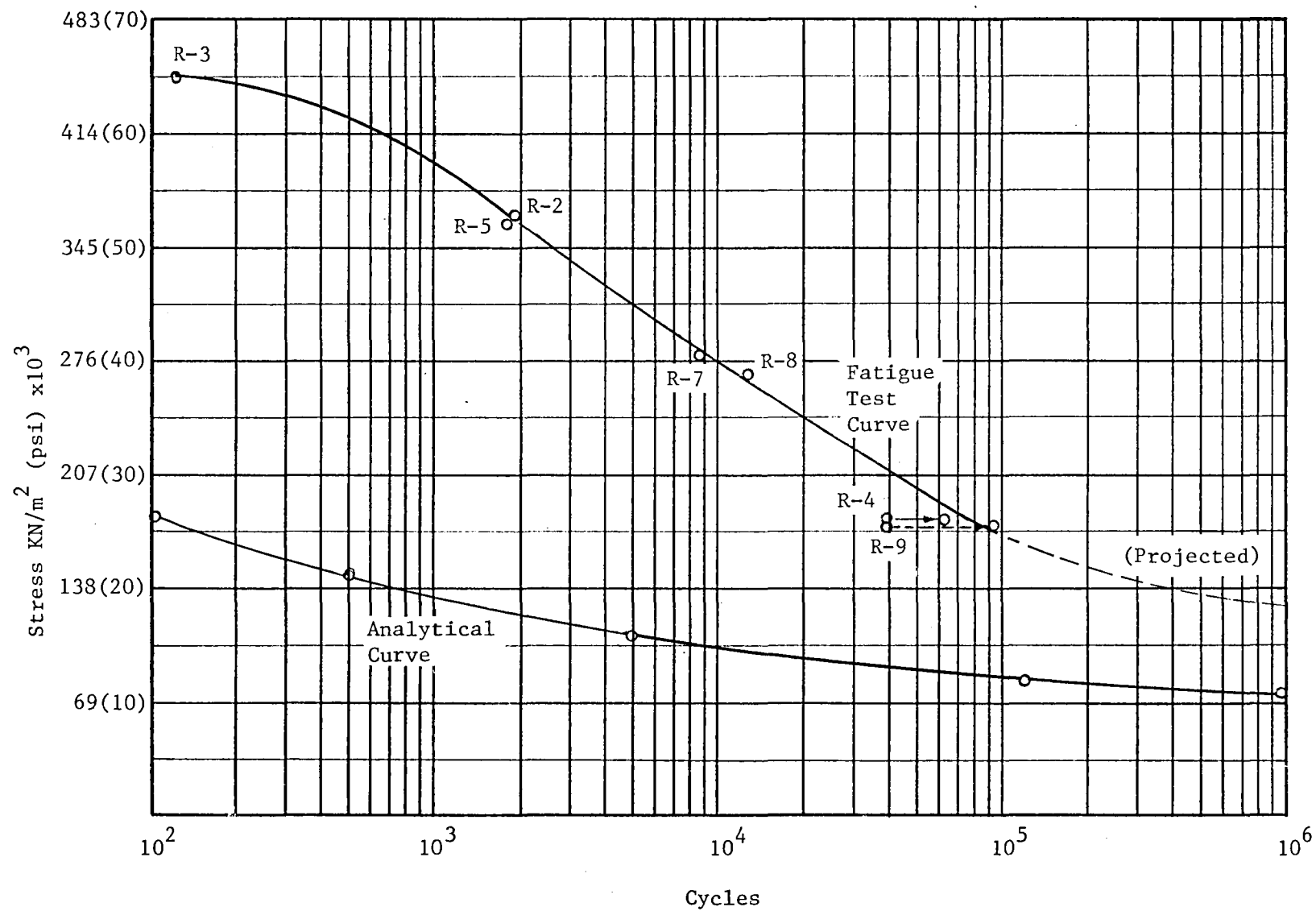


Figure II-12 CFME Trunnion Laminate S/N Curve
for Ambient Temperature

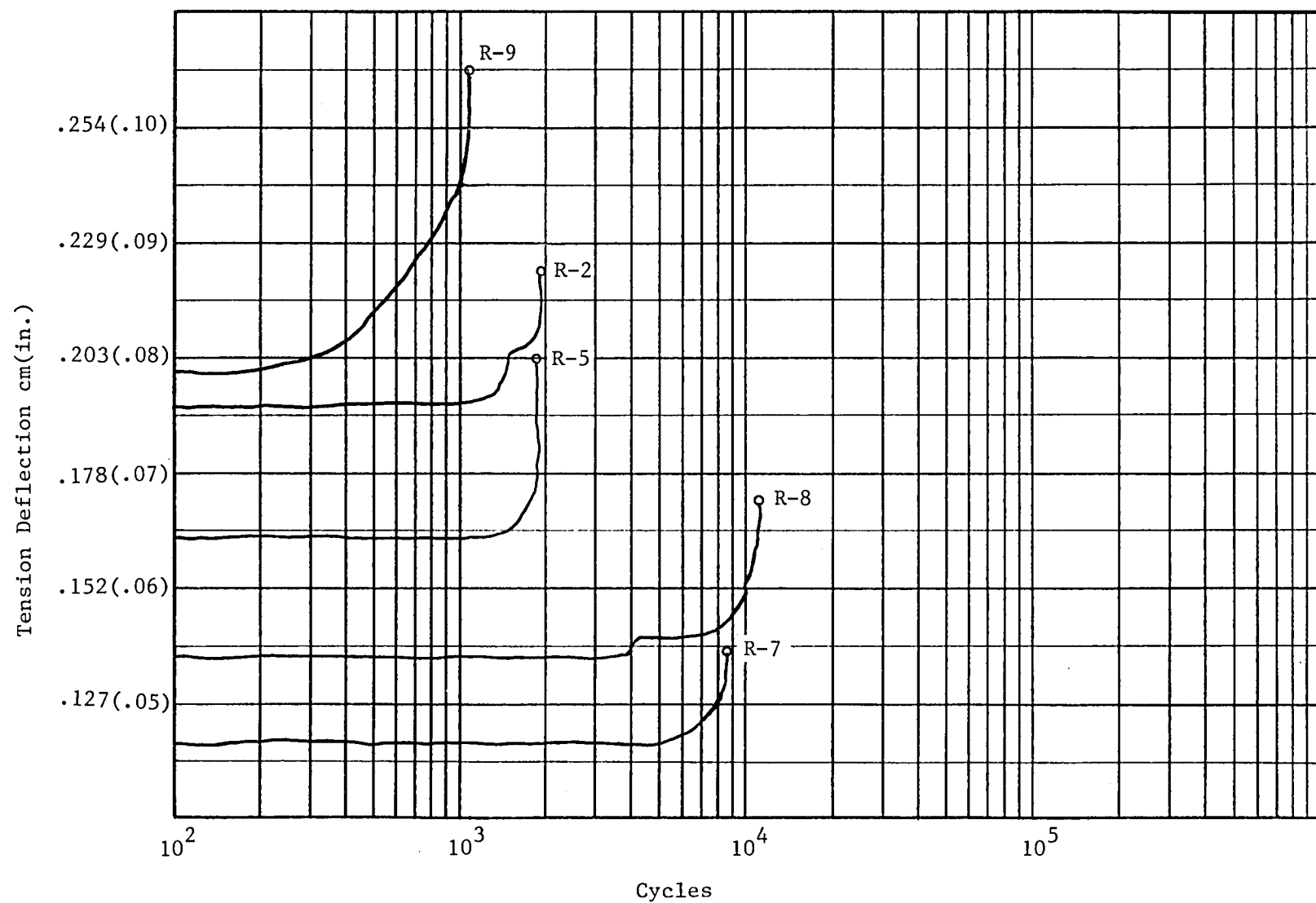


Figure II-13 Ambient Temperature Laminate Specimen
Test Deflection Data

Failures listed in Table II-3 and the resulting S/N curve generated from the data (Figure II-12) consisted of catastrophic yielding of the entire laminate to the imposed loading condition. Deflections were analyzed to determine the points at which the deflection started to increase. Figure II-14 shows the ambient temperature S/N curve for the laminate, as well as a lower bound curve generated by selecting the points where deflection started to increase. This lower bound curve can be termed "first indication of laminate stiffness degradation". The area between the two curves is characterized by a rapid loss in specimen stiffness until catastrophic failure occurs at the upper limit. In all cases, a 10% increase in deflection almost corresponds to catastrophic failure of the specimen.

The deflection was composed of the following components:

- 1) Test fixture deflection;
- 2) Specimen deflection;
- 3) Specimen movement in the fixture.

Test fixture deflection was a near constant component, as was the specimen movement in the test fixture clevis. The main component, however was due to the specimen deflection which was a direct result of the load applied and the specimen configuration. The specimen configuration, or design, contributed to the overall deflection results obtained from the testing by inducing stress concentrations in the transition section and at the bolt hole locations. It is difficult to speculate whether stiffness degradation (deflection increase) was a result of failure in the laminate or due to specimen design. The end result, however, lies in the S/N curve generated from the catastrophic yielding of the laminate regardless of how the failure was induced. Deflection data indicate that the stiffness of the laminate was maintained throughout the major portion of the fatigue cycling, as shown in Figure II-14. A typical failed ambient test specimen is shown in Figure II-15.

F. Liquid Hydrogen Temperature Fatigue Test Results

Results of the LH₂ temperature fatigue tests are presented in Table II-4. Specimens were tested at the same 100%, 80%, 60%, and 40% levels of the baseline 12,000 lb load used for the ambient temperature tests.

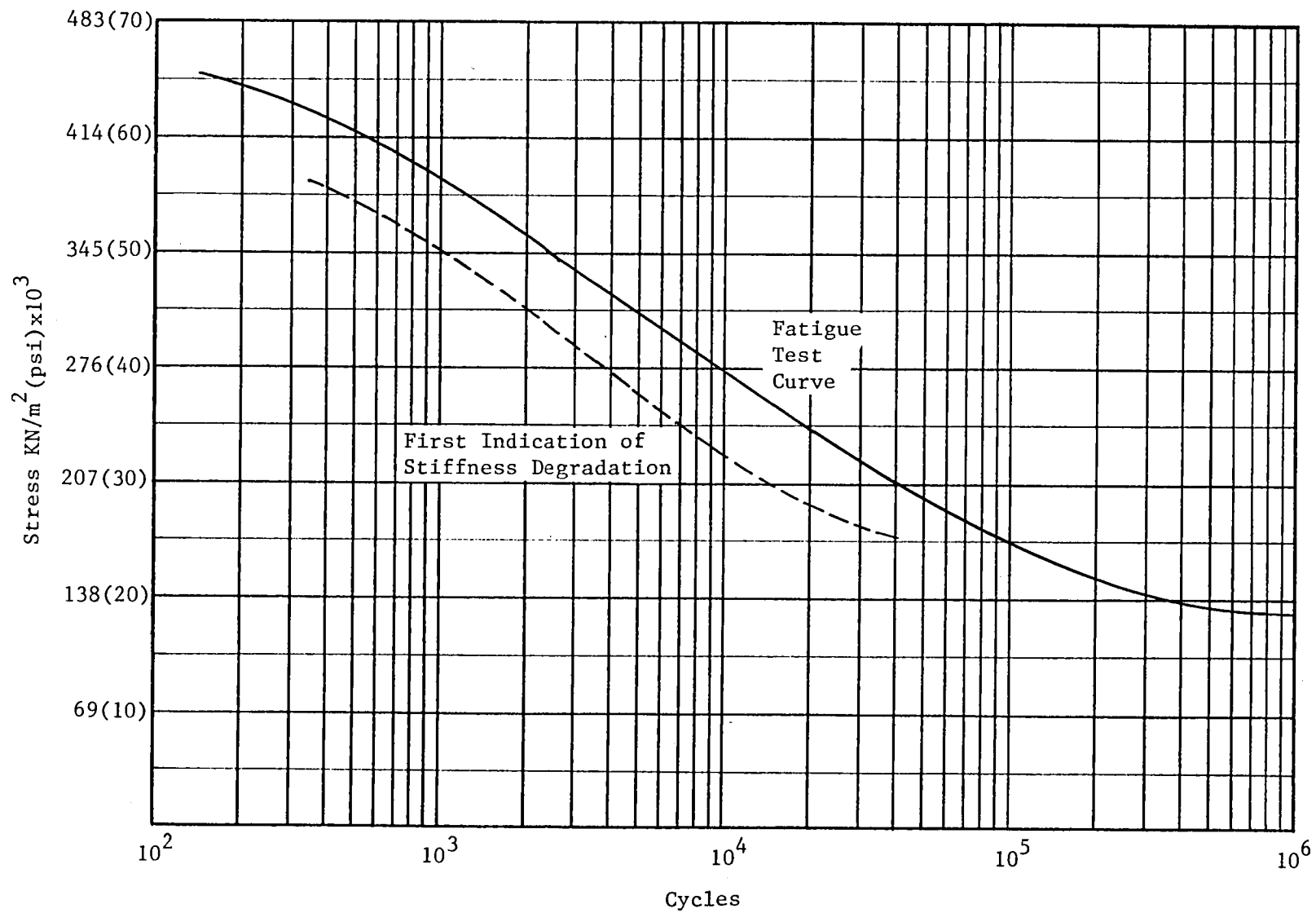
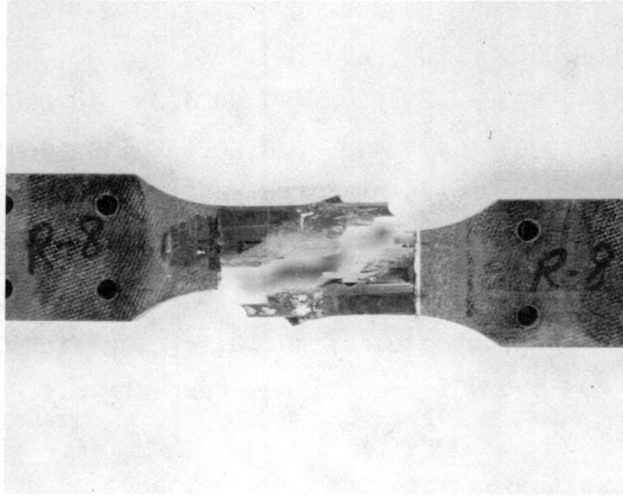
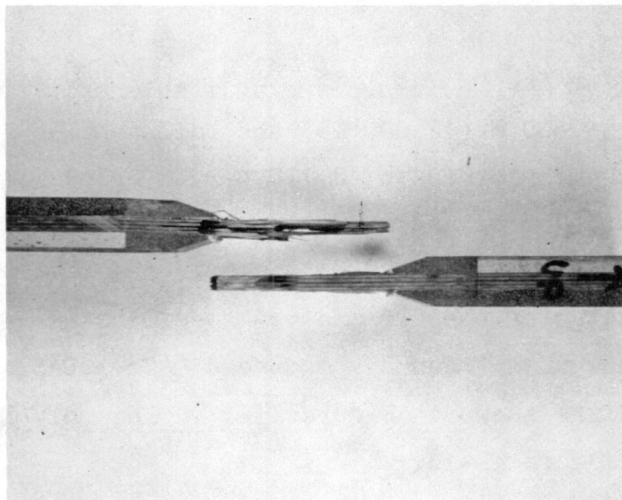


Figure II-14 CFME Trunnion Laminate Stiffness Degradation



Top View



Side View

Figure II-15 Failed Ambient Test Specimen R-8

Table II-4 Liquid Hydrogen Temperature Fatigue Test Results (R = -1)

<u>Specimen Number</u>	<u>Loading Amplitude</u>		<u>Stress Amplitude</u>		<u>Cycles to Failure</u>	<u>Loading Condition</u>
	<u>N</u>	<u>(lb)</u>	<u>kN/m²</u>	<u>(psi)</u>		
H-1	32,040	(7,200)	285,660	(41,400)	40,000*	60%
H-3	42,720	(9,600)	351,900	(51,000)	8,000*	80%
H-4	21,360	(4,800)	179,400	(26,000)	100,000*	40%
H-5	53,400	(12,000)	442,980	(64,200)	581	100%

* Test stopped with no failure when cycle limit was reached.

Limits were increased to 8,000 cycles, 40,000 cycles and 100,000 cycles for the 80%, 60% and 40% conditions, respectively.

Figure II-16 shows the ambient temperature specimen data S/N curve and the LH₂ data plotted for comparison. A projected cryogenic temperature S/N curve is also shown and represents the lower limit of the available data.

Deflection data for the LH₂ tests are available only for specimen (H-5), which was loaded to 53,400 N (12,000 lb) and failed at 581 cycles, and for specimen (H-3), which was loaded to 42,720 N (9,600 lb) with no failure after 8,000 cycles. Again, the failure at 581 cycles occurred at the bolt holes rather than the gage section and was thus considered to be a conservative data point. Deflection data for the 40% and 60% specimens were not documented due to recorder limitations when frequency exceeded 2 Hz. Deflection data for specimen H-3 and H-5 are shown in Figure II-17. The only LH₂ test specimen to fail is shown in Figure II-18.

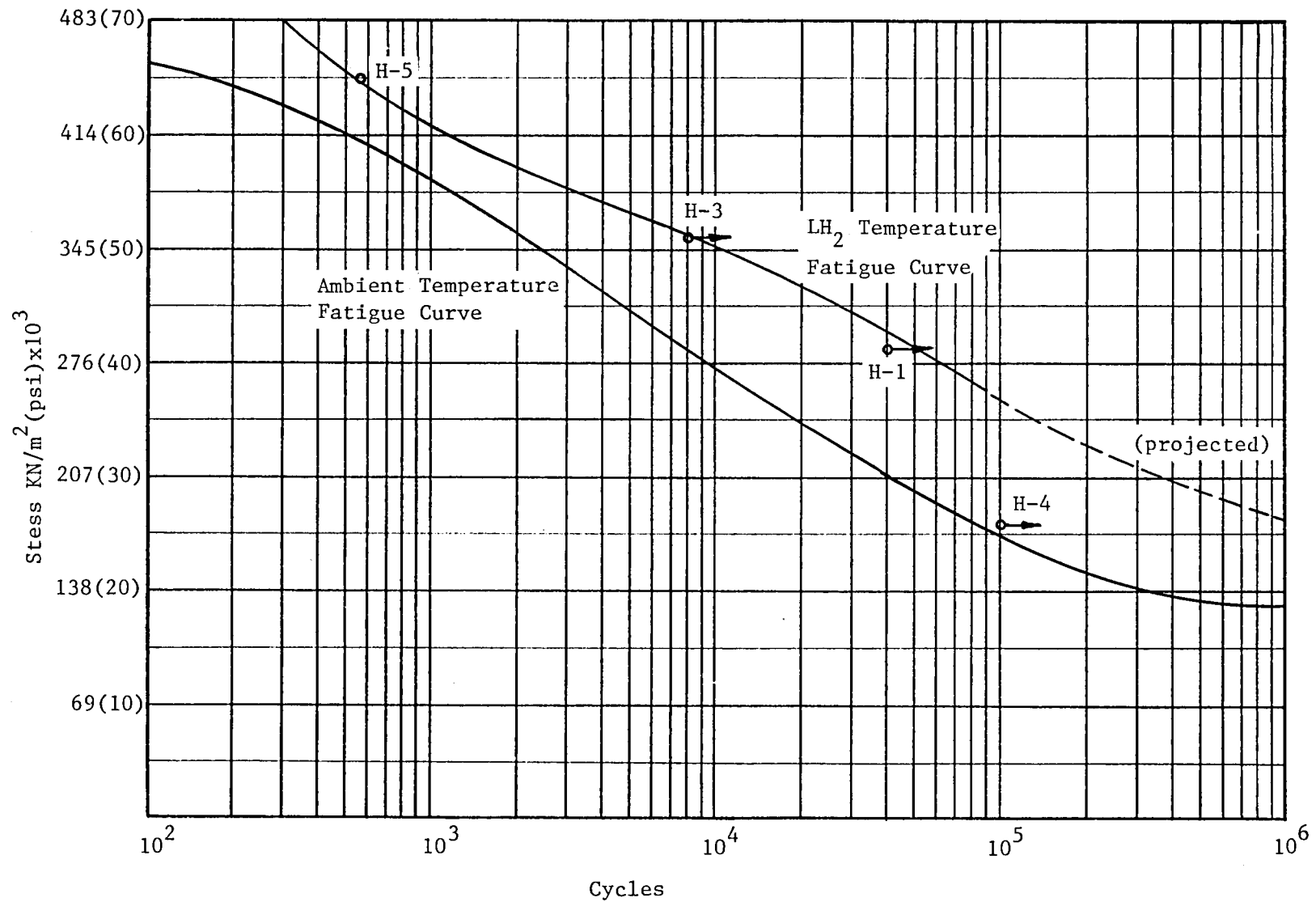


Figure II-16 CFME Trunnion Laminate LH₂
Temperature S/N Curve

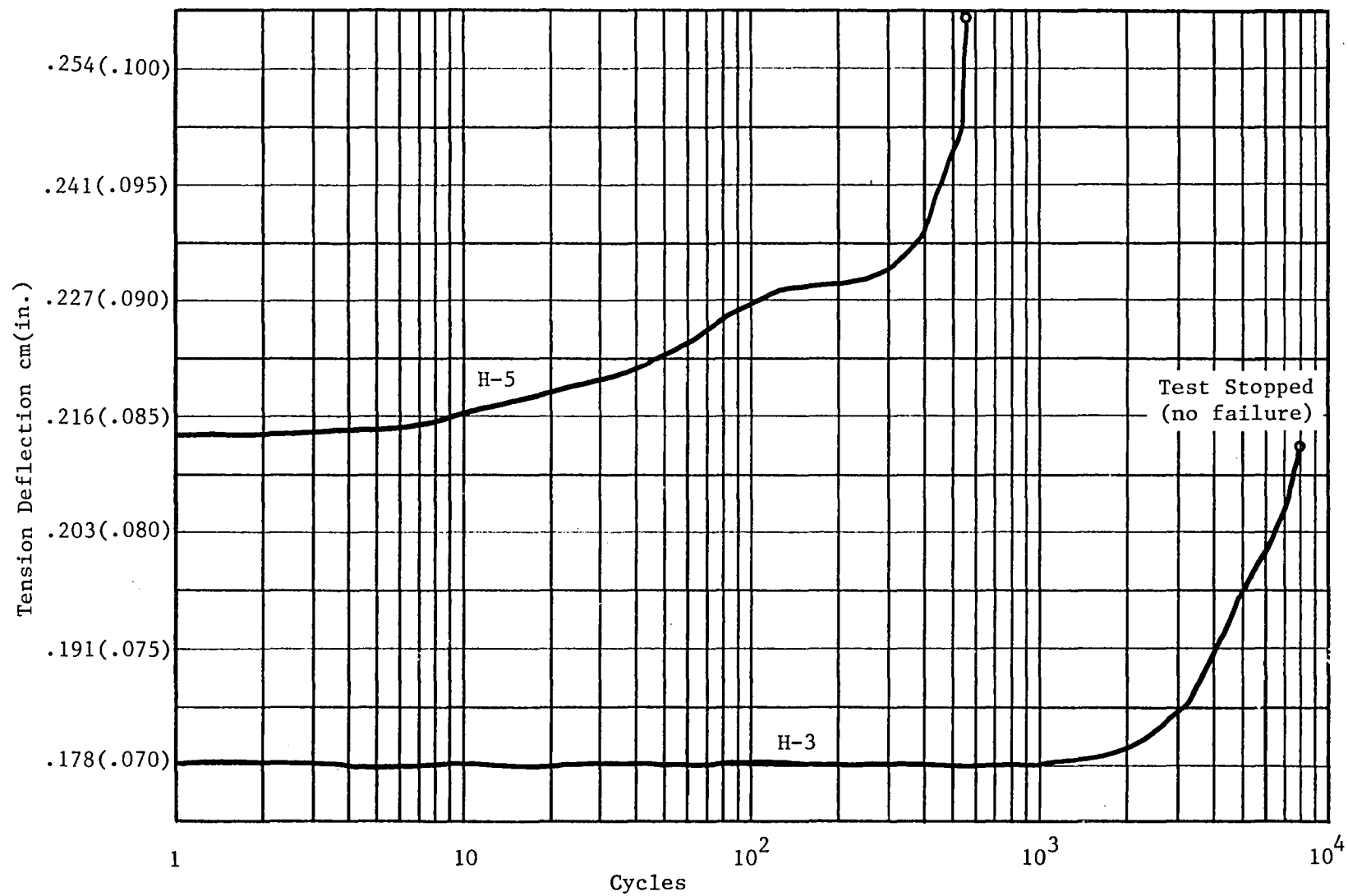
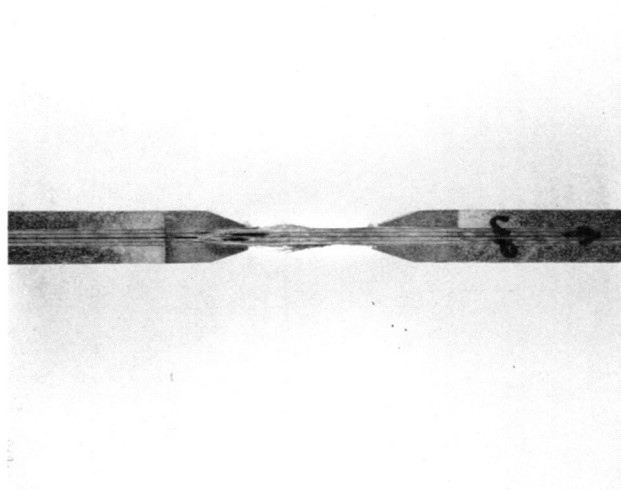


Figure II-17 CFME Trunnion Laminate Deflection at
LH₂ Temperature



Top View



Side View

Figure II-18 Failed LH_2 Test Specimen H-5

III. CFME TRUNNION DESIGN ASSESSMENT (Task II)

All Task I data indicate that the CFME trunnion laminate is significantly stiffer (and stronger) than suggested from the properties used during the original analysis. Stiffness increases as the laminate temperature decreases and the maximum cycle test limits for three of the four cryo-loading conditions were reached before failure occurred. Ambient temperature fatigue tests showed significantly increased cycle life beyond that indicated by the original analytical S/N curve.

Results obtained from specimens with thickness variations from 0.48-cm (0.190-in.) to 0.45-cm (0.178-in.) indicated that the original 0.51-cm (0.2-in.) nominal laminate thickness material was not compromised from a stiffness standpoint by being somewhat thinner than expected. In fact, it was expected that the reduced thickness (a result of resin flow during cure) would result in a reduction in thermal conductivity of the completed trunnion without sacrificing any load carrying capability.

One of the concerns resulting from the original CFME trunnion fatigue analysis was the high cumulative damage factor of 0.813 calculated for seven missions using a scatter factor of four on the number of fatigue cycles. This value was derived using laminate properties that were much lower than those obtained by Task I fatigue tests. Analysis of CFME trunnion cumulative damage factor based on Task I test data resulted in a damage of less than 0.1. This factor is much less than the 0.35 damage factor calculated for the pressure vessel and vacuum jacket. Based on these results, the trunnion is a low criticality item in the CFME liquid hydrogen supply tank. Results from Task I fatigue testing indicate that the trunnion laminate longitudinal S/N curve compares favorably with S/N curves for stainless steel and aluminum (see Figure III-1).

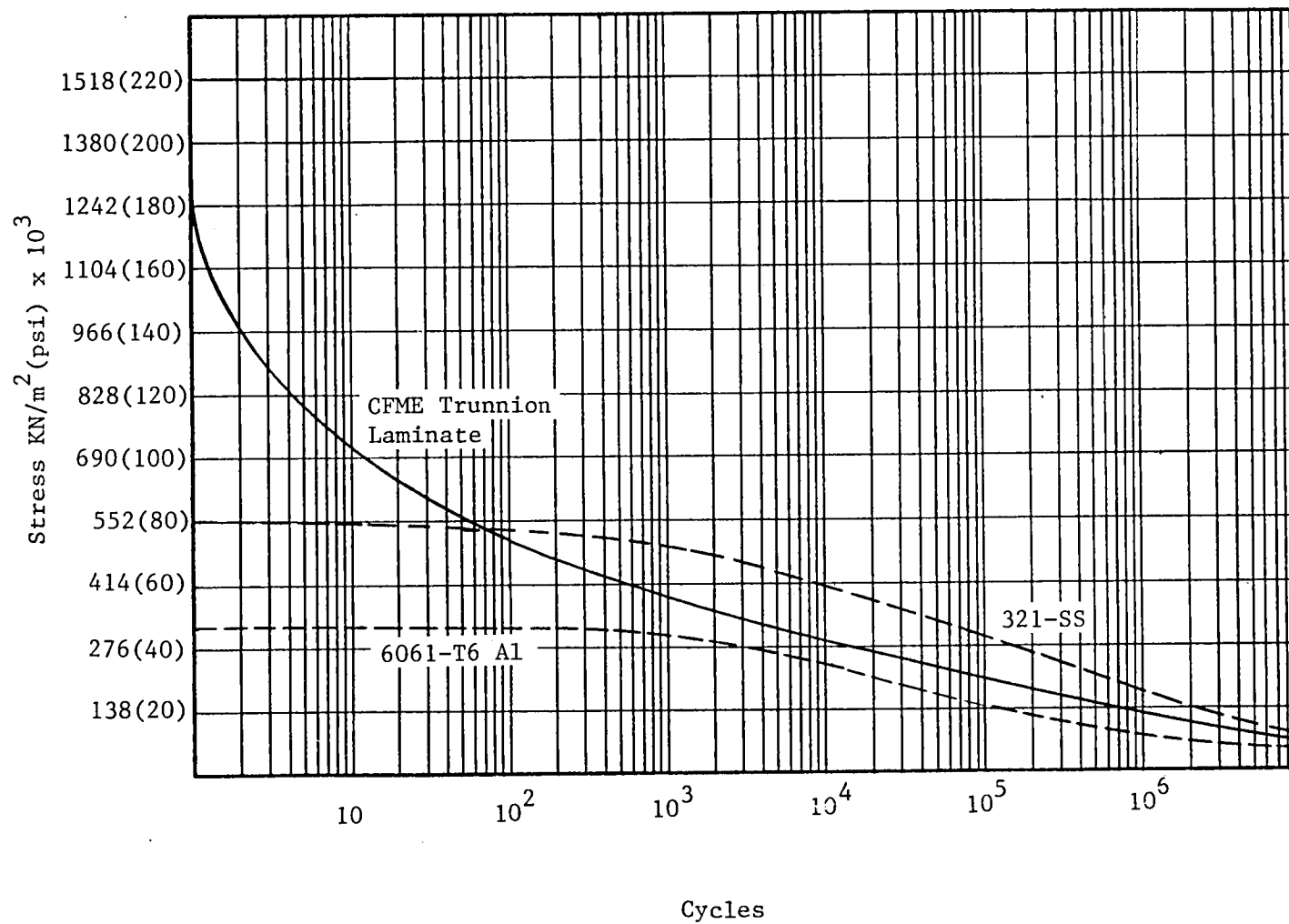


Figure III-1 CFME Trunnion Laminate S/N Curve
Comparison with 321 SS and 6061-T6 Al

A. Stress and Dynamic Analysis

The trunnions were designed based on load factors defined during the CFME design (Ref 4). The design limit load factors (DLLF) are a combination of quasi-static load factors (LF_{QS}) and random load factors (LF_R), as delineated in Table III-1.

Table III-1 - Design Load Factors

Axis	LF_{QS}	LF_R^*	DLLF
X_O	$\pm 4.3g$	$\pm 9.4g$	$\pm 13.7g$
Y_O	± 1.4	± 9.4	± 10.8
Z_O	± 10.6	± 9.4	± 20.0

* 2σ random load factor

These load factors were based on the Spacelab Payload Accomodation Handbook, SLP/2104 (Ref 6) and a preliminary random vibration evaluation. (Ref. 4)

A review of the prior trunnion analysis was initiated to insure that loading and spectral conditions planned for the Task III trunnion fatigue test were proper. A verification of the critical loading conditions for the CFME trunnion test was completed; results are summarized by the diagrams in Figure III-2. The analysis indicated that the original limit loading conditions, shown in Figure III-3, required updating due to the following:

1. An increase of 57.2 kg (26 lb) in the supported weight on the trunnions not accounted for in the original analysis. This effect contributes the largest increase in load at P_1 and P_2 .
2. Consideration of moment effect of pressure vessel C.G. offset in the X-Y plane (see Reference 4, page 249). This effect adds load in the X component direction and thereby increases P_1 and P_2 .

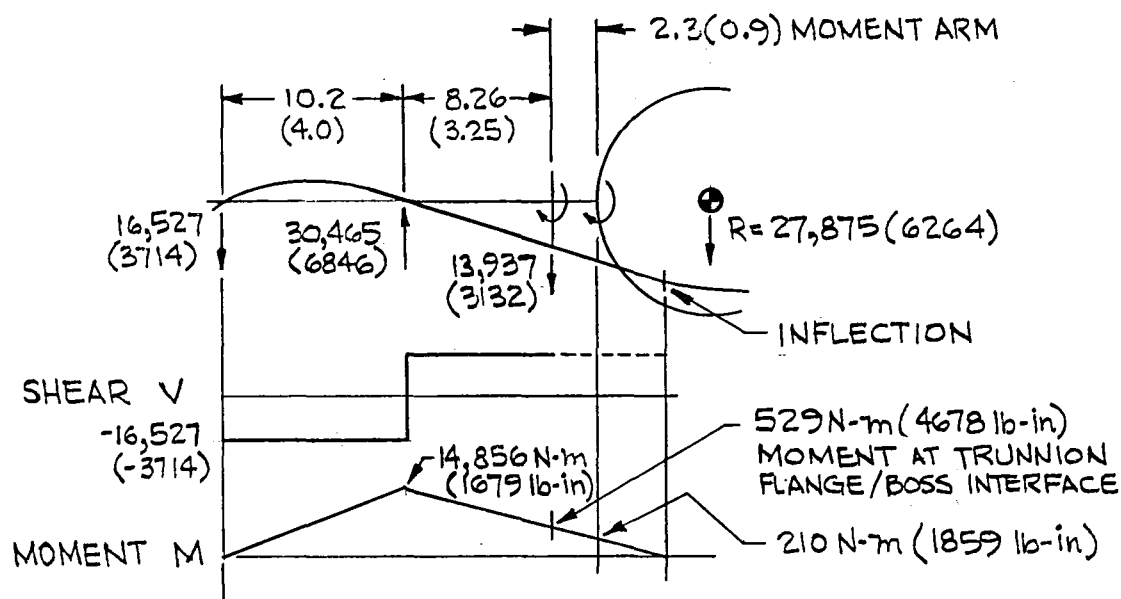
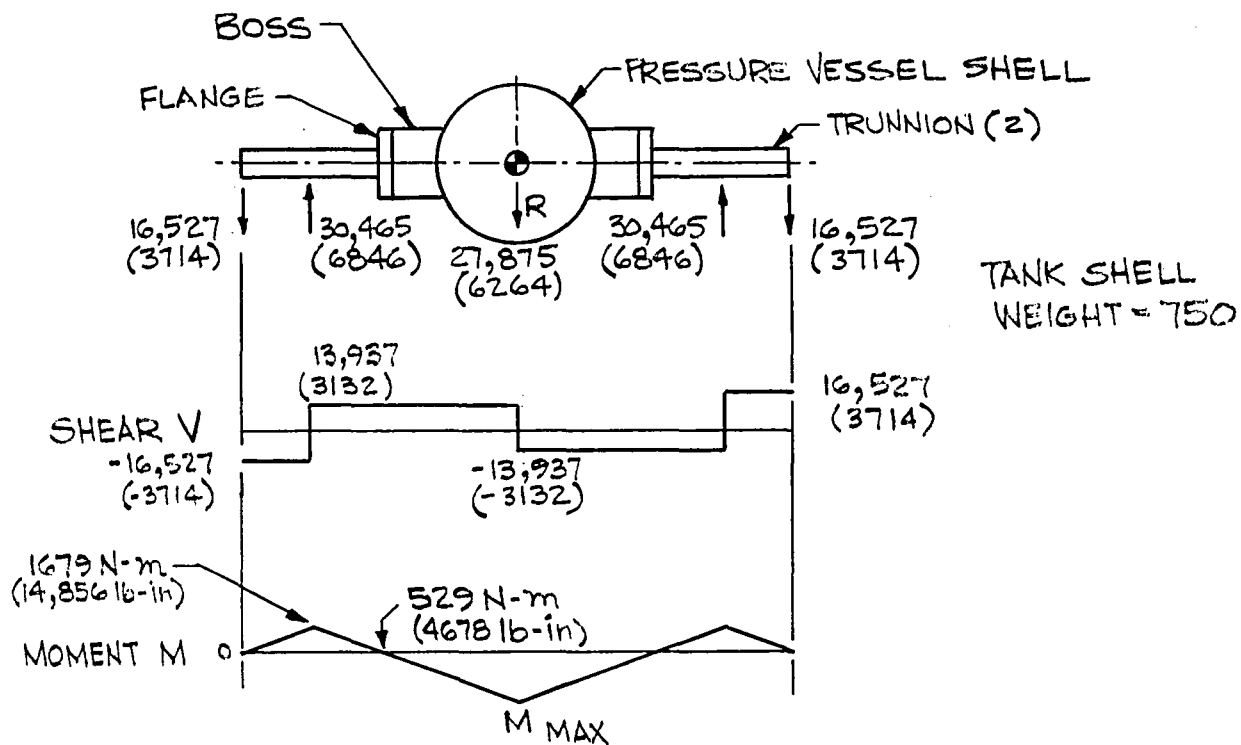
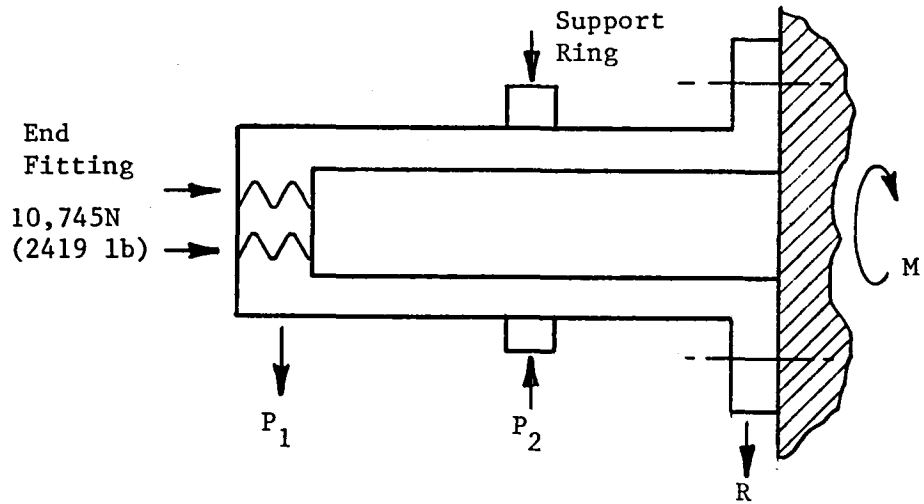


Figure III-2 CFME Trunnion Stress Analysis Diagrams

ORIGINAL LOADING CONDITIONS



	P_1	P_2	R	M
Loading Condition 1:	8055N (1810 lb)	20,136N (4525 lb)	12,082N (2715 lb)	0 N-m (0 in.-lb)
Loading Condition 2:	7552N (1697 lb)	19,633N (4412 lb)	12,082N (2715 lb)	182 N-m (1612 in.-lb)

NEW LOADING CONDITION

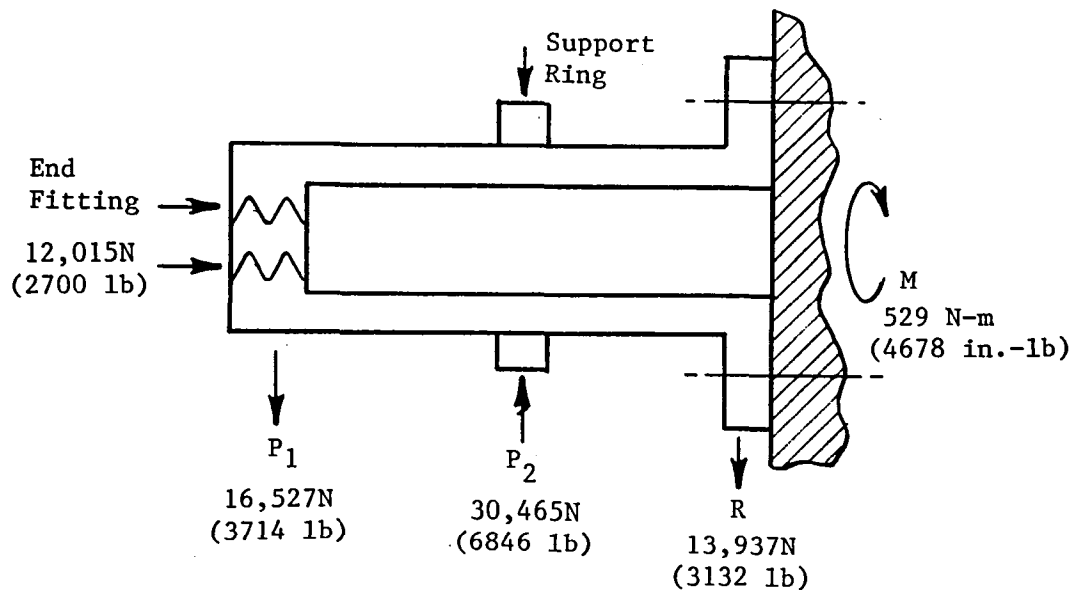


Figure III-3 Trunnion Fatigue Loading Conditions

3. Consideration of the 2.29-cm (0.9-in.) moment arm measured between the center of the membrane shell and the trunnion flange/boss interface. This effect increases the resultant loads (reactions) P_1 and P_2 .
4. The original loading condition 1 was found to be inconsistent with the final stress analysis because of an imbalance of 131.42 N-m (1163 in-lb) moment that was not shown. Also, loading condition 2 was unconservative in that the moment acted as a relieving moment, when in fact this moment should have been considered as a reinforcing moment for worse case conditions.

The new loading conditions for the trunnion fatigue tests are also shown in Figure III-3. Stress analysis and dynamic computer modeling indicated that a loading condition with a resulting moment at the flange was more critical in the area of the spacer while imposing, at the same time, the greater stress at the flange. Therefore, the trunnions were tested in fatigue using the most critically determined loading case which resulted in the higher trunnion stress.

An evaluation of the loading spectrum for the CFME trunnion fatigue tests was conducted, as well as a review of the results of the dynamic fatigue analysis. The results indicated that the defined test loads were a good representation of the actual trunnion loading and were conservative in nature. In addition, the Rayleigh distribution for the loading spectrum was verified. This distribution was applied only to the portion of each load corresponding to the random load factors (LF_R). The portion of each load corresponding to the quasi-static load factors (LF_{QS}) was treated as a base load under the Rayleigh-distributed random loads. The static limit loads were taken as the 2σ value for the random distribution loading.

During The CFME dynamics and loads analysis, a random vibration analysis (Ref 4) was conducted to verify the random vibration load factor. The dynamic analysis compared the trunnion loads calculated by the finite element dynamic loads analysis and the detail stress analysis (based on the above Table III-1). The maximum stress (limit) from the dynamic analysis (Ref. 7) was $191,820 \text{ kN/m}^2$ (27.8 KSI), which compares well with the stress analysis value of $183,540 \text{ kN/m}^2$ (26.6 KSI). Hence, it was felt that the design limit load factors in Table III-1 were reasonable.

The loading conditions presented in Table III-2 were derived for the trunnion fatigue tests. This loading spectrum encompasses the 2σ random vibration load over a 20,000 cycle distribution (which is four times the cycles encountered over seven missions). Margin testing (shown in Table III-3) was derived so that testing above limit load (2σ) could be accomplished. These values correspond to a 3σ distribution over 2,540 delta fatigue cycles which would be applied after the trunnion successfully passed the 20,000 cycle fatigue test. We proposed going above the limit load (and cycle maximum) for conservatism which should be adequate to encompass the following:

1. Modeling inaccuracies;
2. Future possible design changes;
3. Changing shuttle environments;
4. The statistical chance that the 2σ level could be exceeded.

Table III-2 20,000 Cycle Fatigue Loading (0 to 2σ)

<u>Cyclic Axial Load, N (lb)</u>	<u>Cyclic P_1 Load, N (lb)</u>	<u>Cyclic P_2 Load, N (lb)</u>	<u>σ</u>	<u>Cycles 0σ to 2σ = 20,000</u>
3649/-534 (820/-120)	9372/5794 (2106/1302)	17275/10680 93882/2400)	.4	1780
6786/-3671 (1525/-825)	12055/3110 (2709/699)	22223/5732 (4994/1288)	1.0	7320
9924/-6809 (2230/-1530)	14738/427 (3312/96)	27167/788 (6105/177)	1.6	7600
10969/-7854 (2465/-1765)	15633/-467 (3513/-105)	28818/863 (6476/-194)	1.8	1860
12015/8900 (2700/-2000)	16527/-1362 (3714/-306)	30465/-2510 (6846/-564)	2.0	1440

Table III-3 2,540 Cycle Fatigue Loading Margin Testing (2σ to 3σ)

<u>Cyclic Axial Load N, (lb)</u>	<u>Cyclic P_1 Load N, (lb)</u>	<u>Cyclic P_2 Load N, (lb)</u>	<u>σ</u>	<u>Cycles 2σ to 3σ = 2,540</u>
15152/-12037 (3405/-2705)	19211/-4045 (4317/-909)	34413/-7458 (7958/-1676)	2.6	2060
17244/-14129 (3875/-3175)	21000/-5834 (4719/-1311)	38711/-10756 (8699/-2417)	3.0	480

B. Trunnion Design Modifications

Details defining trunnion fabrication were added to conceptual drawings 849CFME1035 and 849CFME1036 which were prepared under the CFME Design Contract (NAS3-21591). Whereas the basic trunnion designs have remained unchanged, the details required to define assembly of the items necessitated drawing modifications included in Figures III-4 and III-5 (Rev A of the referenced drawings).

Changes made include the following:

1. Two extra plies of S-glass unidirectional material were added to the laminate layup to provide a thickness close to the original 0.51 cm (0.20 in.). The resulting laminate was slightly stiffer and stronger longitudinally. In order to maintain laminate symmetry, the two extra plies were added between the existing +45/-45 cloth plies producing the following layup:

$$(-45/0_3/+45/0_3/+45/+0_2/-45/0_3/+45/0_3/-45)$$

A trial cylindrical layup of this laminate resulted in a thickness of 0.50 \pm 0.01-cm (0.195 \pm .005-in.).

2. Flange and end fitting fabrication details were added and pre-fabricated disc reinforcement material was included.

3. Details for flange end tab orientation were added.

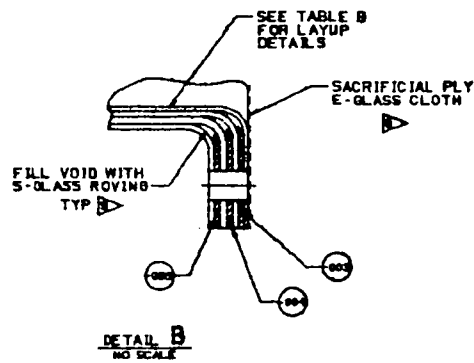
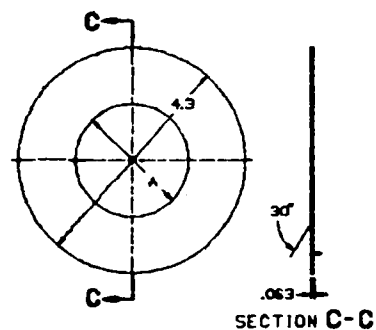
4. General details and notes to define trunnion assembly were added.

5. Two 1/8-in. holes in the trunnion cylinder positioned midway between the spacer and the flange were added as well as two 1/8-in. holes in the spacer configuration. These holes will accomodate flight instrumentation wiring routing and will aid evacuation of the enclosed trunnion/vacuum jacket cavities.

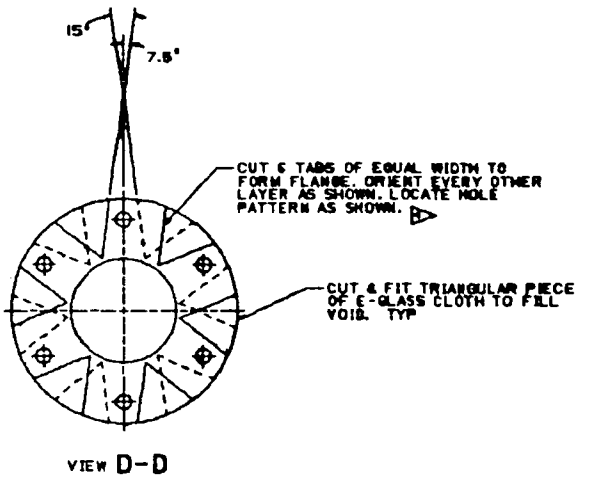
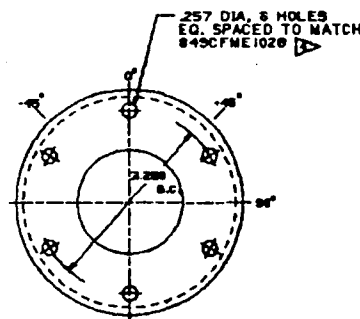
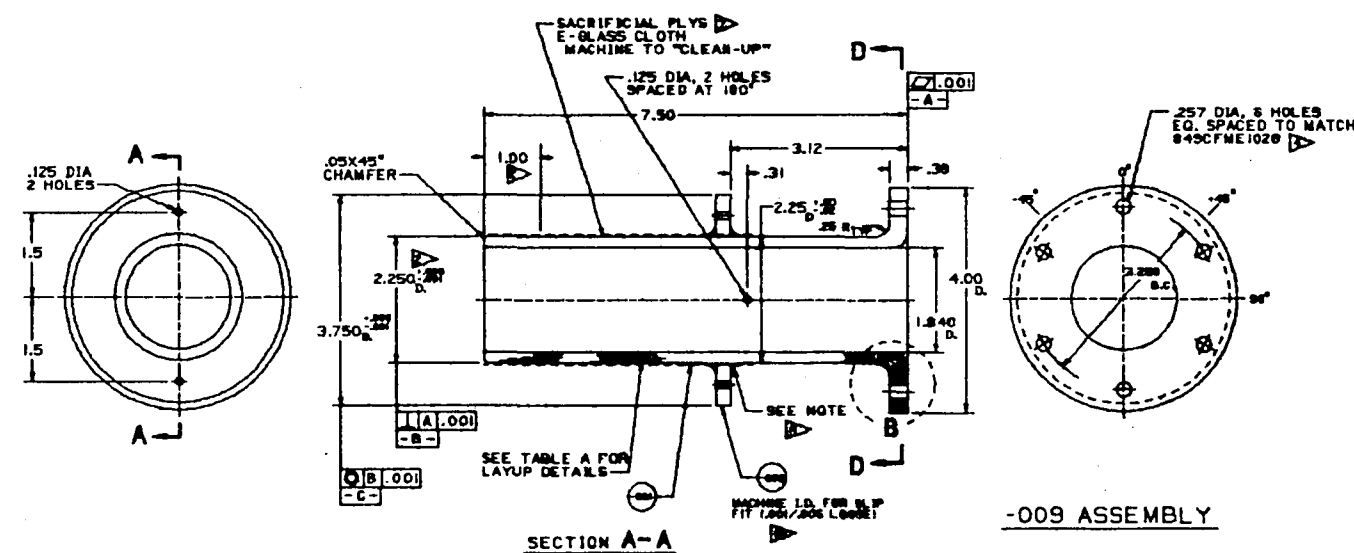
TABLE A (TRUNNION)									
45°	0°	45°	0°	45°	0°	45°	0°	45°	0°
.008	.032	.008	.032	.008	.032	.008	.032	.008	.032

TABLE B (FLANGE)									
45°	0°	45°	0°	45°	0°	45°	0°	45°	0°
.008	.040	.008	.040	.008	.040	.008	.040	.008	.040

ITEM	DESCRIPTION	QTY
1	1.0241 E-GLASS CLOTH	1
2	1.0081 E-GLASS CLOTH	1
3	1.0081 E-GLASS CLOTH	1



- NOTES:
- ABBREVIATIONS PER MIL-STD-12C.
 - HOLD 2.250 DIA. \pm .000 TOL 1.00 FROM END OF PART.
 - MATERIAL REQUIREMENT FOR TRUNNION:
 - WOVEN FIBERGLASS CLOTH PREIMPREGNATED WITH EPOXY RESIN PER EM CODE H66SH.
 - UNIDIRECTIONAL FIBERGLASS MATERIAL IMPREGNATED WITH EPOXY RESIN PER EM CODE H679 TBD.
 - DRILL HOLES THROUGH CYLINDER END MATERIAL.
 - EACH OF 3 DEBULK OPERATIONS WILL BE ACCOMPLISHED BY WRAPPING THE CYLINDER WITH 1 LAYER OF 1 INCH SHRINK TAPE APPLIED AT 3 WRAPS/INCH. HEAT AT 175 \pm 10°F FOR 1 HR \pm 5 MIN.
 - FINAL DEBULK AND CURE WILL BE ACCOMPLISHED BY WRAPPING THE CYLINDER WITH 3 LAYERS OF 4 WRAPS/INCH LAYER. CURE AT 250 \pm 10°F FOR 2 HRS \pm 10 MIN; 300 \pm 10°F FOR 1 HR \pm 5 MIN; 350 \pm 10°F FOR 2 HRS \pm 10 MIN.
 - 3 PLYS (1.0241) OF E-GLASS CLOTH ARE TO BE ADDED AS SACRIFICIAL MACHINING MATERIAL AT THE TRUNNION END AND EXTENDING BACK FOR 5 INCHES.
 - 1 PLY (1.0081) OF E-GLASS CLOTH IS TO BE ADDED AS SACRIFICIAL MACHINING MATERIAL AT THE TRUNNION FLANGE.
 - FILL VOID WITH PRE-PREG S-GLASS ROVING, 20 END, HTS.
 - BOND -.002 TO THE TRUNNION CYLINDER AS SHOWN WITH EAS34NA ADHESIVE PER MP00043. SHORE HARDNESS PER MP IS THE ONLY TEST REQUIRED.
 - WRAP PRE-PREG S-GLASS ROVING ON EACH SIDE OF -.002 SPACER TO HEIGHT AND WIDTH OF .28. CURE AND MACHINE AS SHOWN.



ITEM	DESCRIPTION	QTY	UNIT	REVISION	DATE	BY	CHKD	APP'D
1	1.0241 E-GLASS CLOTH	1						
2	1.0081 E-GLASS CLOTH	1						
3	1.0081 E-GLASS CLOTH	1						

ITEM	DESCRIPTION	QTY	UNIT	REVISION	DATE	BY	CHKD	APP'D
1	1.0241 E-GLASS CLOTH	1						
2	1.0081 E-GLASS CLOTH	1						
3	1.0081 E-GLASS CLOTH	1						

Figure III-5. CFME Floating Trunnion Assembly

6. An uncertainty in the material properties of the vendor supplied preformed 0.64-cm (1/4-in.) E-glass sheet material selected for spacer use resulted in the development of a quasi-isotropic 36-ply laminate of pre-pregnated E-glass cloth which became a separate lay-up and installed subassembly of the trunnion configuration. Analysis of spacer loadings using the known properties of the new lay-up resulted in increasing the spacer thickness from 0.64-cm (1/4-in.) to 0.79-cm (5/16-in.).

7. Potential delamination of the plies at the trunnion cylinder/flange radius became a concern under the fatigue loading conditions. Complexities of the laminate configuration in this area made analysis highly questionable based on unknowns and assumptions which would have to be made. By increasing the thickness of the metal ring support installed on the flange (which formerly was used to distribute bolting loads uniformly around the flange) and creating an area of close fit at the radius, additional load support and some possible delamination prevention were provided. In this manner, uncertainties were minimized and design confidence was increased. Figure III-6 shows details of the back-up ring and Figure III-7 shows the ring installation on the trunnion. The ring was installed during trunnion fabrication before the spacer was put in place.

Many of the above changes were the direct result of fabricating three simplified development trunnion assemblies where flange and end fitting configurations were simulated. Various cure techniques were evaluated and filler material was added in end fitting and cylinder/flange transitions to prevent excessive void areas.

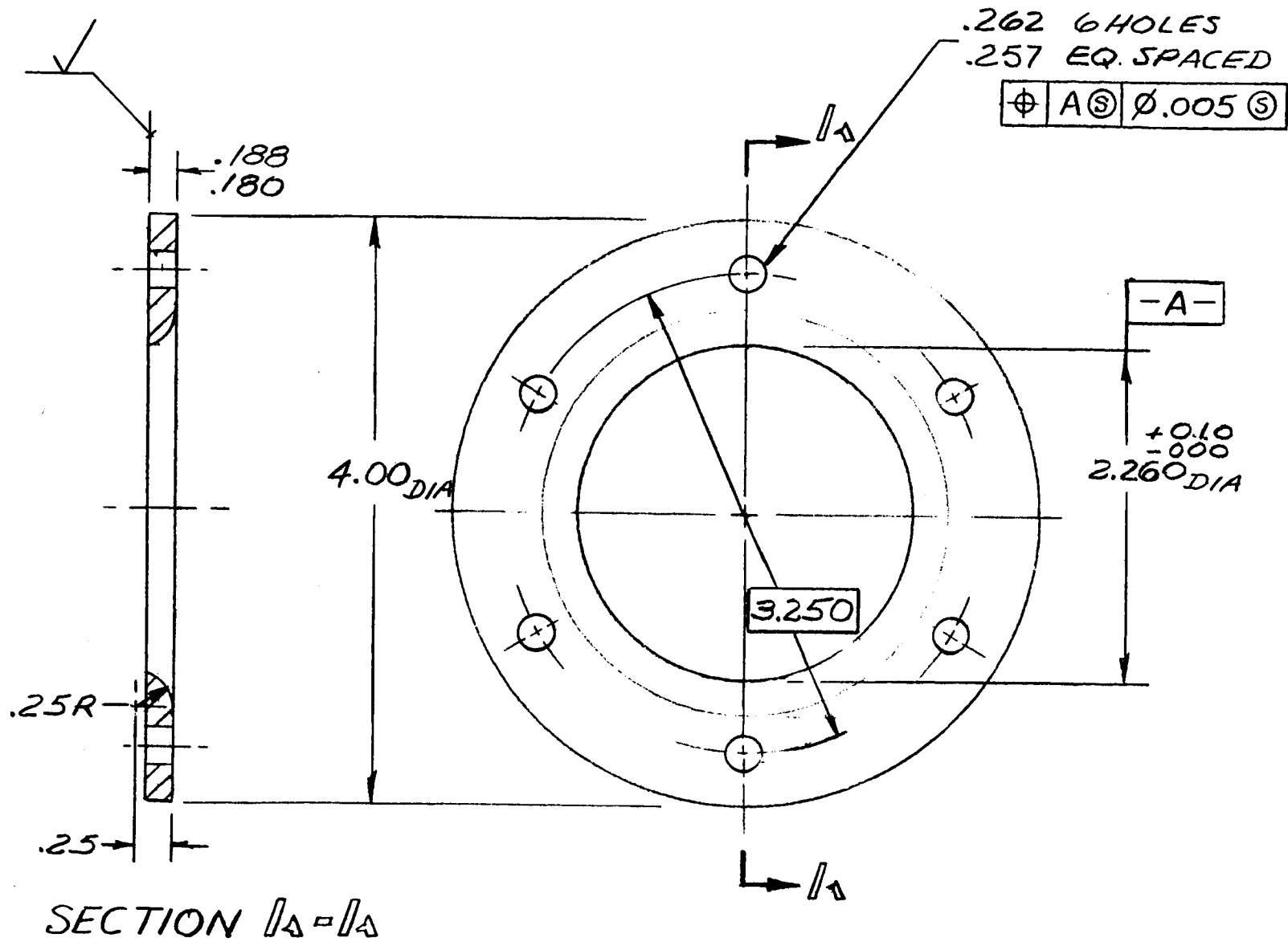
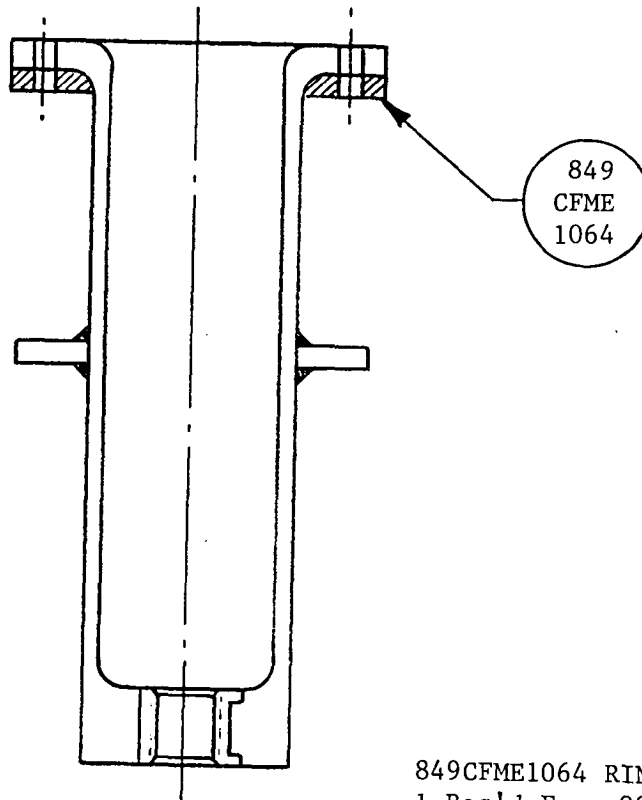
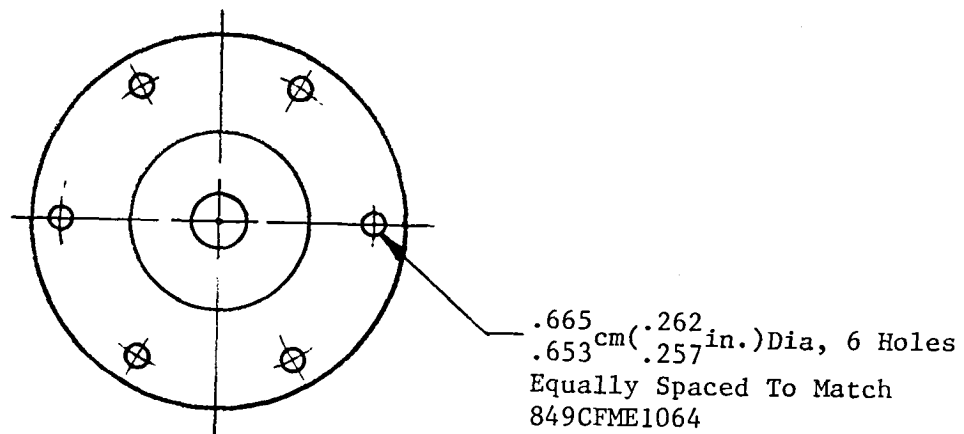


Figure III-6 Back-up Ring Assembly



849CFME1064 RING, BACKUP
 1 Req'd For -009 Assy

Figure III-7 Back-up Ring Installation

IV. DETERMINATION OF CFME TRUNNION STRUCTURAL INTEGRITY (Task III)

The Task III effort consisted of the following activities:

1. Definition of test philosophy;
2. Test plan preparation;
3. Test fixture design and fabrication;
4. Test fixture installation;
5. Manufacturing Process Plan preparation;
6. Test trunnion fabrication;
7. Test procedure preparation;
8. Trunnion structural integrity fatigue testing;
9. Fatigue testing data reduction;
10. Deliverable trunnion fabrication.

The following sections detail the Task III effort.

A. Test Philosophy

The prime objective of the Task III fatigue testing was to verify the capability of the trunnions to survive the fatigue environment imposed by four times the seven mission cycles over a distribution up to and including limit load. Further testing (up to and including ultimate load) was performed to establish design margin. Testing was as follows:

- 1) Each of the three test trunnions (2 floating and 1 fixed) were fatigued for 20,000 cycles over a distribution up to and including the 2σ limit loads, as previously shown in Table III-2.
- 2) One fixed and one floating trunnion were tested for margin for an additional 2,540 cycles starting at the 2σ load and ending with the 3σ (ultimate) loading condition, as previously shown in Table III-3.
- 3) All trunnions were then loaded to failure. A comparison was made of cumulative damage of the floating trunnions between the 2σ and 3σ cases.

B. Trunnion Fabrication

The following details the fabrication process for trunnion manufacture per drawing 849CFME1035 (fixed trunnion). A similar procedure was used for floating trunnion fabrication (less end fitting details). Figures IV-1 and IV-2 show revision B to the trunnion drawings, which represents the trunnion "as-built" configuration.

The fabrication steps were:

- 1) Fabricate disc, bushing and spacer details.
- 2) Verify fiberglass E-glass pre-preg cloth and S-cloth pre-preg roving material traceability (properties, shelf life, etc.).
- 3) Prepare lay-up mandrel (Figure IV-3) by spraying with release agent. Install mandrel to winding lathe. Install -002 bushing to mandrel.
- 4) Lay up one layer of sacrificial cloth on flange per eng. dwg. Table C.
- 5) Lay up one -45° E-glass cloth layer and three layers of S-glass roving per eng. dwg. Table A, B and C. Orient flange tabs per eng. dwg. View E-E.
- 6) Install -004 and -011 disc. Attach top constraint fixture (Figure IV-4). Fill void areas with hoop oriented S-glass roving pre-preg per eng. dwg. Note 9.
- 7) Wrap de-bulk shrink tape per eng. dwg. Note 5. Install flange constraint fixture (Figure IV-5).
- 8) Perform first de-bulk per eng. dwg. Note 5.
- 9) Lay up $+45^{\circ}$ E-glass cloth layer and three layers of S-glass roving per eng. dwg. Table A, B, and C. Orient tabs per eng. dwg. View E-E.

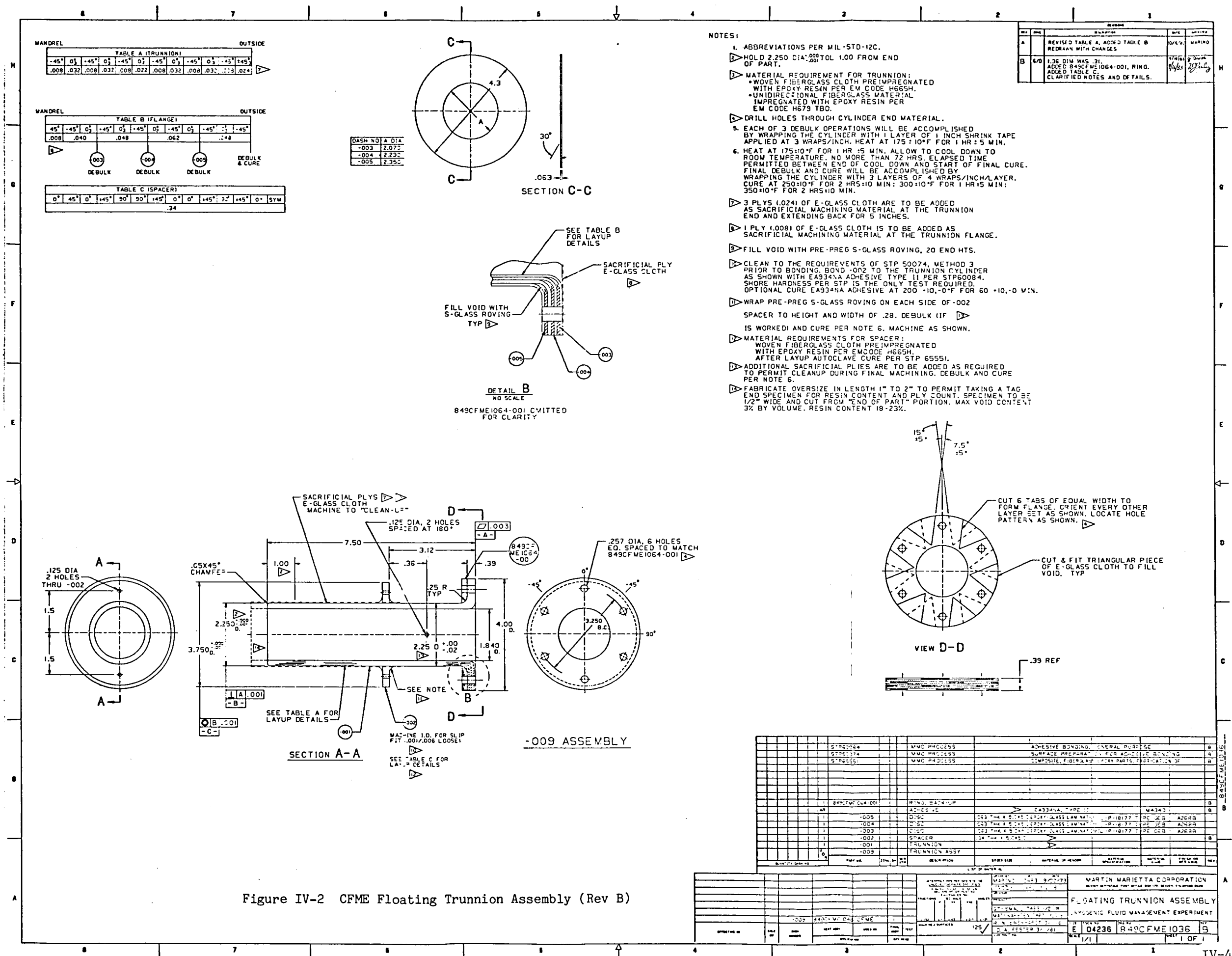


Figure IV-2 CFME Floating Trunnion Assembly (Rev B)

1 001 + 002 BOLTED
TOGETHER TO BE
MATCH MACHINED

2 1/4-20 BOLT, 1.00
IN LENGTH

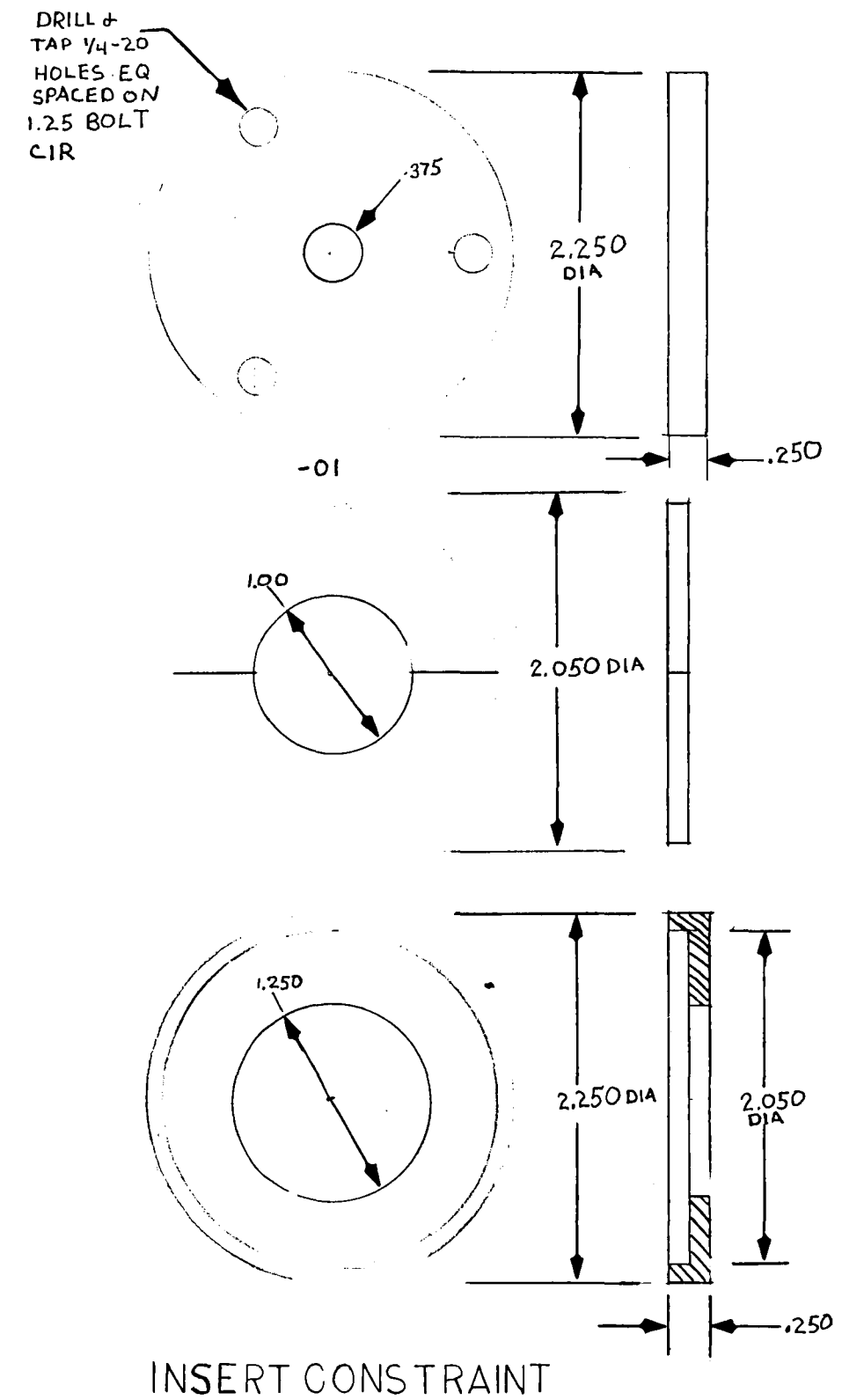
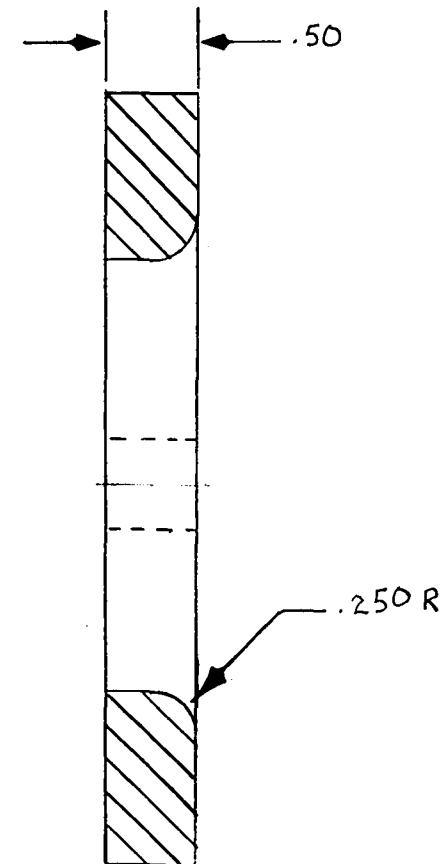
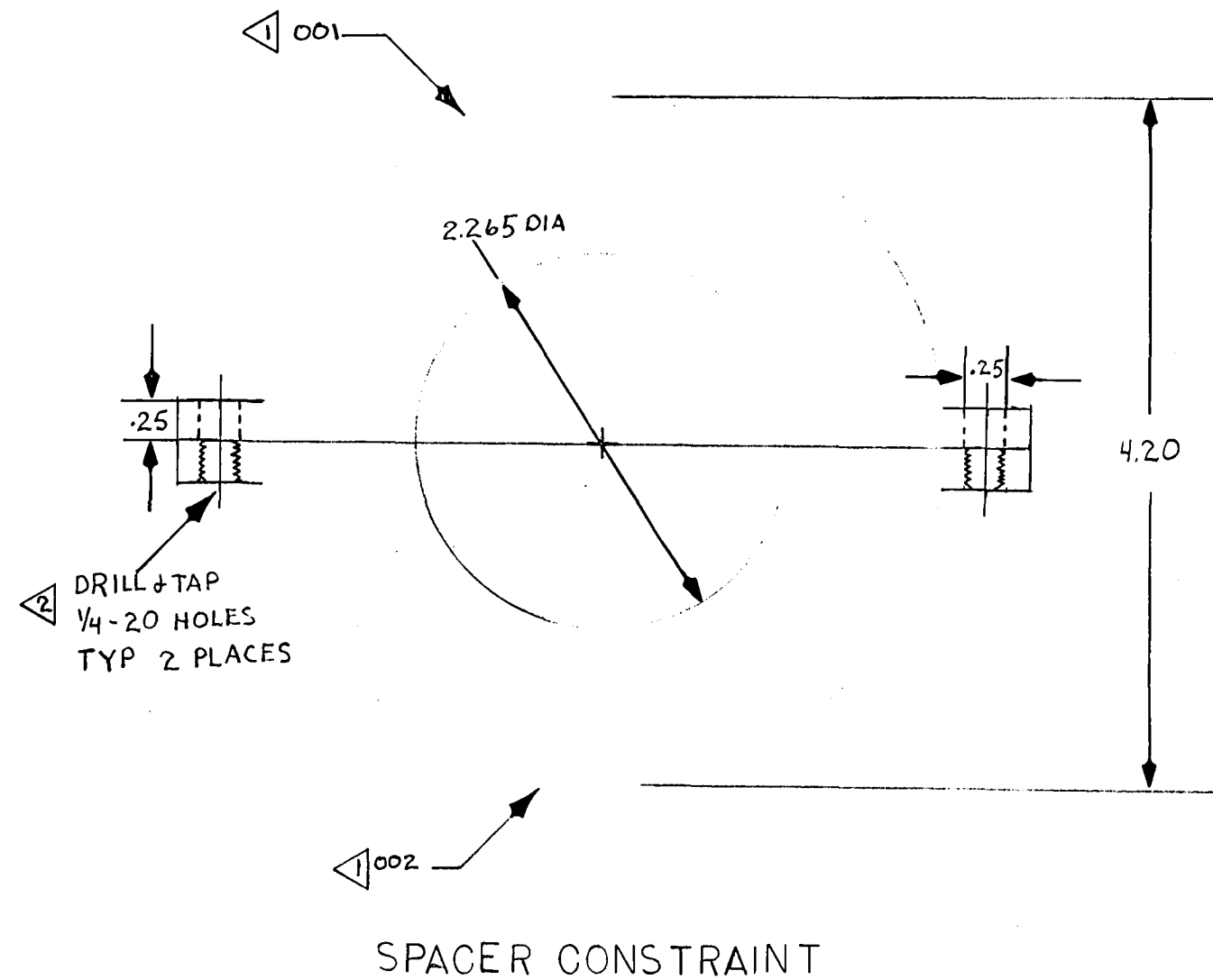


Figure IV-4 End Insert and Spacer Constraint Tooling

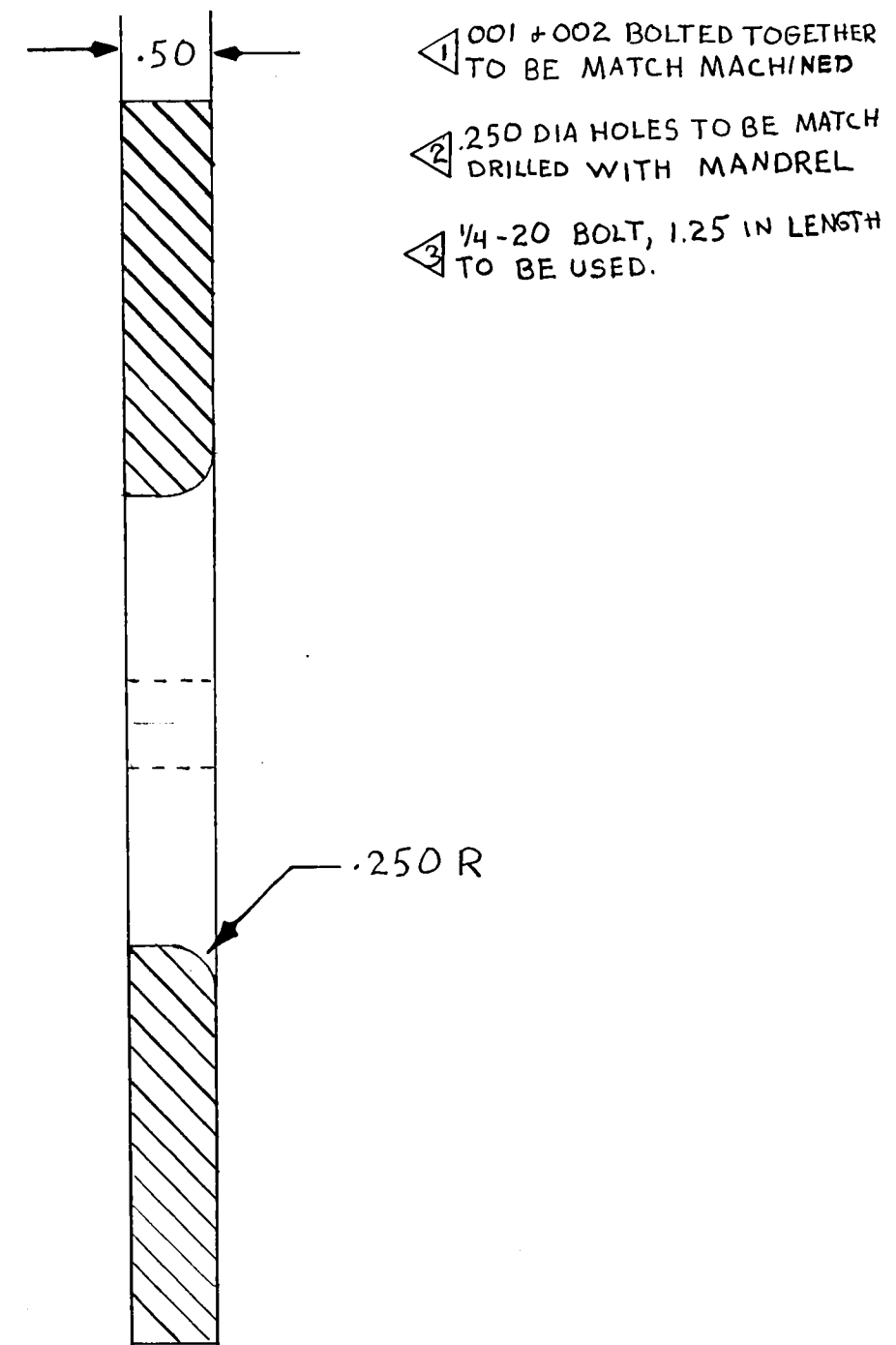
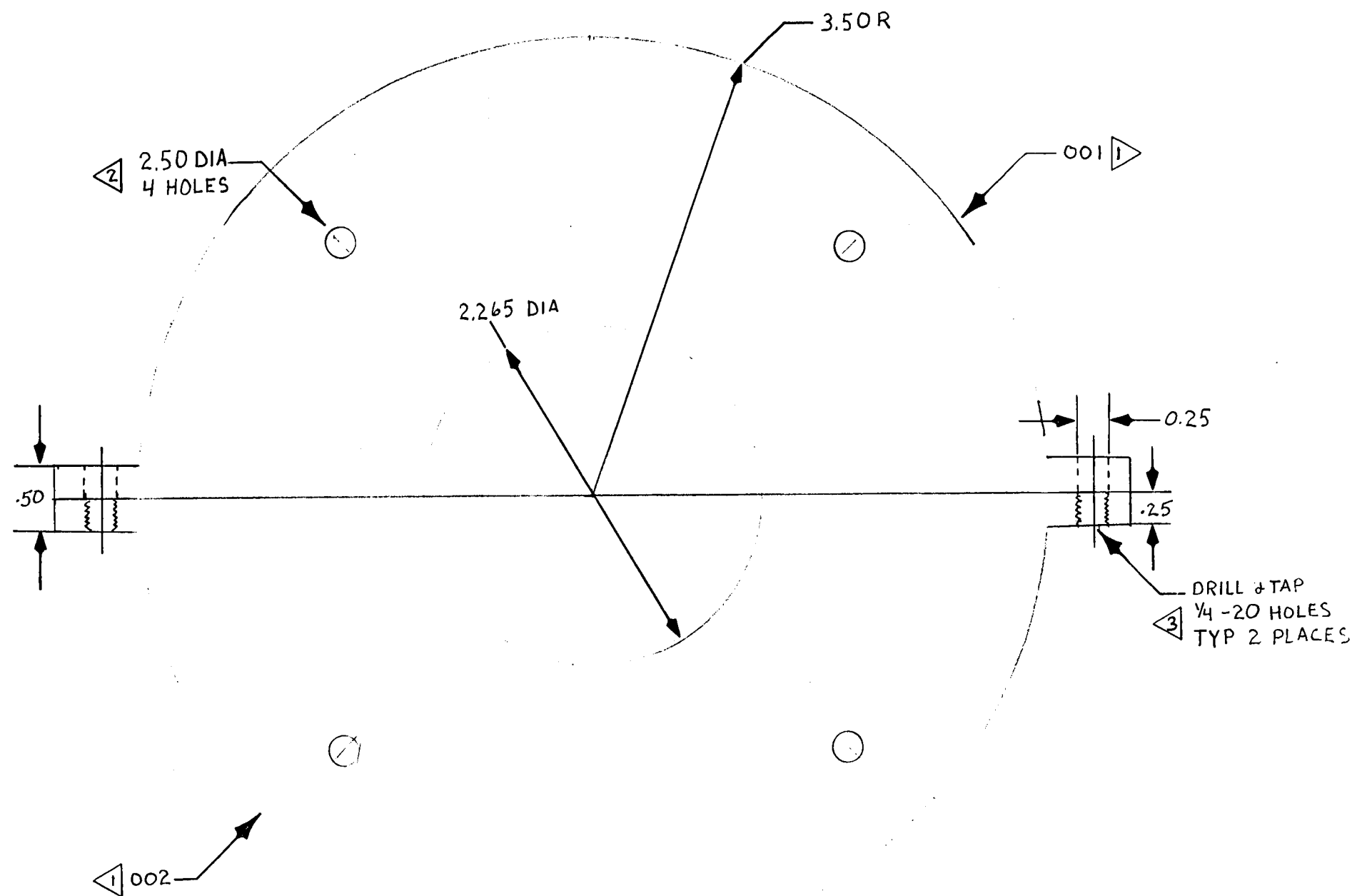


Figure IV-5 Flange Constraint Tooling

- 10) Install -006 and -012 disc. Bond -006 disc per eng. dwg. Note 10. Attach top constraint fixture (Figure IV-4). Fill void areas with hoop oriented S-glass roving pre-preg per eng. dwg. Note 9.
- 11) Wrap de-bulk shrink tape per eng. dwg. Note 5. Install flange constraint fixture (Figure IV-5).
- 12) Perform second debulk per eng. dwg. Note 5.
- 13) Lay up two layers of S-glass roving and one layer of -45° E-glass cloth per eng. dwg. Table A, B and C. Orient tabs per eng. dwg. View E-E.
- 14) Install -005 disc. Bond disc per eng. dwg. Note 10.
- 15) Lay up three layers of S-glass roving per eng. dwg. Table A, B and C. Orient flange tabs per eng. dwg. View E-E.
- 16) Install -003 and -013 disc. Attach top constraint fixture (Figure IV-4). Fill void areas with hoop oriented S-glass roving pre-preg per eng. dwg. Note 9.
- 17) Wrap de-bulk shrink tape per eng. dwg. Note 5. Install flange constraint fixture (Figure IV-5).
- 18) Perform third de-bulk per eng. dwg. Note 5.
- 19) Lay up one $+45^{\circ}$ layer of E-glass cloth and three layers of S-glass roving per eng. dwg. Table A, B and C. Orient flange tabs per eng. dwg. View E-E.
- 20) Fill void areas with hoop oriented S-glass roving pre-preg per eng. dwg. Note 9. Apply top constraint fixture (Figure IV-4).
- 21) Lay up three plies of $+45^{\circ}$ E-glass sacrificial cloth per eng. dwg. Table A and B per Note 7.

- 22) Wrap final de-bulk and cure shrink tape per eng. dwg. Note 6.
Install flange constraint fixture (Figure IV-5).
- 23) Perform final de-bulk and cure per eng. dwg. Note 6.
- 24) Drill 0.318-cm (0.125-in.) diameter holes in trunnion body and spacer per eng. dwg. (4 places).
- 25) Fabricate 849CFME1064-001 back-up ring.
- 26) Install 1064-001 back-up ring to trunnion flange.
- 27) Match drill 0.653-cm (0.257-in.) diameter holes (6 places) to trunnion flange as shown on eng. dwg. View E-E.
- 28) Rough machine 5.715-cm (2.250-in.) diameter to $5.740 + 0.25/-0.000$ cm ($2.260 + .010/-0.000$ in.)
- 29) Install -008 spacer by matching ID to obtain a slip fit over the machined trunnion end of $.003/.015$ cm ($.001/.006$ in.) Maintain 7.925-cm (3.12-in.) dimension.
- 30) Bond -008 spacer to trunnion per eng. dwg. Note 11.
- 31) Add S-glass roving pre-preg reinforcement per eng. dwg. Note 12.
Install spacer constraining fixture.
- 32) Cure per eng. dwg. Note 6.
- 33) Final machine $5.715 + .000/-0.0025$ cm ($2.250 + .000/-0.001$ in.) diameter, $9.525 + .000/-0.0025$ cm ($3.750 + .000/-0.001$ in.) diameter, datum A face, and 0.127-cm (.05-in.) x 45 chamber radii at end face.
- 34) Perform quality dimensional inspection.

Figure IV-6 shows the floating trunnion manufacturing tooling mandrel. Flange constraint tooling (Figure IV-5) is also used in floating trunnion assembly.

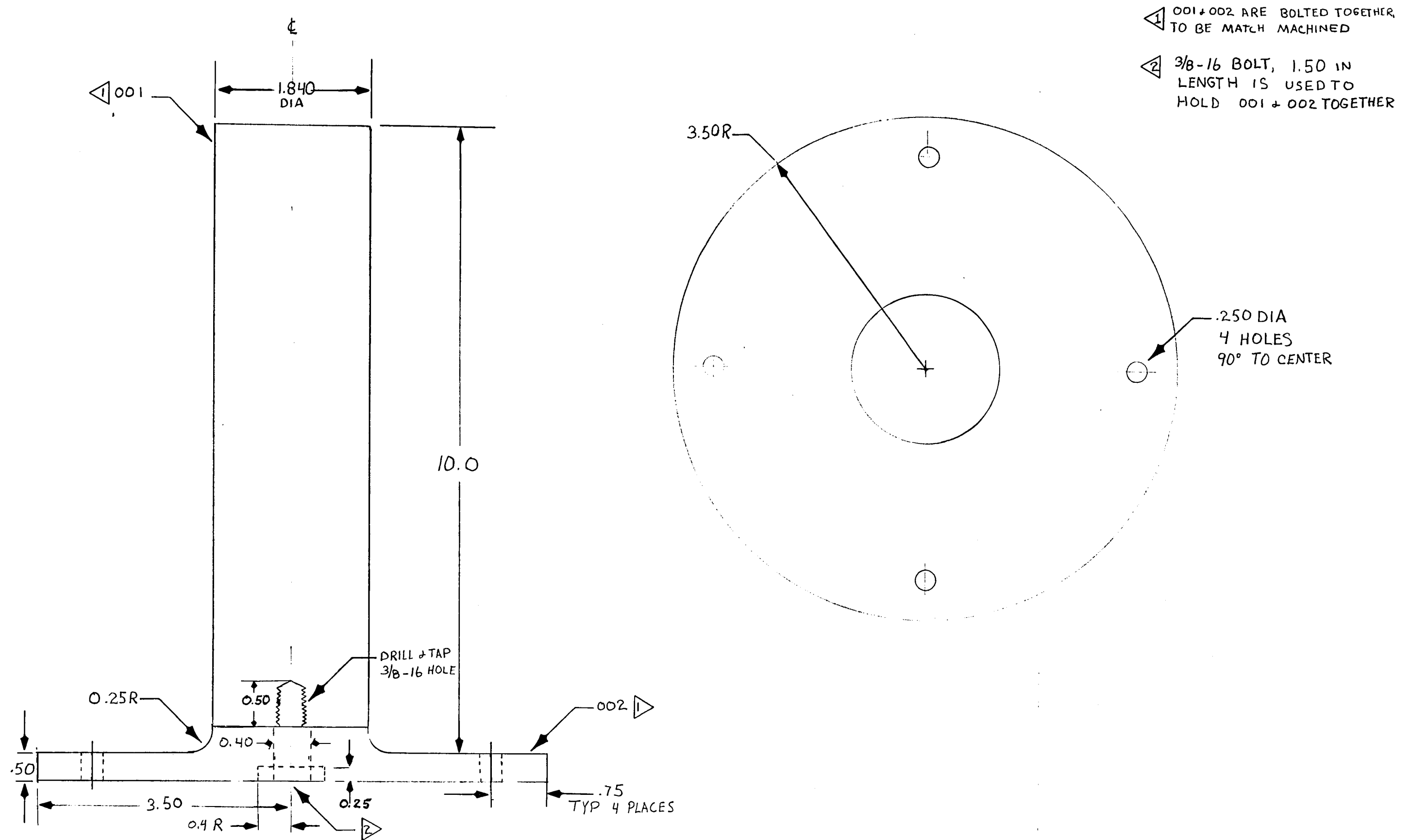


Figure IV-7 shows a side and an end view of a completed fixed trunnion configuration. Figure IV-8 shows a front and a side view of a completed floating trunnion configuration.

C. Structural Fatigue Test Fixture

The test fixture for the CFME trunnion fatigue assessment is shown in Figure IV-9. It consisted of the test trunnion rigidly bolted to a fixed support stand. Transverse and axial loads were applied using load-cell-controlled hydraulic actuators. Test fixture supports interfaced with the actuators to impart the required loads into the trunnion spacer, end, and threaded fitting (for the fixed configuration only). Proper alignment was provided by accurate placement of the actuator fixed supports on the flat test cell bed. Maintaining proper centerline and perpendicularity positions aided in load alignment as well. Figure IV-10 shows the details of the test fixturing required to secure the load actuators to the trunnion. Strain gage and deflection gage instrumentation locations for the test trunnions are shown in Figure IV-11.

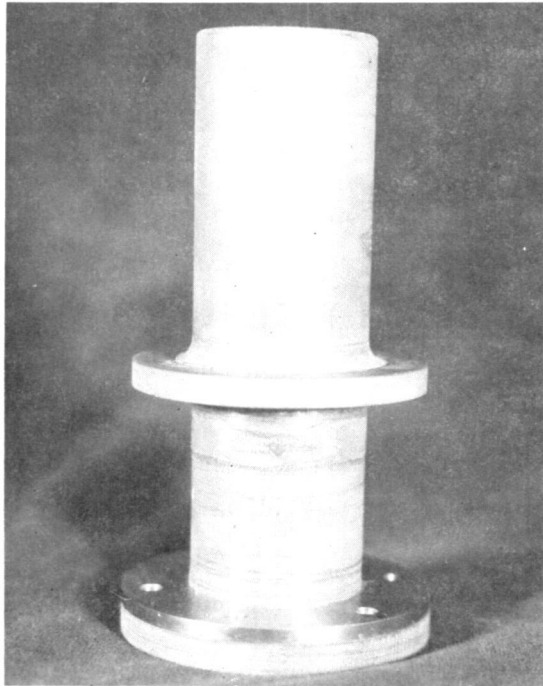
D. Structural Fatigue Test Description

1. Test Objective

The objective of this test was to verify the structural integrity of the CFME trunnions used to support the CFME liquid hydrogen storage tank by demonstrating the capability to survive seven-mission-life fatigue testing.

2. Test Specimens

Three trunnions were tested. One was manufactured according the revised drawing 849CFME1036 (fixed type which includes a threaded titanium insert) while two were manufactured according to revised drawing 849CFME1035 (floating type with an open end). The cylindrical portion of the trunnion was composed of fiberglass/epoxy composite similar to that used in the test specimen for the laminate mechanical properties tests.

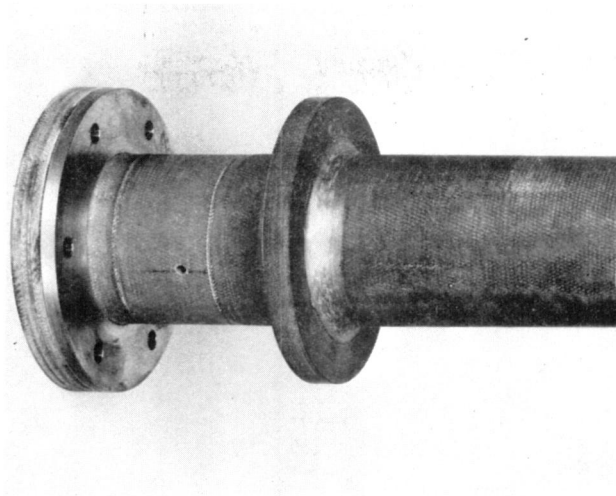


Side View

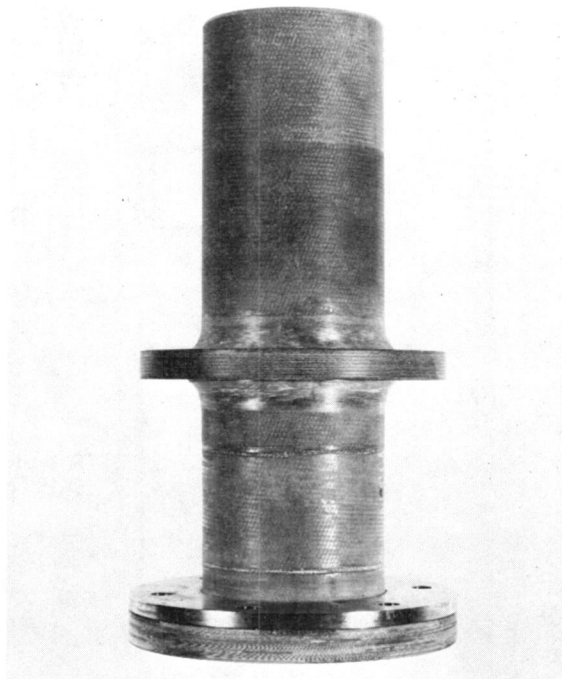


End View

Figure IV-7 Fixed Trunnion Configuration



Partial End View



Side View

Figure IV-8 Floating Trunnion Configuration

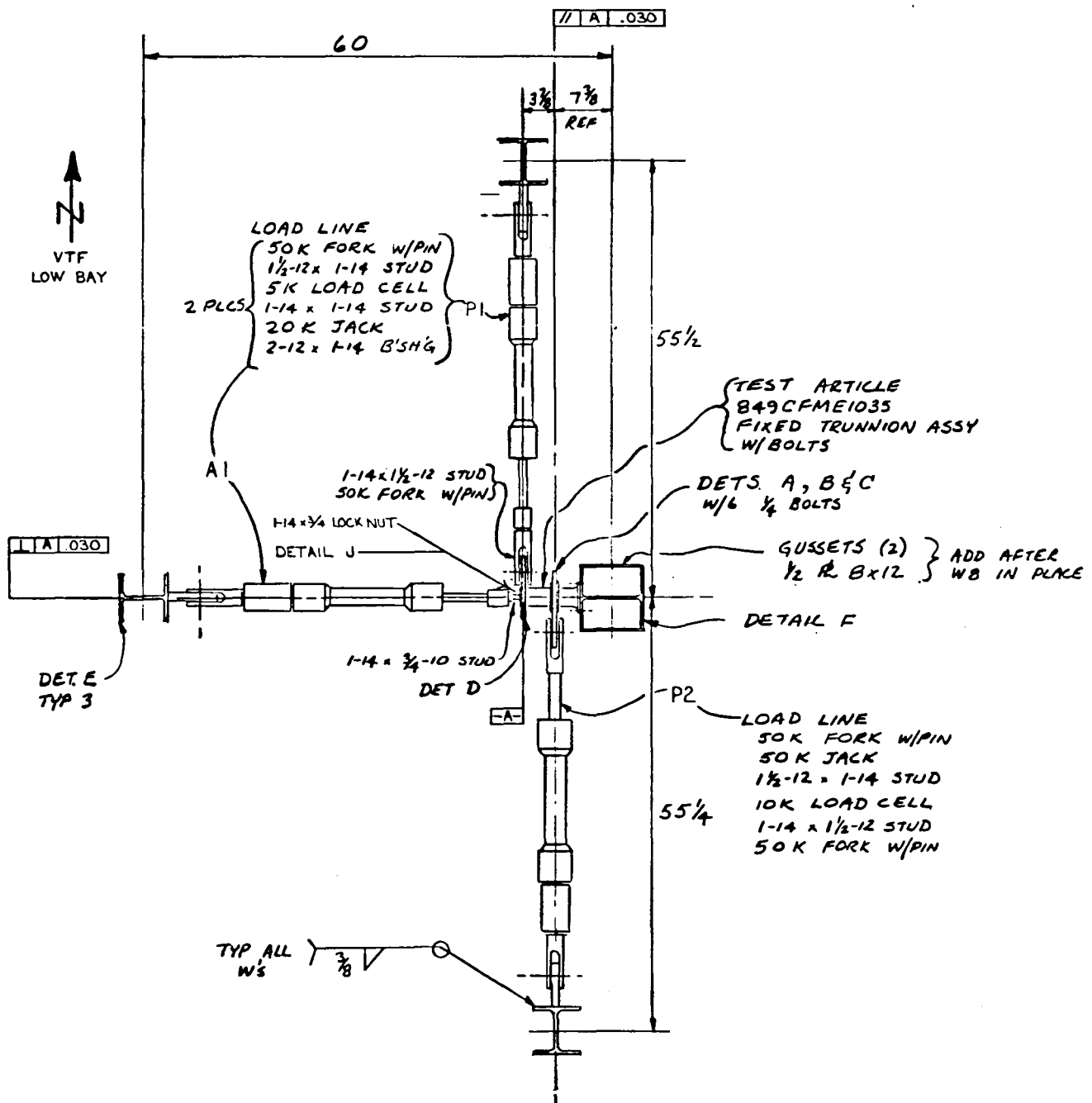
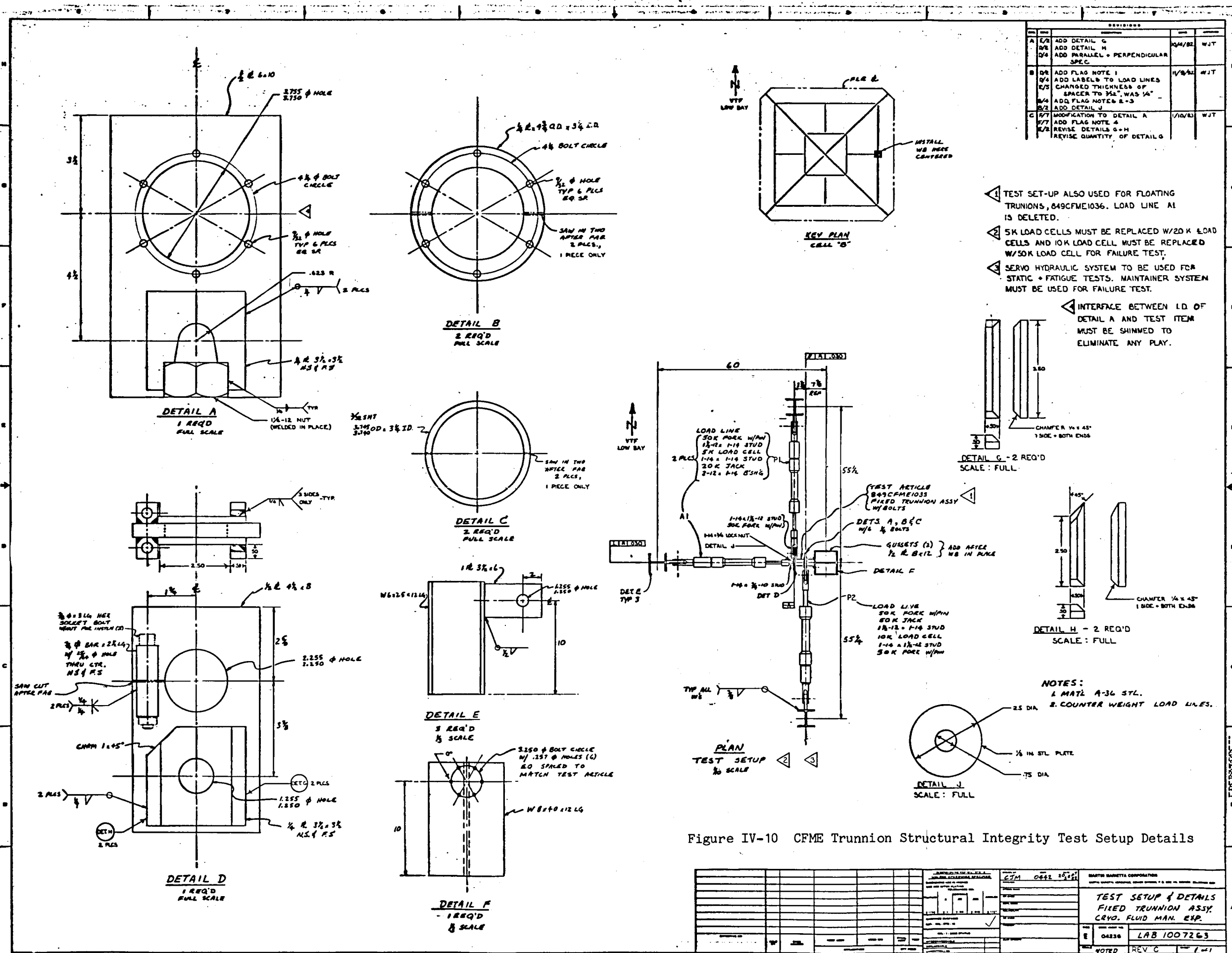


Figure IV-9 CFMF Trunnion Fatigue Test Setup



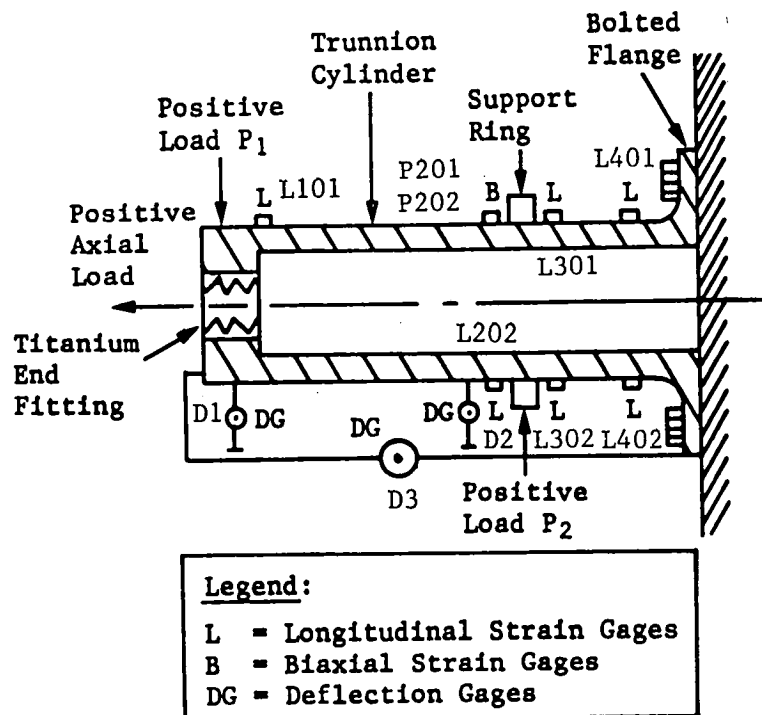


Figure IV-11 CFMF Trunnion Test Instrumentation Locations

3. Test Configuration

Each of the three test trunnions were tested in fatigue using the test setup shown in Figure IV-9. Actuators 1 and 2 connected with the trunnion by support rings which uniformly distributed the loads. Actuator 3 had a threaded end to mate with the titanium insert on the fixed trunnion and was not used for floating trunnion tests since no axial load is imposed.

4. Specimen Instrumentation

All three test trunnions were instrumented with strain and deflection gages which were aligned in the Z-Y plane as shown in Figure IV-11. Loads were also applied in this plane.

5. Floating Trunnion Testing

Two floating trunnions were tested separately in fatigue using the following approach:

Prior to fatigue cycling, loads were applied in a concurrent and linear manner in static increments of 10% of the limit loads up to and including the limit load (shown in Figure III-3) so that baseline strain and deflection gage readings could be obtained. A load/deflection curve was generated to establish an individual trunnion deflection "signature" for later comparison.

Loads P_1 and P_2 , as shown in Figure III-3, were applied and relaxed in a concurrent and synchronized linear manner utilizing the loading spectrum given in Table III-2 until a total number of 20,000 fatigue cycles were applied. Loads are shown in the positive sense and consist of a fixed base quasi-static load under a Rayleigh-distributed random load. Only the random loads were cycled (in tension and compression) while the quasi-static loads remained fixed with the following magnitudes in the positive direction:

Axial quasi-static load	1558 N (350 lb)
P ₁ quasi-static load	7583 N (1704 lb)
P ₂ quasi-static load	13977 N (3141 lb)

One stress cycle consisted of the concurrent application of loads P₁ and P₂ by actuators 1 and 2 until the maximum loading condition was achieved followed by relaxing the loads concurrently until the minimum loading condition was achieved. Loading directions were reversed only when the minimum loading became negative (see Table III-2). The spectrum was applied to the floating trunnions in the following manner until 20,000 cycles were reached:

<u>Load Setting</u>	<u>Cycles</u>
3	7600
2	7320
1	1710
4	1860
5	1440

Another static test was performed after the fatigue test was completed. Loads were applied in a concurrent and linear manner (starting at zero) in increments of 10% of the limit load (shown in Figure III-2) so that strain and deflection gage readings could be compared with those obtained prior to the start of the test. Increments were taken up to and included 150% of limit load. This test constituted a proof loading of the trunnion. Margin testing was then conducted on one floating trunnion using the distribution shown in Table III-3 for 2,540 cycles. Both floating trunnions were then static tested to failure.

6. Test Description for Fixed Trunnions

One fixed trunnion was tested separately in fatigue using the following approach:

Prior to fatigue cycling, loads were applied in a concurrent and linear manner in static increments of 10% of the limit loads up to and including the limit load, in a manner similar to that which was performed on the floating trunnions. Next, all three loads (Axial, P_1 and P_2 as shown in Figure III-3) were applied and reduced in a concurrent and synchronized linear manner utilizing the loading spectrum given in Table III-3 until a total number of 20,000 fatigue cycles were applied. Loads and cycles were applied and changed in a similar manner as for the floating trunnion.

After the fatigue test was complete, another static test was performed with loads applied in 10% increments of limit load until 150% of limit load was reached. Margin testing was then conducted using the distribution shown in Table III-3 for 2,540 cycles. The fixed trunnion was then static tested to failure.

7. Failure Modes

Any structural degradation which resulted in the inability of the trunnion to withstand the loading spectrum constituted a failure. Possible failure modes could be caused by delamination, cracks, splits, or material rupture. Occurrence of any of these modes at any point prior to static failure testing would constitute a trunnion failure.

E. Trunnion Fatigue Test Results

Results of the trunnion structural integrity tests are summarized in Table IV-1.

Table IV-1
Trunnion Test Summary

Trunnion Type	Static Test to 100% of Limit Loads	20,000 Cycle Fatigue Test*	2540 Cycle+ Margin Test	Static Test to 150% of Limit Loads (Design Ult)	Static Test to Rupture (% of Limit Load)	(% of Ult Load)
Fixed (S/N 001)	X	X	X	X	190	127
Floating (S/N 001)	X	X	X	X	210	140
Floating (S/N 002)	X	X		X	230	153

Note:

* See Table III-2

+ See Table III-3

(X indicates successful completion of this test)

All of the trunnions exceeded the design fatigue load carrying requirement (no failure at 20,000 cycles of distributed load). One fixed and one floating trunnion were subjected to margin testing for an additional 2540 cycles at loads which included design ultimate without failure. All trunnions were then loaded to failure with margins of 27% to 53% recorded (based on ultimate load). In each instance, primary failure occurred adjacent to the support ring, as predicted. Figure IV-12 shows a failed fixed trunnion in the test system.

1. Test Data Discussion

Figure IV-13 shows static test deflection data for S/N 001 and 002 floating trunnions. In both cases, data were obtained before testing and after fatigue cycling of 22,540 and 20,000 cycles respectively for S/N001 and S/N002. After test deflection data for gages D_2 and D_3 when compared to

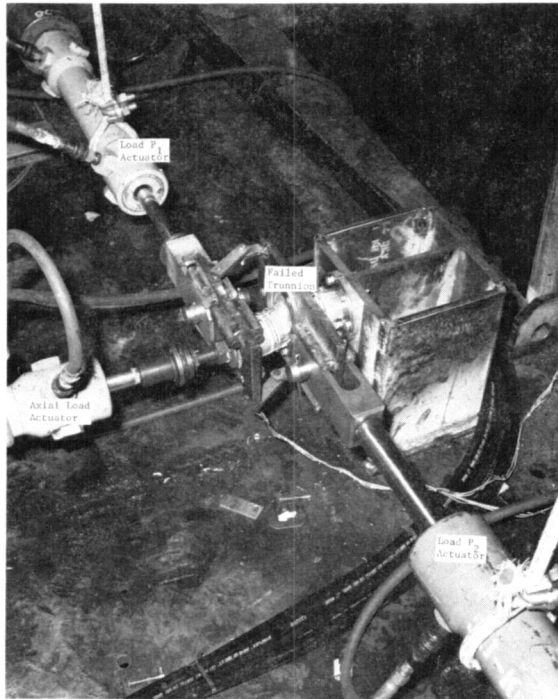


Figure IV-12 Failed CFME Fixed Trunnion in Fatigue Test Setup

before test data indicate slight increases in trunnion deflection for S/N001. Data for S/N002 indicates virtually identical before and after test indications.

Figure IV-14 shows static test strain data for representative strain gages installed on S/N001 and S/N002 floating trunnions. Data were collected before and after test in a similar manner as deflection data. After test strain data for all gages (L202, L301 and L401) indicate increased strain for S/N001 when compared with before test indications. Data for S/N002 indicates virtually identical strains before and after test measurements.

Data presented in Figures IV-13 and IV-14 for the two tested floating trunnions indicate the following:

1. Fatigue loading to 20,000 cycles over the assumed profile up to and including limit load does not produce any detectable damage to the component.
2. Fatigue loading for an additional 2540 cycles from limit load to ultimate load produces only slight detectable damage (reduction in modulus) equivalent to a 13% reduction of the ultimate capability at failure.

Figures IV-15 and IV-16 present similar static test deflection and strain data for the S/N001 fixed trunnion which was loaded for 22,540 cycles over an assumed profile up to and including ultimate load. The deflection data indicates an increase in deflection after the test (an indication of damage due to reduction in modulus). However, strain gage data indicates almost no change in before and after indications. This data supports the conclusion that minimal damage resulted from the cycling.

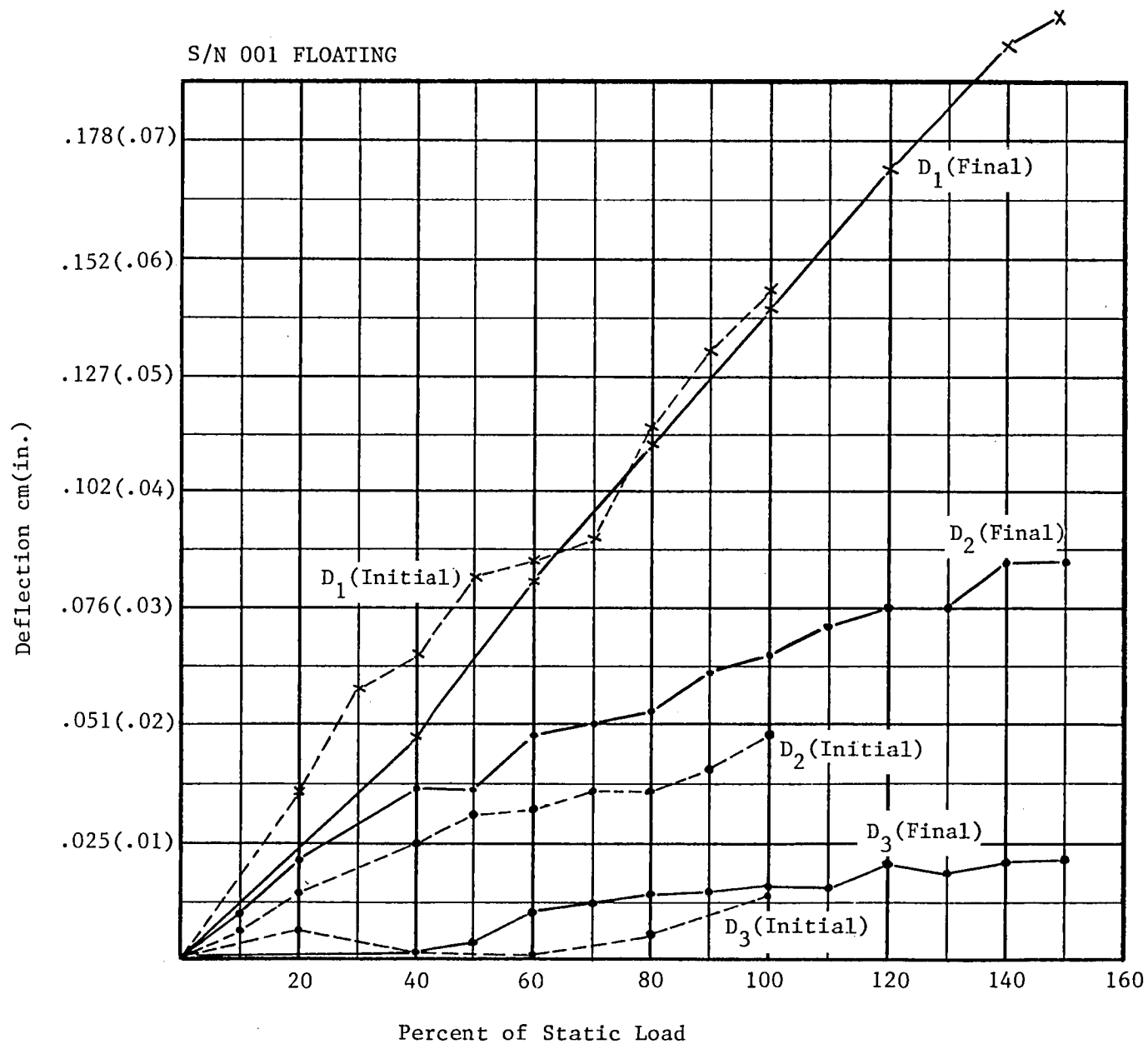


Figure IV-13 Floating Trunnion Static Test Deflection Data

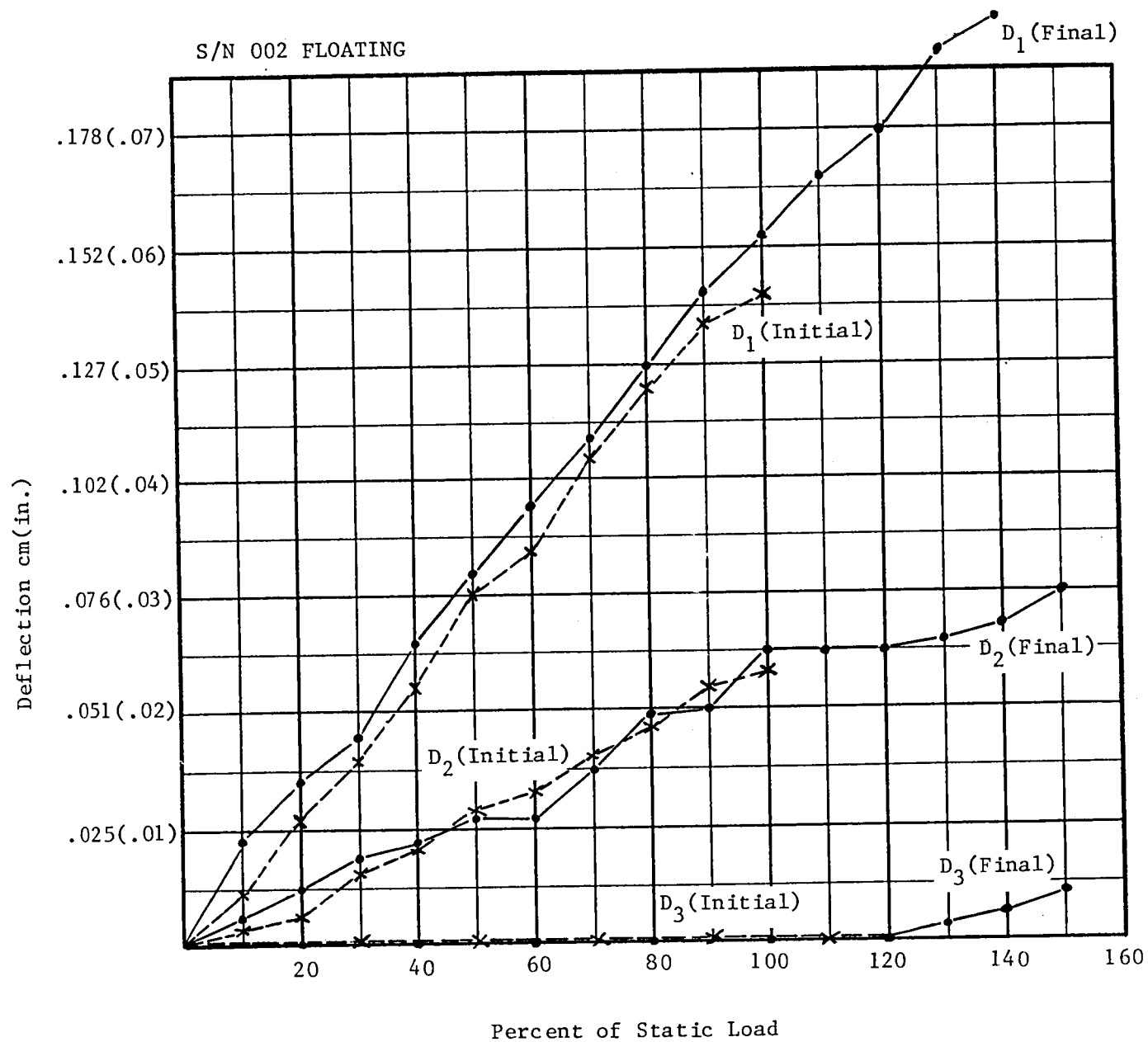


Figure IV-13 (Concl'd)

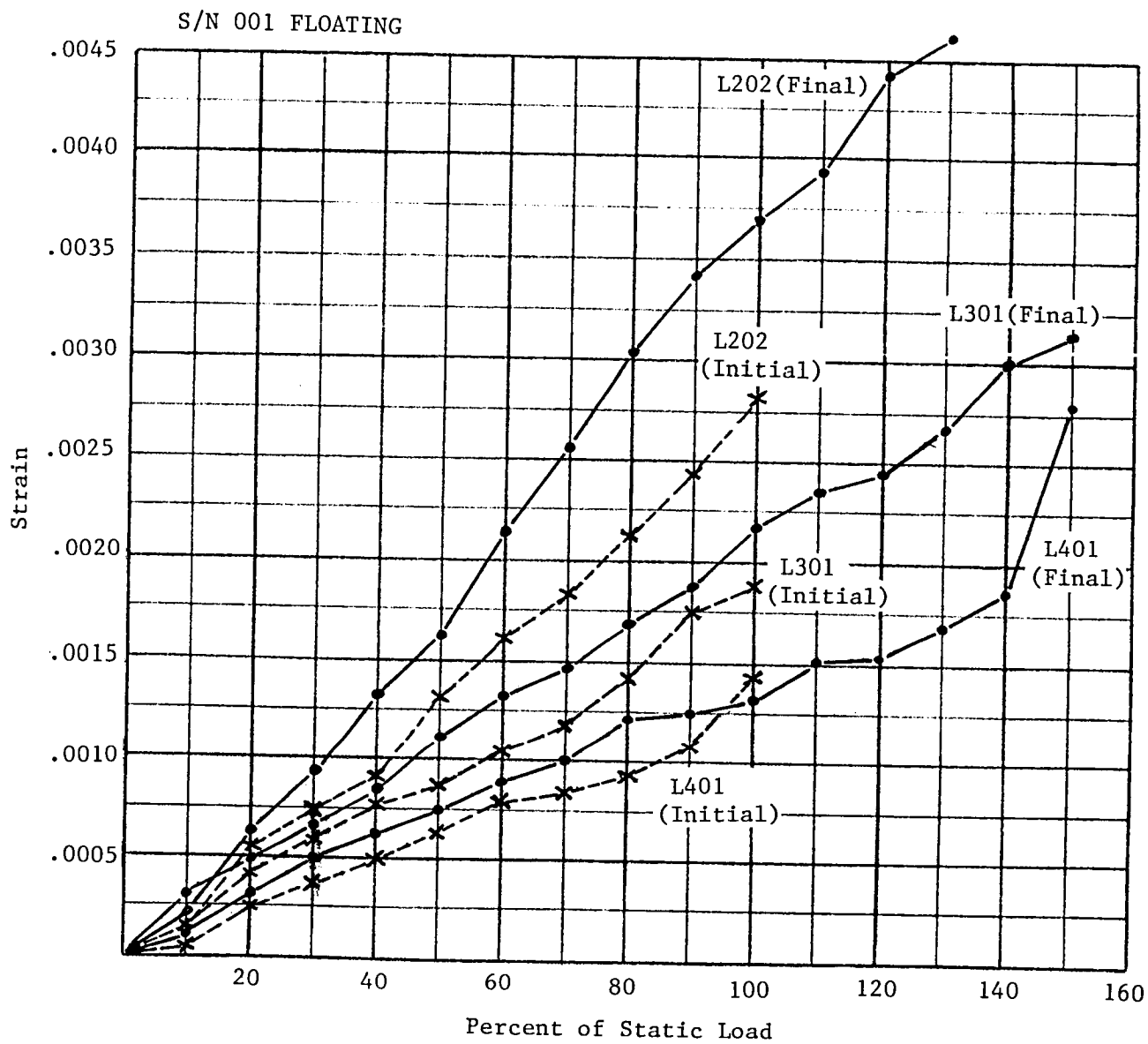


Figure IV-14 Floating Trunnion Static Test Strain Data

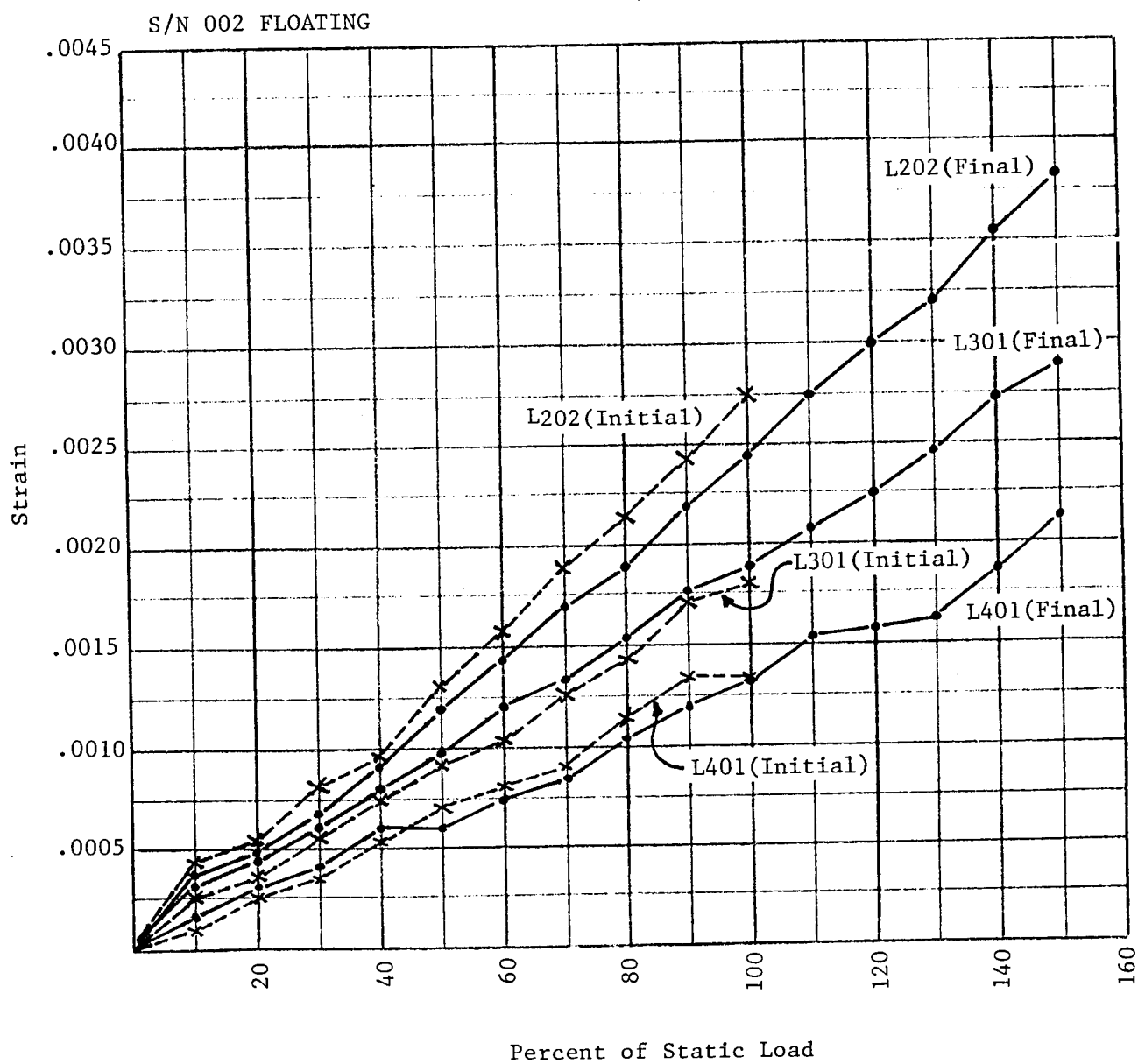


Figure IV-14 (Concl'd)

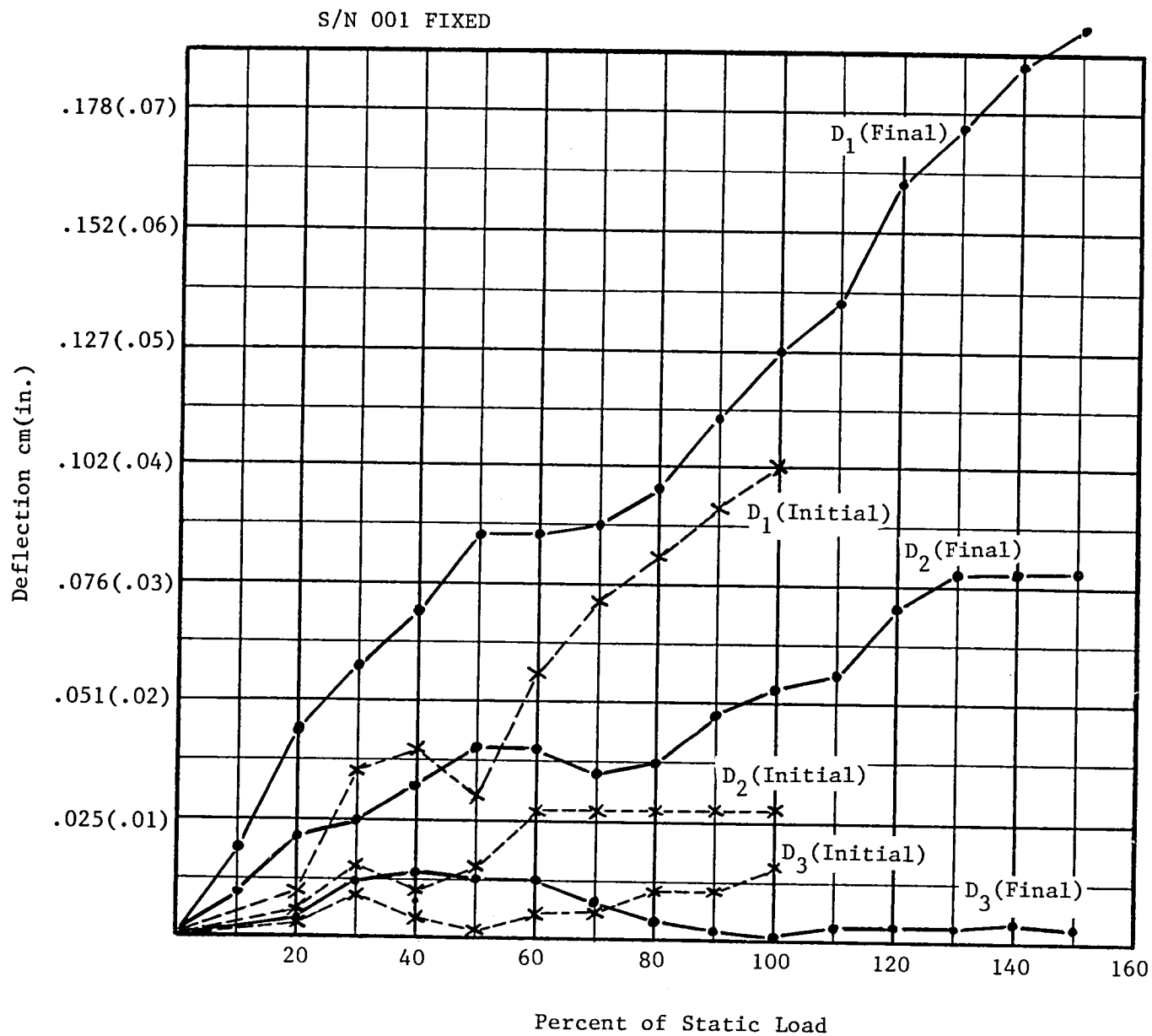


Figure IV-15 Fixed Trunnion Static Test Deflection Data

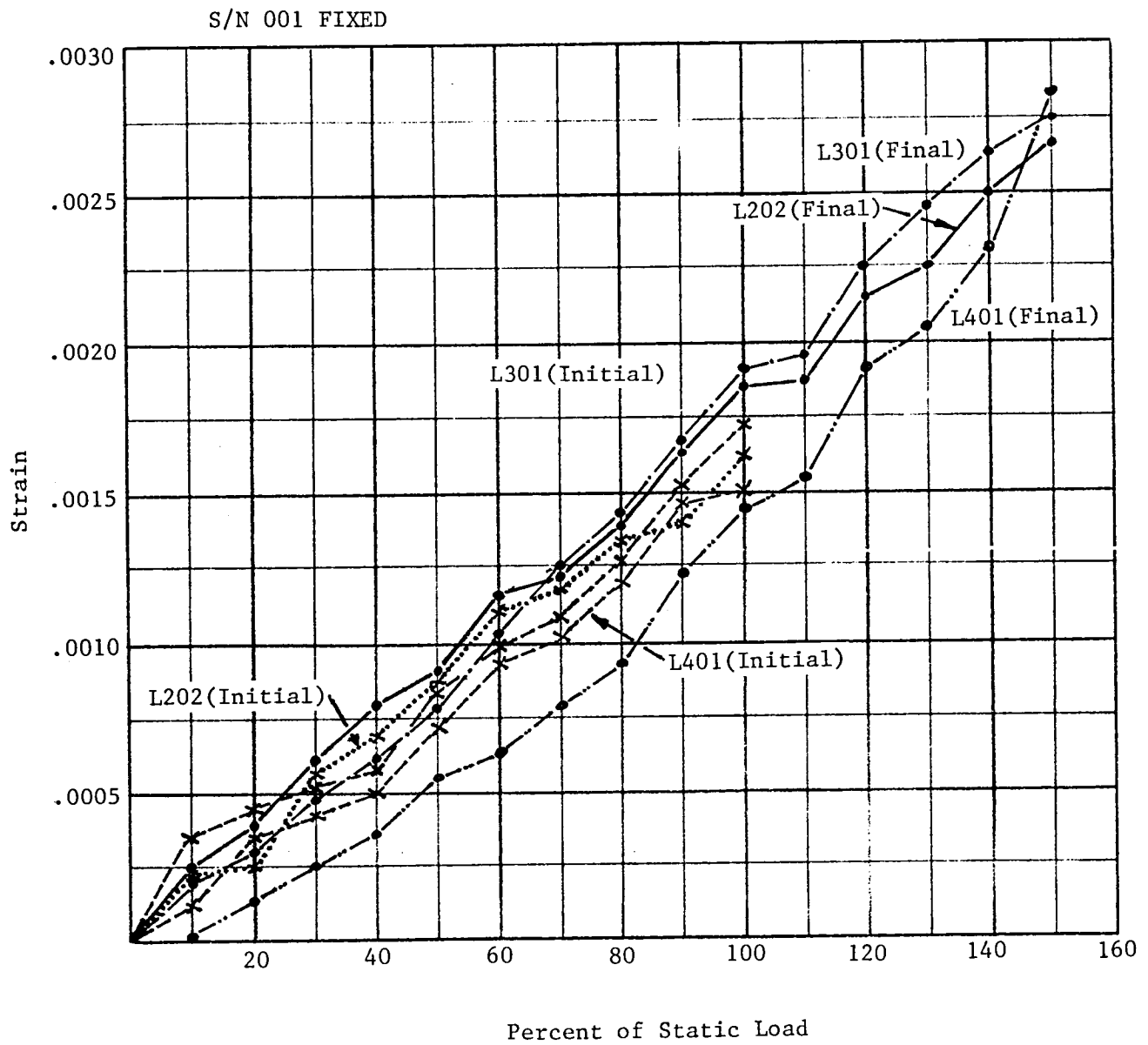


Figure IV-16 Fixed Trunnion Static Test Strain Data

2. Comparison of Test Data to Pre-Test Analysis

The loading conditions used in the trunnion fatigue tests were obtained by combining the quasistatic loads and the 2σ random loads to obtain the trunnion limit loads. The static determination of the test loads compared very well with the loads indicated in the CFME Dynamic Analysis (Reference 7). The two independent analyses compared stresses in the outer fiber based on simple beam theory and assuming a homogeneous, isotropic material for the trunnions.

The trunnion laminate is actually non-homogeneous and anisotropic. Therefore, the outer fiber stress is a function of the longitudinal strain, the circumferential strain, and the outer layer material properties. Circumferential strain was measured at one location on the fixed-end trunnion outer fiber. A rough value of the stress at this location was computed using anisotropic relationships for the two measured strains. This computed stress is within 11% of the stress predicted for this point before test which assumed an isotropic, homogenous material. Considering the assumptions in the pre-test analysis and reduction of the test data, these stresses compare closely, indicating that the test was performed properly and that the loads were applied to the trunnions in a manner which compared to predicted loading conditions.

Evaluation of the trunnion strength should be based on any degradation seen in the measured strain and deflection data. There is insufficient test data to accurately transform the strains in the outer fibers to stresses in the trunnions at more than the one location discussed above since the calculated stresses are based on assumed values of elastic modulus which is gradually being reduced due to accumulated damage.

V. CONCLUSIONS AND RECOMMENDATIONS

A. Conclusions

Obtained material properties data indicate that the CFME trunnion laminate has a stiffness which will adequately meet the imposed loading requirements for use in the CFME trunnion design. The trunnion designs, both floating and fixed, exceeded the design load carrying requirement without failure when subjected to margin testing up to ultimate load. Further capability was demonstrated by static testing to failure which in all cases occurred far in excess of the design ultimate value.

B. Recommendations

The CFME Trunnion Verification Testing Program has proven the design concept with sufficient margin to classify the flight assembled trunnions in a very high confidence category. We recommend that the delivered flight and test article trunnions be allocated for use on the CFME Program.

APPENDIX A

ABBREVIATIONS AND ACRONYMS

Al	aluminum
CFME	Cryogenic Fluid Management Experiment
CFMF	Cryogenic Fluid Management Facility
DLLF	design limit load factor
cm	centimeter
eng.	engineering
dwg.	drawing
g	force of Earth's gravity
Hz	hertz
in.	inch
kN	kilo newton
KSI	one thousand pounds per square inch
lb	pounds
LeRC	Lewis Research Center
LFqs	quasi-static load factors
LFr	random load factor
LH ₂	liquid hydrogen
m	meter
N	newton
preg	impregnated
psi	pounds per square inch
S/N	Stress versus Cycles
s/n	serial number
SS	stainless steel
ult	ultimate

REFERENCES

1. R. N. Eberhardt, W. J. Bailey and D. A. Fester, CFME Final Report, MCR-81-597, Martin Marietta Denver Aerospace, Denver, Colorado, October 1981.
2. W. J. Bailey and R. J. McMannon, CFME Trunnion Verification Test Plan, CFME-T-82-1, Martin Marietta Denver Aerospace, Denver, Colorado, February 1982.
3. R. D. Karsten, T. M. Small and R. L. Berry, CFME Trunnion Test Plan, CFME-80-32, Martin Marietta Denver Aerospace, Denver, Colorado, July 1981.
4. R. L. Berry, L. J. Demchak, T. M. Small and S. W. Wirth, Structural Analysis Final Report - CFME, MCR-81-600, Martin Marietta Denver Aerospace, Denver, Colorado, July 1981.
5. W. J. Bailey, P. R. Kerstetter and S. W. Pawlowski, CFME Trunnion Verification Test Plan - Rev A, CFME-T-82-1, Martin Marietta Denver Aerospace, Denver, Colorado, September 1982.
6. Spacelab Payload Accomodation Handbook, SLP/2104 Issue 1, Rev 2, 31 July 1979.
7. S. W. Pawlowski, CFME Trunnion Fatigue Testing Loading Spectrum, MMC-0482/82-251, Martin Marietta Denver Aerospace, Denver, Colorado, August 1982.

FINAL REPORT DISTRIBUTION LIST - CR 168310

<u>Name</u>	<u>No. of Copies</u>
National Aeronautics & Space Administration Lewis Research Center 21000 Brookpark Road Cleveland, OH 44135	
Attn: Space Technology Section, MS 500-305	1
Technical Utilization Office, MS 7-3	1
Technical Report Control Office, MS 5-5	1
AFSC Liaison Officer, MS 501-3	2
Library, MS 60-3	2
Office of Reliability & Quality Assurance, MS 500-211	1
H. J. Kasper, Project Manager, MS 500-107	10
E. P. Symons, MS 501-8	10
D. A. Petrash, MS 501-5	1
J. F. DePauw, MS 501-8	1
T. H. Cochran, MS 501-5	1
E. W. Kroeger, MS 501-8	1
D. R. Glover, MS 501-8	1
J. C. Aydelott, MS 501-6	1
National Aeronautics & Space Administration Headquarters Washington, D. C. 20546	
Attn: RS/Director, Space Systems Division	1
MFA/F. Hrach	1
RTP/F. W. Stephenson	1
MPT/L. Edwards	1
RST/E. Gabris	1
RST/M. Quviello	1
RSS/R. Carlisle	1
EM/L. Demas	1
National Aeronautics & Space Administration Goddard Space Flight Center Greenbelt, MD 20771	
Attn: Library	1
A. Sherman, MS 713	1

<u>Name</u>	<u>No. of Copies</u>
National Aeronautics & Space Administration John F. Kennedy Space Center Kennedy Space Center, FL 32899	
Attn: Library	1
CS-SED-4/M. Matis	1
CS-SED-31/M. Haddad	1
DD-MED-43/G. Reuterskiold	1
National Aeronautics & Space Administration Ames Research Center Moffett Field, CA 94035	
Attn: Library	1
P. Kittel, MS 244-7	1
National Aeronautics & Space Administration Langley Research Center Hampton, VA 23365	
Attn: Library	1
National Aeronautics & Space Administration Johnson Space Center Houston, TX 77001	
Attn: Library	1
EP2/R. Kahl	1
LP/C. M. Vaughn	1
EN3/C. J. LeBlanc	1
National Aeronautics & Space Administration George C. Marshall Space Flight Center Huntsville, AL 35812	
Attn: Library	1
EP43/L. Hastings	1
EP43/A. L. Worlund	1
PD22/U. Hueter	1
Jet Propulsion Laboratory 4800 Oak Grove Drive Pasadena, CA 91103	
Attn: Library	1
D. Young, MS 183-501	1
G. Klein, MS 125-224	1

NASA Scientific & Technical Information Facility
P. O. Box 8757
Baltimore/Washington International Airport

Attn: Accessioning Department 10

Defense Documentation Center
Cameron Station - Bldg. 5
5010 Duke Street
Alexandria, VA 22314

Attn: TISIA 1

National Aeronautics & Space Administration
Flight Research Center
P. O. Box 273
Edwards, CA 93523

Attn: Library 1

Air Force Rocket Propulsion Laboratory
Edwards, CA 93523

Attn: LK/G. Haberman 1
LKDM/Lt. A. Tolentino 1
LKCC/R. A. Silver 1

Aeronautical Systems Division
Air Force Systems Command
Wright Patterson Air Force Base
Dayton, OH 45433

Attn: Library 1

Air Force Office of Scientific Research
Washington, DC 20333

Attn: Library 1

Aerospace Corporation
2400 E. El Segundo Blvd.
Los Angeles, CA 90045

Attn: Library - Documents 1

Beech Aircraft Corporation
Boulder Facility
Box 9631
Boulder, CO 80301

Attn: Library 1
R. A. Mohling 1

Bell Aerosystem, Inc.
Box 1
Buffalo, NY 14240

Attn: Library 1

Boeing Company
P. O. Box 3999
Seattle, WA 98124

Attn: Library 1
C. L. Wilkensen, MS 8K/31 1

Chrysler Corporation
Space Division
P. O. Box 29200
New Orleans, LA 70129

Attn: Library 1

McDonnell Douglas Astronautics Co.
5301 Balsa Avenue
Huntington Beach, CA 92647

Attn: Library 1

General Dynamics Corp./Convair Division
5001 Kearny Villa Road
San Diego, CA 92138

Attn: Library 1
R. Bradshaw 1

Missiles & space Systems Center
General Electric Company
Valley Forge Space Technology Center
P. O. Box 8555
Philadelphia, PA 19101

Attn: Library 1

IIT Research Institute
Technology Center
Chicago, IL 60616

Attn: Library

1

Lockheed Missiles & Space Company
P. O. Box 504
Sunnyvale, CA 94087

Attn: Library

1

Battelle Memorial Institute
Columbus Labs
505 King Avenue
Columbus, Ohio 43201

Attn: E. Rice

1

Space Division
Rockwell International Corp.
12214 Lakewood Blvd.
Downey, CA 90241

Attn: Library
A. Jones

1

1

Northrop Research & Technology Center
1 Research Park
Palos Verdes Peninsula, CA 90274

Attn: Library

1

TRW Systems, Inc.
1 Space Park
Redondo Beach, CA 90278

Attn: Tech. Lib. Document Acquisitions

1

National Science Foundation, Engr. Div.
1800 G. Street, NW
Washington, D. C. 20540

Attn: Library

1

Florida Institute of Technology
M. E. Department
Melbourne, FL 32901

Attn: Dr. T. E. Bowmann

1

RCA/AED
P. O. Box 800
Princeton, NJ 08540

Attn: D. Balzer

1

Southwest Research Institute
Department of Mechanical Sciences
P. O. Drawer 28510
San Antonio, TX 78284

Attn: H. Norman Abramson
Franklin Dodge

1

1

McDonnell Douglas Astronautics Co.-East
P. O. Box 516
St. Louis, MO 63166

Attn: G. Orton
W. Regnier

1

1

Xerox Electro-Optical Systems
300 North Halstead
Pasadena, CA 91107

Attn: R. Richter

1

Science Applications, Inc.
1200 Prospect Street
P. O. Box 2351
La Jolla, CA 92037

Attn: M. Blatt

1

DARPA
Attn: Dr. R. Sepucha
1400 Wilson Blvd.
Arlington, VA 22209

1

